

# CHEMICAL ENGINEERING SCIENCE

## GENIE CHIMIQUE

VOL. 9

1958

No. 1

### Studies on ion exchange—IV

#### Kinetic theory of ion exchange

K. KLAMER, C. VAN HEERDEN and D. W. VAN KREVELEN

Central Laboratory, Staatsmijnen in Limburg, Geleen, Netherlands

(Received 12 December 1957)

**Abstract**—A suggestion that it might be possible to describe equilibria between ion exchangers and electrolyte solutions in analogy with membrane equilibria (Part II) has been followed up to determine the influence of some variables on the kinetics of ion exchange. It is proved that at low concentrations of the solution the mass transfer through a liquid film around the grain is rate-determining for the process, whereas at high concentrations the rate-determining step is the diffusion within the grain (Boyd *et al.*). It is predicted that during a given process the relative influences of these two diffusion mechanisms need not always be constant.

The quantitative treatment of the process in a column in which no instantaneous establishment of equilibrium occurs is generally very difficult from a mathematical point of view. With isotherms having a negative curvature the break-through curve will, however, in the end assume a stationary shape, when all concentrations travel through the column at the same rate.

The treatment of this asymptotic approach is comparatively easy; in order to compute the break-through curve it is only necessary to measure the mass transfer coefficients of liquid film and grain; this may be done graphically.

**Résumé**—Afin de déterminer l'influence d'un nombre de variables sur la cinétique de l'échange d'ions, il a été donné suite à la suggestion (Part II) qu'il serait possible sous certaines conditions de décrire les équilibres entre l'échangeur d'ions et les solutions d'électrolytes en analogie avec les équilibres de membrane. Il a été prouvé qu'à une basse concentration de la solution le transport de matière à travers un film de liquide enveloppant le grain est déterminant pour la vitesse de marche du processus tandis qu'à des concentrations élevées, la vitesse est déterminée par la diffusion à l'intérieur du grain (Boyd *et al.*). Il est prédit que, durant un processus déterminé, il n'est pas nécessaire que les influences relatives de ces deux mécanismes de diffusion soient toujours constantes.

Le traitement quantitatif du processus dans une colonne où il n'y a pas d'établissement instantané d'équilibre est en général très difficile au point de vue mathématique. Toutefois dans le cas d'isothermes à courbure négative la courbe de traversée aura finalement une forme stationnaire, quand toutes les concentrations passent à travers la colonne à la même vitesse.

Le traitement de ces approximations asymptotiques est relativement facile; pour calculer la courbe de traversée il est seulement nécessaire de mesurer les coefficients du transport de matière du film de liquide et du grain; ceci peut être effectué par moyen graphique.

**Zusammenfassung**—Die Vorstellung, dass man Gleichgewichte zwischen Ionenaustauschern und elektrolytischen Lösungen in Analogie zu Membran-Gleichgewichten (Teil II) beschreiben kann, wurde zur Bestimmung des Einflusses einiger Veränderlichen auf die Kinetik des Ionenaustausches weiter entwickelt. Es wurde bestätigt, dass bei kleinen Konzentrationen der Lösung der Stoffübergang durch eine Flüssigkeitsschicht um das Korn geschwindigkeitsbe-

stimmend für den Prozess ist, während bei hohen Konzentrationen der geschwindigkeitsbestimmende Schritt die Diffusion innerhalb des Korns ist (Boyd u.a.). Man kann voraussagen, dass während eines gegebenen Prozesses der relative Einfluss dieser beiden Diffusionsmechanismen nicht immer konstant zu sein braucht.

Die quantitative Behandlung des Prozesses in einer Säule, in der sich das Gleichgewicht nicht unmittelbar einstellt, erweist sich im allgemeinen als sehr schwierig vom mathematischen Standpunkt aus. Wenn die Isothermen eine negative Krümmung haben, so wird die Durchbruchkurve sich einer stationären Lage annähern, wenn alle Konzentrationen mit der gleichen Geschwindigkeit durch die Säule strömen.

Die Behandlung dieser asymptotischen Annäherung ist verhältnismässig einfach. Um die Durchbruchkurve zu berechnen, braucht man nur den Stoffübergangskoeffizienten der Flüssigkeitsschicht und des Korns zu messen. Dies kann auf graphischem Wege geschehen.

In the preceding part [1] we compared the capacity of ion exchangers under practical conditions with the capacity that can be calculated from equilibrium considerations. As kinetic factors slow down the process the actual capacities are lower than those found by calculation. Therefore, the present part of our article will deal with the kinetic theory of ion exchange.

#### 1. QUALITATIVE CONSIDERATIONS ON THE KINETICS OF ION EXCHANGE

Over 30 years ago DONNAN [2], in a survey of the theory on membrane equilibria, pointed in passing to the resemblance between the processes occurring on a membrane and those met with in ion exchange. The experimental results described in Part II [3] tends to support DONNAN's remarks. It seems useful further to examine this resemblance, as it may provide an insight into the kinetics of ion exchange.

Formally it may be said that three mechanisms may determine the rate of ion exchange, namely: (a) diffusion of ions from the solution through a liquid film to the exchanger surface and vice versa; (b) diffusion of ions in the exchanger particles and (c) chemical reaction between the groups on the exchanger and ions in solution.

Some authors thought they must conclude from their experiments that the rate was determined by a chemical reaction inside the exchanger. Thus NACHOD and WOOD [4, 5], like JUDA and CARRON [6], correlated their experiments with a bimolecular reaction equation. However, it is unlikely that chemical kinetics should play an important part in ion exchange; the rate of ion reactions in solutions is determined by diffusion

phenomena, and it is difficult to imagine why a similar rule should not apply to ion exchangers, in which the diffusion of ions is slower by one order than it is in solutions (HOLM [7], BOYD and SOLDANO [8]).

The cause of the improbable results obtained by these authors may be that in the mathematical treatment of experimental results sometimes a chemical reaction cannot be distinguished from film diffusion (BOYD, ADAMSON and MYERS [9], ADAMSON and GROSSMAN [10]).

At present it is assumed that only film and particle diffusion can be rate-determining factors and this assumption is borne out by practical results. There is an important difference between these two types of diffusion, in that diffusion through a liquid film depends, partly, on the velocity of the solution with respect to the particle, whereas particle diffusion does not.

We shall now examine whether it is possible *a priori* to make predictions about the relative influences of film and particle diffusion in different cases. For the present we shall assume that both film and particle diffusion play a part, and that equilibrium - viz. a Donnan equilibrium - exists at the interface. The assumption of equilibrium at the interface implies a transition of ions from the solution into the exchanger, and vice versa, which is very rapid as compared with the diffusion through solution or exchanger.

Then the number of ions transferred per unit of particle area is (cf. Fig. 1)

$$N_A = k_L a (\alpha - \alpha_i) = k_R (q_i - q) \quad (1)$$

In this formula  $k_L$  and  $k_R$  are the transfer coefficients in the liquid film and exchanger respectively; they both denote rates. The general

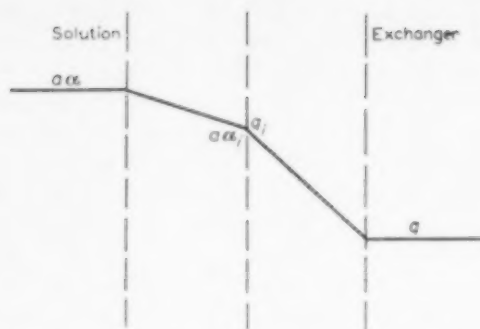


FIG. 1. Changes in concentration at the particle surface.

applicability of the last term in the above equation may be doubted, the more since the particle is not flat but spherical, so that much more complicated diffusion equations are to be expected (cf., e.g. BOYD *et al.* [9]). Recently, however, GLUECKAUF [11] demonstrated by calculation that the simple equation given above is a good approximation also for particle diffusion, and that it may be used for computing columns, provided the position of the equilibria is not too extreme ( $q$  is the mean concentration in the particle). For this reason use will be made chiefly of this approximate equation.

If the number of dissociated groups in the exchanger be  $g$ , the Donnan equilibrium at the interface may be expressed as:—

$$\frac{q_i}{g - q_i} = \frac{\alpha_i}{1 - \alpha_i} \quad (2)$$

or

$$\alpha_i = \frac{q_i}{g} \quad (3)$$

From equations (1) and (3) it follows that:—

$$N_A = \frac{\alpha g - q}{\frac{1}{k_R} + \frac{g}{k_L a}} \quad (4)$$

Prevalence of particle diffusion gives:—

$$N_A = k_R (f(\alpha) - q) \quad (5)$$

whereas, if diffusion through a liquid film is slower than particle diffusion, we get:—

$$N_A = k_L a (\alpha - \alpha_{eq}) \quad (6)$$

For exchange of bivalent for monovalent ions we may write:—

$$\frac{q_i}{(g - q_i)^2} = \frac{\alpha_i}{(1 - \alpha_i)^2 a}$$

If  $\alpha_i$  is small we may then use the approximations  $\alpha_i = \frac{aq_i}{g^2}$  and

$$N_A = \frac{\alpha \frac{g^2}{a} - q}{\frac{1}{k_R} + \frac{g^2}{a^2} \cdot \frac{1}{k_L}} \quad (7)$$

If  $q_i \simeq g$ , the following equations hold:

$$\alpha_i = 1 - \frac{g - q_i}{\sqrt{ag}} \quad \text{and} \quad N_A = \frac{g - (1 - \alpha) \sqrt{ag} - q}{\frac{1}{k_R} + \sqrt{\frac{g}{a}} \cdot \frac{1}{k_L}} \quad (8)$$

From (7) and (8) it is seen that the relative influence of  $a$  and  $g$  on the reaction mechanism of bivalent-monovalent exchange is the same as with monovalent-monovalent exchange (cf. equation (4)). Also equations (5) and (6) hold for bivalent-monovalent exchange.

From equations (4), (7) and (8) the following conclusions may be drawn:

(a) *The higher the concentration in solution, the greater the chance that particle diffusion is an important factor.* This has been shown experimentally by BOYD *et al.* [9]. A theoretical example may further illustrate this point. For  $k_L$  and  $k_R$  the following formulae may be given:

$$k_L = D_L/d \quad (9)$$

$$k_R \simeq D_R/0.1r \quad (10)$$

Equation (9) follows directly from the first law of Fick and (10) from GLUECKAUF's [11] equation:

$$k' = 15D/r^2 \quad (11)$$

in which, for our case  $k'$  is equal to

$$k_R \cdot \frac{\text{particle surface area}}{\text{bed volume}} = k_R \cdot \frac{3(1 - \beta)}{r} \quad (12)$$

If now  $\beta = 0.5$ , equations (11) and (12) lead directly to equation (10).

If we further assume  $D_L = D_R \cdot 10$ ;  $d = 5 \cdot 10^{-4}$  cm<sup>2</sup>;  $r = 0.05$  cm and  $g = 2000$  m equiv/l., it follows from (9) and (10) that  $k_L \cong 100 k_R$ .

If now  $a = 2$  m equiv/l., we get  $k_L \frac{a}{g} \cong 0.1 k_R$  so that, according to equation (4), film diffusion must dominate; if  $a = 200$  m equiv/l., then  $k_L \frac{a}{g} \cong 10 k_R$ , in which case particle diffusion is the rate-determining factor.

(b) If a strongly acid exchanger ( $H^+$  form) is contacted with a buffer solution,  $a$  is not constant throughout the process but varies from  $a_0$ , at the start, to a low value. In buffer solutions any influence of particle diffusion will disappear and the influence of the diffusion through the liquid film remains.

(c) The greater  $g$ , the more chance that diffusion through a liquid film comes to be rate-determining. This cannot easily be verified through experiments, as it is, in general, necessary to work with different types of exchanger which, owing to differences in porosity, for example, may render the interpretation of the comparison extremely dubious; a difference in porosity causes a difference in the effective value of  $r$  (cf. equation (10)). Moreover,  $D_R$  itself depends on the degree of cross-linking, on the capacity of the exchanger and, probably, also on the concentration in solution [12].

(d) Only for monofunctional strongly acid exchangers, such as Dowex 50, can  $g$  be equalized to the total capacity. For polyfunctional or weakly acid exchangers  $g$  varies with the degree of loading ("degree of occupation") of the exchanger. If a weakly acid exchanger loaded with  $Na^+$  ions is brought into the  $H^+$  form (or rather the  $HX$  form) by means of hydrochloric acid,  $g$  is at first very great and decreases in the course of the process. With polyfunctional or weakly acid exchangers any influence of film diffusion will eventually be lost in favour of particle diffusion.

(e) If a buffer solution is led over a column containing a polyfunctional exchanger ( $H^+$  form) it is difficult to predict anything ( $a$  and  $g$  both

increase when break-through occurs). Presumably there are many possibilities in this case. As far as is known in weakly acid exchangers the influence of particle diffusion is predominant. Experiments carried out by McGARVEY and THOMPSON [13] with Amberlite IRC 50 and calcium bicarbonate solutions at least point in this direction, as will be explained in another paper. CONWAY, GREEN and REICHENBERG [14] draw the same conclusion from their experiments in which this exchanger was neutralized with sodium hydroxide (cf. also BAUMAN [15]). We may therefore state that experiments with buffer solutions have shown particle diffusion to play an important part.

(f) From what was said in (b) and (d) it is seen that in a given experiment the relative influences of film and particle diffusion may be subject to variations. The literature does not show this to have been found before. However in our kinetic experiments which are described in a forthcoming paper such cases have been found.

## 2. THE GENERAL BASE OF ADSORPTIVE PERCOLATION IN A COLUMN, SLOWED DOWN BY TRANSFER PHENOMENA

If there is no equilibrium in the column the material balance applies:—

$$v \left( \frac{\partial c}{\partial x} \right)_t + \gamma \left( \frac{\partial c}{\partial t} \right)_x + S \left( \frac{\partial q}{\partial t} \right)_x = 0 \quad (13)$$

Instead of the equilibrium equation we now get a kinetic equation of the following type:—

$$\left( \frac{\partial q}{\partial t} \right)_x = F(c, q) \quad (14)$$

A combination of equations (13) and (14), together with the limit conditions, must enable us to solve any given case. Such a solution, in which  $c$  and  $q$  are given as functions of  $x$  and  $t$  respectively, will, even for simple cases, be highly complicated mathematically and difficult to work with (THOMAS [16], GOLDSTEIN [17, 18]). We shall therefore try to find out if, perhaps, there are asymptotic solutions which, although limited in their applicability, render possible the kinetic interpretation of the experiments by virtue of their simplicity.



Below we shall consider—unless otherwise stated—a column for which at  $t = 0$  and  $x \geq 0$ , the quantity  $q = 0$ ; this is to be loaded with a solution of concentration  $c_0$ . After a short time  $t$  the relation between  $q$  and  $c$  will be as shown in Fig. 2, in which the initial state coincides with the horizontal axis.

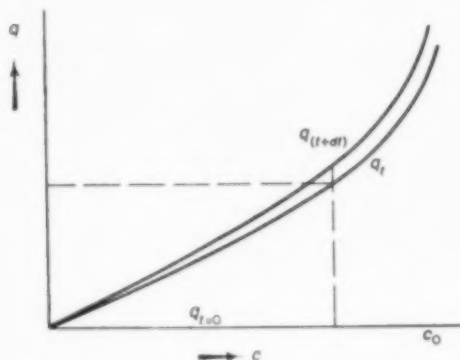


FIG. 2. Kinetic relation  $q_t(c)$ .

This curve will rise with time, or, in other words,  $\left(\frac{\partial q}{\partial t}\right)_c$  is positive and  $\left(\frac{\partial c}{\partial t}\right)_q$  is negative. We shall express each of these differential quotients in a formula:—

$$dq = \left(\frac{\partial q}{\partial x}\right)_t dx + \left(\frac{\partial q}{\partial t}\right)_x dt \quad (15)$$

If  $v_c$  is the velocity at which a given liquid concentration moves through the column, then  $dx = v_c dt$ ; and hence:—

$$(dq)_c = \left(\frac{\partial q}{\partial x}\right)_t v_c dt + \left(\frac{\partial q}{\partial t}\right)_x dt \quad (16)$$

and:—

$$\left(\frac{\partial q}{\partial t}\right)_c = \left(\frac{\partial q}{\partial x}\right)_t (v_c - v_q) = \left(\frac{\partial q}{\partial t}\right)_x \left(1 - \frac{v_c}{v_q}\right) \quad (17)$$

where  $v_q$  is the velocity at which a given concentration  $q$  moves through the column.

During the loading of a column  $\left(\frac{\partial q}{\partial x}\right)_t < 0$ , and, as  $\left(\frac{\partial q}{\partial t}\right)_c > 0$ , we may conclude that  $v_q > v_c$ . This conclusion may also be drawn from the

expression for  $\left(\frac{\partial c}{\partial t}\right)_q$  which can be derived in an analogous way:—

$$\left(\frac{\partial c}{\partial t}\right)_q = \left(\frac{\partial c}{\partial x}\right)_t (v_q - v_c) = \left(\frac{\partial c}{\partial t}\right)_x \left(1 - \frac{v_q}{v_c}\right) \quad (18)$$

where, for the reason mentioned above,  $\left(\frac{\partial c}{\partial x}\right)_t < 0$ .

From  $v_q > v_c$  it consequently follows that the concentration front in the adsorbent will tend to catch up with the proceeding concentration front in the liquid and will eventually coincide with it.

**2.1. Linear isotherms.** This case is completely analogous to the problem of heat transfer from a flowing medium to a fixed bed. For the sake of simplicity, calculations are often made on the assumption that the isotherms are straight, but in experiments this simplification can only seldom be tolerated (Boyd, *et al.* [19]). Therefore, it may suffice here to refer to Section 2.3, as with the isotherms showing a negative curvature, the front here tends to adopt a stationary shape although less strongly.

**2.2. Isotherms with positive curvature.** ( $f''(c) > 0$ ; cf. Fig. 3). The question is now whether the eventual value of  $q$  is equal to  $f(c)$ .

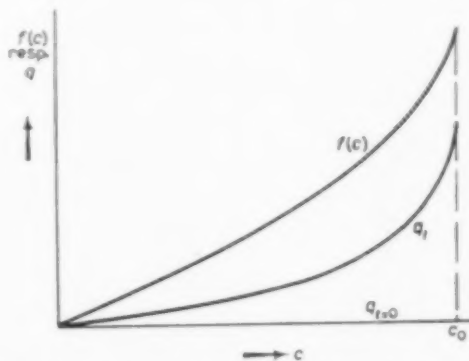


FIG. 3. Kinetic relation  $q_t(c)$  if the isotherm has a positive curvature.

Although this seems to be so, it is difficult to prove. It may be remarked, however:—

That also if eventually equilibrium should be reached,  $v_c$  is equal to  $v_q$ , as:—

$$v_q = -\frac{\left(\frac{\partial q}{\partial t}\right)_x}{\left(\frac{\partial q}{\partial x}\right)_t} = -\frac{\left(\frac{\partial f(c)}{\partial t}\right)_x}{\left(\frac{\partial f(c)}{\partial x}\right)_t} = -\frac{f'(c)\left(\frac{\partial c}{\partial t}\right)_x}{f'(c)\left(\frac{\partial c}{\partial x}\right)_t} = v_c \quad (19)$$

That data in the literature point to the possibility of circumstances under which, practically speaking, equilibrium will be established. For instance, GLUECKAUF [20] compares the statically measured equilibrium between  $\text{Cu}^{2+}$  and  $\text{H}^+$  ions for Zeo-Karb, with the curve that can be calculated from the continuous elution curve (Part II [3]), assuming equilibrium to be established in the column. The equilibrium curve and the calculated curve coincided.

SUJATA, BANCHERO and WHITE [21] led sodium chloride solutions over Dowex 50 in the  $\text{K}^+$  form (the  $\text{K}^+$  ion is more strongly adsorbed on this exchanger than the  $\text{Na}^+$  ion), and found an elution curve which indicated the establishment of equilibrium in the exchanger. The experiments of WHEATON and BAUMAN [22], already mentioned in Part III [1], point in the same direction.

It cannot be said that  $v_c = v_q$  implies the existence of equilibrium. However, experimental data do point to a chromatogram of the same appearance as that obtained at instantaneous establishment of equilibrium.

2.3. *Isotherms with negative curvature*, ( $f''(c) < 0$ ; cf. Fig. 4). For isotherms having a negative curvature it can be proved that the maximum values of  $q$  are given by the chord passing through  $(0, 0)$  and  $(c_0, f(c_0))$  (Fig. 4).

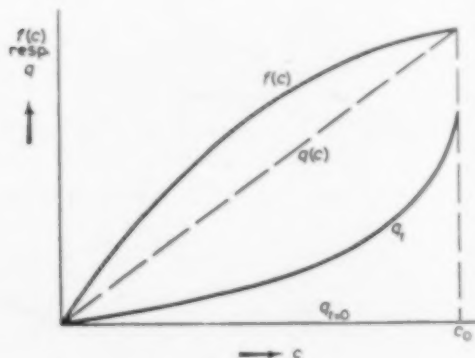


FIG. 4. Kinetic relation  $q_t(c)$  if the isotherm has a negative curvature.

Assume that eventually ( $q_t''(c) < 0$ ). The value of  $v_c$  derived from the material balance is:—

$$v_c = \left(\frac{\partial x}{\partial t}\right)_c = \frac{v}{\gamma + S\left(\frac{\partial q}{\partial c}\right)_x} \quad (20)$$

$v_q$  is defined by

$$v_q = -\left(\frac{\partial x}{\partial t}\right)_q = -\frac{\left(\frac{\partial q}{\partial t}\right)_x}{\left(\frac{\partial q}{\partial x}\right)_t} = -\frac{\left(\frac{\partial q}{\partial c}\right)_x \left(\frac{\partial c}{\partial t}\right)_x}{\left(\frac{\partial q}{\partial c}\right)_t \left(\frac{\partial c}{\partial x}\right)_t} = \left(\frac{\partial q}{\partial c}\right)_x v_c \quad (21)$$

If, finally,  $v_q = v_c$ , then  $\left(\frac{\partial q}{\partial c}\right)_x = \left(\frac{\partial q}{\partial c}\right)_t$ . After substitution of this equation in (20) and subsequent differentiation it appears that  $dc/dc$  would be positive. From a physical point of view this situation is unreal, in analogy to that discussed in Part I [23] for the instantaneous establishment of equilibrium.

Consequently, the eventual situation will be

$$\frac{dq}{dc} = \frac{f(c_0)}{c_0} \quad (22)$$

from which it follows that:

$$q = \frac{f(c_0)}{c_0} c \quad (23)$$

Here  $q$  is a function of  $c$  alone.

In the end the concentration front in the liquid will coincide with the concentration front in the adsorbent; this event is characterized by the fact that all concentrations have the same forward velocity from that moment. We are then concerned with a so-called stationary sharp front.

If information is desired about the kinetic behaviour of an adsorbent it is advisable to study the desorption at  $f''(c) > 0$  and the adsorption at  $f''(c) < 0$ ; this is due to the fact that in both cases a sharp front will eventually result, which: (a) can be much more easily treated mathematically than a widening front and (b) in principle, cannot ever lead to a situation indistinguishable from equilibrium.

This had already been found in the experiments by SUJATA *et al.* [21], mentioned above: when sodium chloride solutions were passed over  $\text{K}^+$ -Dowex 50 (widening front). A situation resembling the instantaneous establishment of

equilibrium was obtained, whereas when potassium chloride solutions were led over Na<sup>+</sup>-Dowex 50 (sharp front) a kinetic effect was clearly observed.

For this reason many investigators have studied the sharp front (GLUECKAUF and COATES [24], HIESTER and VERMEULEN [25], MICHAELS [26], SILLÉN [27], VERMEULEN [28], VERMEULEN and HUFFMAN [29], LAPIDUS and ROSEN [30] and BADDOUR, GOLDSTEIN and EPSTEIN [31]).

Unlike other authors we shall not attempt to express the equilibria in formulae. The quantity which must necessarily be known, the driving force, will be determined graphically.

The discussions given in the previous paragraphs have been illustrated in the Table. This Table also shows the result of analogous observations on isotherms in which inflexion points occur.

### 3. THE BREAK-THROUGH CURVE FOR A STATIONARY SHARP FRONT

The object of this section is to give a description of the way in which mass transfer coefficients can be determined from a stationary break-through curve. In this connexion it is shown how the driving force for film and particle diffusion can be determined. Furthermore it is proved that an inflexion point in the curve corresponds with a maximum in the driving force. Finally, attention is drawn to characteristic differences between

particle and film diffusion from which, by using experimental data, it can be derived which of the two mechanisms is rate-determining.

3.1. *The stationary break-through curve in chromatographic processes in general.* Substitution of equation (23) in equation (14) gives:—

$$\left(\frac{\partial c}{\partial t}\right)_x = \frac{c_0}{f(c_0)} F(c) \quad (24)$$

With  $x = l$ , this equation gives the slope of the break-through curve of the column.  $F(c)$  depends on the rate-determining mechanism. In case particle diffusion is rate-determining, equation (24) (see equation 5) becomes:—

$$\left(\frac{\partial c}{\partial t}\right)_x = \frac{c_0}{f(c_0)} k_R a' (f(c) - q) \quad (25)$$

where  $a'$  is the particle area per unit bed volume,  $\left(\frac{\partial c}{\partial t}\right)_{x=l}$  can be measured, and the driving force can be graphically determined from Fig. 5; therefore  $k_R$  can be calculated.

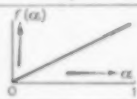
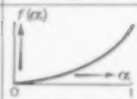
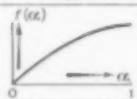
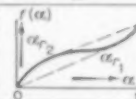
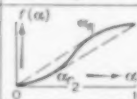
A significant point in the break-through curve is the inflexion point. This corresponds with the maximum value of the driving force  $f(c) - q$ :—

$$\left(\frac{\partial^2 c}{\partial t^2}\right)_x = \frac{c_0}{f(c_0)} k_R a' \left(f'(c) - \frac{f(c_0)}{c_0}\right) \left(\frac{\partial c}{\partial t}\right)_x = 0$$

for (see Fig. 5):—

$$f'(c_b) = \frac{f(c_0)}{c_0} \quad (26)$$

Table 1. Characteristics of ion exchangers

TYPE OF ISOTHERMS	I	II	III	IV	V
A SHAPE OF $f(\alpha)$					
B VALUE OF $q (= q_i / \alpha)$ AS A FUNCTION OF $\alpha$ (ACCORDING TO EQUATION 3)	CONSTANT	INCREASING	DECREASING	FIRST DECREASING, THEN INCREASING	FIRST INCREASING, THEN DECREASING
C RELATIVE INFLUENCE $k_i$ AS COMPARED WITH $k_0$ AS A FUNCTION OF $q$	CONSTANT	INCREASING	DECREASING	FIRST DECREASING, THEN INCREASING	FIRST INCREASING, THEN DECREASING
D FRONT AT ADSORPTION	STATIONARY AT $t = \infty$	WIDENING → EQUILIBRIUM	STATIONARY IN COURSE OF TIME	$0 < \alpha < \alpha_{f1}$ LIKE D III; $\alpha_{f1} < \alpha < \alpha_0$ LIKE D II	$0 < \alpha < \alpha_{f2}$ LIKE D II; $\alpha_{f2} < \alpha < \alpha_0$ LIKE D III
E BEST SUITED FOR KINETIC INVESTIGATION	(THEORY ON HEAT TRANSFER IN FIXED BED)	DESORPTION	ADSORPTION	$0 < \alpha < \alpha_{f1}$ : ADSORPTION; $\alpha_{f1} < \alpha < \alpha_0$ : DESORPTION	$0 < \alpha < \alpha_{f2}$ : DESORPTION; $\alpha_{f2} < \alpha < \alpha_0$ : ADSORPTION

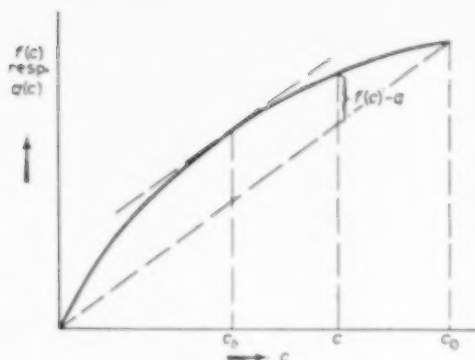


FIG. 5. Determination of the driving force in particle diffusion.

If film diffusion is rate-determining, equation (24) (see equation (6)) becomes:—

$$\left(\frac{\partial c}{\partial t}\right)_x = \frac{c_0}{f(c_0)} k_L a' (c - c_{eq}) \quad (27)$$

The driving force  $c - c_{eq}$  can be read from Fig. 6 and  $k_L$  can be calculated from the measured slope of the break-through curve by means of equation (27).

Here again an inflexion point in the break-through curve is determined by the maximum of the driving force  $c - c_{eq}$  :—

$$\left(\frac{\partial^2 c}{\partial t^2}\right)_x = \frac{c_0}{f(c_0)} k_L a' \left\{ 1 - \frac{f(c_0)}{f'(c)} \right\} \left(\frac{\partial c}{\partial t}\right)_x = 0$$

for

$$f'(c) = \frac{f(c_0)}{c_0} \quad (28)$$

Concentration  $c$ , which satisfies equation (28), corresponds with a concentration  $c_b$  in the fluid (see Fig. 6.)

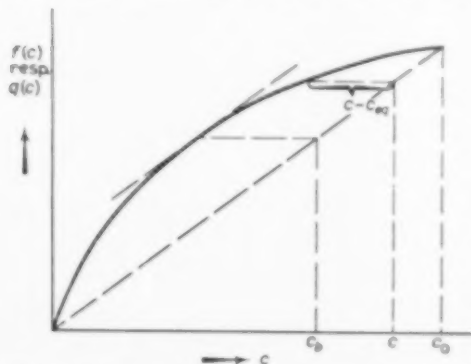


FIG. 6. Determination of the driving force in film diffusion.

Determination of the break-through curves at different linear velocities  $V = (v/S)$  and different  $a'$  values must yield different results for particle and film diffusion because  $k_L$  is also a function of the Reynolds number.

3.2. *The stationary break-through curve in ion exchange processes in particular.* Ion exchange differs in some respects from chromatographic processes in general; for particle diffusion the equation becomes:—

$$\left(\frac{\partial x}{\partial t}\right)_x = \frac{x_0}{f(x_0)} k_R a' \{f(x) - q\} \quad (29)$$

whereas for film diffusion one gets instead of equation (27) the following relationship:—

$$\left(\frac{\partial x}{\partial t}\right)_x = \frac{x_0}{f(x_0)} k_L a' (x - x_{eq}) \quad (30)$$

showing that the shape of the break-through curve varies in proportion with the ion concentration in solution  $a$  (provided that the equilibrium curve and hence  $x_{eq}$  is not dependent on  $a$ ).

Column design, in which the calculation of the break-through curves constitutes an essential step, requires that the values of  $k_R$  and  $k_L$  be known. Our experimental work therefore will be aimed at determining these quantities using the basic equations (25), (27), (29) and (30). This will be dealt with in Part V of this series of papers.

#### NOTATION

$a$ = total ion concentration in solution	$\text{ML}^{-3}$
$a'$ = particle area per unit of bed volume	$\text{L}^{-1}$
$c$ = concentration in the liquid	$\text{ML}^{-3}$
$D$ = diffusion coefficient	$\text{L}^2 \text{T}^{-1}$
$d$ = thickness of film	$\text{L}$
$g$ = number of dissociated groups on exchanger	$\text{ML}^{-3}$
$f(c)$ = concentration in the adsorbent at the moment when equilibrium is established	$\text{ML}^{-3}$
$f(x)$ = as $f(c)$ for the ion exchanger	
$k_L$ = mass transfer coefficient in liquid film	$\text{LT}^{-1}$
$k_R$ = mass transfer coefficient in exchanger	$\text{LT}^{-1}$
$l$ = length of column	$\text{L}$
$N_A$ = number of ions transferred per unit time and per unit of particle area	$\text{MT}^{-1} \text{L}^{-2}$
$q$ = concentration in adsorbent (mean value)	$\text{ML}^{-3}$

# Studies on ion exchange—IV.

$r$ = radius of the grain	$L$	$\beta$ = fractional free space	
$S$ = cross-sectional area of column	$L^2$	$\gamma$ = free space per unit length of column	$L^2$
$t$ = time	$T$		
$v$ = volumetric rate of flow of liquid	$L^3 T^{-1}$	<i>Indices</i>	
$v_q, v_c$ = rate at which concentrations $q$ and $c$ move through the column	$L T^{-1}$	$b$ = inflexion point	
$x$ = distance to the point where liquid enters the column	$L$	$eq$ = equilibrium	
$\bar{x}$ = equivalent fraction of a given ion in solution		$i$ = interface between liquid and ion exchanger	
$\frac{c_{Na^+}}{a}$ (mean value)		$L$ = liquid	
		$R$ = ion exchanger	
		$r$ = tangent point	
		$t$ = time	
		$0$ = condition before the liquid enters the column	

## REFERENCES

- [1] KLAMER K. and VAN KREVELEN D. W. *Chem. Engng. Sci.* 1958 8 216.
- [2] DONNAN F. G. *Chem. Rev.* 1925 1 73.
- [3] KLAMER K., LINSSSEN J. C. H. and VAN KREVELEN D. W. *Chem. Engng. Sci.* 1958 7 204.
- [4] NACHOD F. C. and WOOD W. J. *Amer. Chem. Soc.* 1944 66 1380.
- [5] NACHOD F. C. and WOOD W. J. *Amer. Chem. Soc.* 1945 67 629.
- [6] JUDA W. and CARRON M. J. *Amer. Chem. Soc.* 1948 70 3295.
- [7] HOLM L. W., *J. Chem. Phys.* 1954 22 1132.
- [8] BOYD G. E. and SOLDANO B. J. *Amer. Soc.* 1953 75 6091.
- [9] BOYD G. E., ADAMSON A. W. and MYERS L. S. J. *Amer. Soc.* 1947 69 2836.
- [10] ADAMSON A. W. and GROSSMAN J. J. *J. Chem. Phys.* 1949 17 1002.
- [11] GLUECKAUF E. *Trans. Faraday Soc.* 1955 51 1540.
- [12] RICHMAN D. and THOMAS H. C. J. *Phys. Chem.* 1956 60 237.
- [13] MCGARVEY F. X. and THOMPSON J. *Industr. Engng. Chem. (Industr.)* 1951 43 741.
- [14] CONWAY D. E., GREEN J. H. S. and REICHENBERG D. *Trans. Faraday Soc.* 1954 50 521.
- [15] BAUMAN W. C. *Ion Exchange* (Edited by F. C. NACHOD) p. 61. Academic Press, New York 1949.
- [16] THOMAS H. A. J. *Amer. Chem. Soc.* 1944 66 1664.
- [17] GOLDSTEIN S. *Proc. Roy. Soc.* 1953 A219 151.
- [18] GOLDSTEIN S. *Proc. Roy. Soc.* 1953 A219 171.
- [19] BOYD G. E., MYERS L. S. and ADAMSON A. W. J. *Amer. Chem. Soc.* 1947 69 2849.
- [20] GLUECKAUF E. *J. Chem. Soc.* 1947 1302.
- [21] SUJATA A. D., BANCHERO J. T. and WHITE R. R. *Industr. Engng. Chem. (Industr.)* 1955 47 2193.
- [22] WHEATON R. M. and BAUMAN W. C. *Industr. Engng. Chem. (Industr.)* 1951 43 1087.
- [23] KLAMER K. and VAN KREVELEN D. W. *Chem. Engng. Sci.* 1958 7 197.
- [24] GLUECKAUF E. and COATES J. J. *J. Chem. Soc.* 1947 1315.
- [25] HIESTER N. K. and VERMEULEN T. *Chem. Engng. Progr.* 1953 48 1658.
- [26] MICHAELS A. S. *Industr. Engng. Chem. (Industr.)* 1952 44 1922.
- [27] SILLÉN L. G. *Ark. Kemi* 1950 2 477.
- [28] VERMEULEN T. *Industr. Engng. Chem. (Industr.)* 1953 45 1664.
- [29] VERMEULEN T. and HUFFMAN E. H. *Industr. Engng. Chem. (Industr.)* 1953 45 1658.
- [30] LAPIDUS L. and ROSEN J. B. *Chem. Eng. Progr. (Symp. Ser. No. 14)* 1954 50 97.
- [31] BADDOUR R. E., GOLDSTEIN D. J. and EPSTEIN P. *Industr. Engng. Chem. (Industr.)* 1954 46 2192.



## Studies on ion exchange—V

### Kinetic measurements

K. KLAMER, J. C. H. LINNSEN and D. W. VAN KREVELEN

Central Laboratory, Staatsmijnen in Limburg, Geleen, Netherlands

(Received 12 December 1957)

**Abstract**—Kinetic experiments are described which were aimed at measuring the mass transfer coefficients of liquid film and particle diffusion. A graphic determination of the driving force of the kinetic process was used. Experiments made with a number of exchangers have shown that :

- (1) Sooner or later the front assumes a stationary shape.
- (2) If film diffusion is rate-determining the coefficient of mass transfer is in good agreement with the value that can be calculated from known dimensionless correlations (VAN KREVELEN *et al.*).
- (3) The rate determining mechanism may depend on the degree to which the charging of the exchanger has proceeded.
- (4) If particle diffusion is the rate determining step, two type of mechanisms may be distinguished : diffusion of ions through the liquid in the gel and exchange in the position of ions fixed on the skeleton of the exchanger.

**Résumé**—Des essais cinétiques sont communiqués, qui avaient pour but de mesurer les coefficients du transfert de masse par diffusion à travers le film liquide et à l'intérieur du grain. On a utilisé une détermination graphique de la force motrice du processus cinétique. Des essais effectués avec un nombre d'échangeurs ont montré les faits suivants :

- (1) Tôt ou tard le front prend une forme stationnaire.
- (2) Si la diffusion à travers le film détermine la vitesse, le coefficient du transfert de masse correspondra bien à la valeur qui peut être calculée à partir des corrélations connues sans dimensions (VAN KREVELEN et collaborateurs).
- (3) Le mécanisme déterminant la vitesse peut dépendre du degré de charge atteint dans l'échangeur.
- (4) Si la diffusion à l'intérieur du grain détermine la vitesse, on pourra distinguer deux types de mécanismes à savoir : diffusion d'ions à travers le liquide dans le gel ou changement de position des ions fixés sur le squelette de l'échangeur.

**Zusammenfassung**—Es werden kinetische Versuche beschrieben, die auf die Messung des Stoffübergangskoeffizienten in der Flüssigkeitsschicht und der Teilchendiffusion abzielten. Die treibenden Kräfte des kinetischen Prozesses wurden graphisch bestimmt. Versuche mit einer Anzahl Austauscher hatten folgendes Ergebnis

- (1) Früher oder später erreicht die Front eine stationäre Form.
- (2) Wenn die Filmdiffusion geschwindigkeitsbestimmend ist, liegt eine gute Übereinstimmung zwischen dem gemessenen Stoffübertragungs-koeffizienten und dem Wert, der aus bekannten dimensionslosen Beziehungen berechnet werden kann (VAN KREVELEN u.a.).
- (3) Der geschwindigkeitsbestimmende Mechanismus kann von dem Grad abhängen, wie die Beladung des Austauschers fortgeschritten ist.
- (4) Wenn die Teilchendiffusion geschwindigkeitbestimmend ist, müssen zwei Mechanismen unterschieden werden : Diffusion der Ionen durch die Flüssigkeit in dem Gel und Platzwechsel von Ionen, die in dem Skelett des Austauschers fixiert sind.

IN Part IV it was shown how the coefficients of mass transfer through the liquid film and within the grain can be derived from the slope of the break-through curve. This paper deals with the determination of the above coefficients on a number of ion exchangers. Such data are needed in column design (Part VI).

### 1. PROCEDURE

Kinetic experiments were carried out on ion exchangers in a column of  $4.5 \text{ cm}^2$  cross-section, using the following variables: quantity of exchanger (50–200 ml), total ion concentration (0.01 and 0.02 N) and rate of flow (normally 2.5 and 5 l/hr).

Both the method of recording the effluent concentration and the interpretation of the experiments require that the rate of flow be kept constant; consequently, special attention was paid to this point. From the literature [1, 2] as well as from our own experience we know that a constant flow rate is often difficult to achieve. The rate controller described by HALL [3] was used; the principles of this are outlined in Fig. 1.

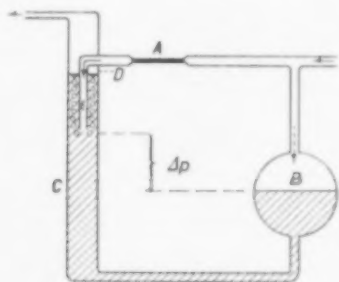


FIG. 1. Principles of the rate controller.

The pressure differential across the capillary  $A$  is  $\Delta p$ . The shaded part of the apparatus is filled with mercury. The diameter of the wide vessel  $B$  is much larger than that of  $C$  minus  $E$ . As a result a variation in preliminary pressure hardly effects the height of the mercury column in  $B$  (as a consequence  $\Delta p$  is constant); on the other hand it produces an equally large variation in back pressure as the level  $D$  of the mercury in  $C$  corresponds with this variation. To ensure

proper operation the dimensions must be so adapted to the anticipated maximum pressure variations that the tube  $E$  will always be immersed in the mercury. The accuracy of the apparatus is determined not only by the pressure variations but also by the ratio between the diameters of  $B$  and of  $C$  minus  $E$ . Fouling of the capillary is prevented by mounting a glass filter before the inlet.

The concentration in the effluent is determined by measuring its electric conductivity. To this end the resistance of a conductivity cell was compared with a fixed resistance in a Wheatstone bridge fed from a 220 V line via a voltage stabilizer. The current in the bridge was rectified and indicated on a millivolt recorder via a potentiometer. Calibration was effected by the use of solutions of known concentration. The temperatures of the liquid, the liquid controller and the conductivity cell were kept constant within about  $0.1^\circ \text{C}$ ; this was done to keep the flow rate constant and to enable the conductivity to be properly measured.

The exchangers examined were the normal commercial products. As a rule they were not separated into fractions, partly in order to ensure that the results would conform as closely as possible with those obtained in practice, partly because the homogeneity of the particle size distribution is merely of secondary importance as compared with the effect of the other variables.

The specific surface area needed for the calculations was derived from the particle size, determined by screen analysis, and the fractional free space in column  $\beta$ . The latter quantity was always assigned a value of 0.5. An exact determination of the fractional free space is not feasible; for example displacement with water-immiscible liquids yields values which depend on the character of the liquid used and moreover deviate considerably from those obtained by centrifuging the wet exchanger.

In all the experiments the concentration profile was assumed to be flat. Disturbances may be caused by the following factors.

- (a) Axial molecular diffusion; considering the low diffusion coefficient in aqueous solutions this effect may be neglected.

- (b) Axial "eddy" diffusion; GLUECKAUF and COATES [4] have shown that this does not give rise to difficulties even when dealing with small particles.
- (c) Axial mixing due to differences in density when the heavier liquid is above the lighter [5]; at the concentration used, no effect of this phenomenon could be demonstrated.
- (d) Shrinkage and swelling; BYRNE and LAPIDUS [6] noted a deviation from the flat concentration profile during contraction. This may have played a part in our experiments with Permutit ES.

It is remarkable that the above workers found the strongly basic anion exchanger Amberlite IRA 400 to swell during loading whereas we observed shrinkage.

Column experiments were carried out with three types of exchangers which are often used in water purification practice: the polyfunctional cation exchanger DUSART VKG, the weakly basic anion exchanger DOWEX 3 and the polyfunctional anion exchanger PERMUTIT ES. With the cation exchanger in the  $H^+$  form we studied the conversion of sodium chloride to hydrochloric acid and with the anion exchangers the adsorption of hydrochloric acid; this corresponds with the practical use of these exchangers in demineralisation processes. As stated in Part IV [7] our investigation has been restricted to the stationary sharp break-through front.

It may be asked whether such a front may occur in the above process with DUSART VKG because the  $Na^+ - H^+$  equilibrium on these ion exchangers shows an inflexion point (Fig. 4A; Part II [8]). That this question must be answered in the affirmative follows from considerations analogous to those given in part IV [7] or from Part I [9] where it has been shown that in the case of instantaneous equilibrium an isotherm with  $f'''(c) > 0$  gives a discontinuous form at  $0 < c < c_{r1}$  as is also observed with isotherms having a negative curvature. The stationary sharp front may then occur at  $0 < \alpha < \alpha_r$  where  $\alpha_r$  is defined by:

$$f'(\alpha_r) = \frac{f(\alpha_r)}{\alpha_r} \quad (1)$$

The adsorption equilibria for hydrochloric acid of Dowex 3 and Permutit ES are represented in Fig. 10, Part II [8]. As can be seen from this graph both isotherms show a negative curvature so that the primary condition for the formation of a stationary front has been satisfied.

## 2. RESULTS

The results are shown in Figs. 2-6.

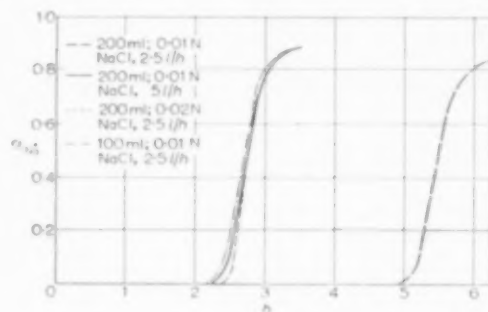


FIG. 2. Kinetic measurements on DUSART VKG.

In Fig. 2 (DUSART VKG) the curves obtained at 100 and 200 ml bed volumes (0.01 N sodium chloride and  $v = 2.5$  l/hr) run parallel; this points to a stationary shape (Part IV [7]). The total ion concentration in solution considerably affects the slope of the break-through curve, the influence of the linear velocity being less pronounced. This indicates that film diffusion has a marked effect (Part IV [7]).

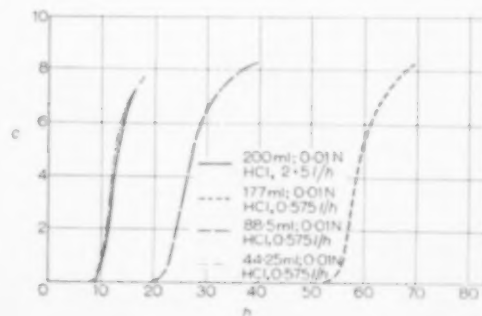


FIG. 3. Kinetic measurements on DOWEX 3.

In Fig. 3 (DOWEX 3) the curves for 44.3 and 88.5 ml bed volumes do not run parallel in

contrast to those for 88.5 and 177 ml. The latter two curves therefore have a stationary shape.

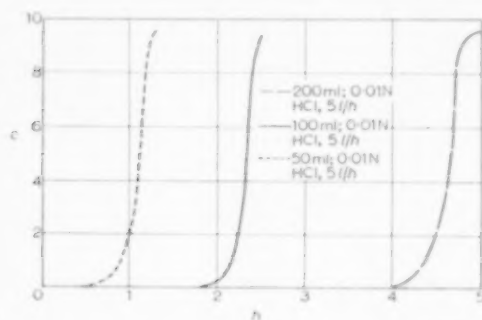


FIG. 4. Kinetic measurements on Permutit ES.

In Fig. 4 (Permutit ES) all the curves obtained with different bed depths run parallel again. As will be demonstrated later the  $\log c$  or  $\log (c_0 - c)$  vs. time curve for this exchanger is partly linear; in Fig. 5 the influence of the

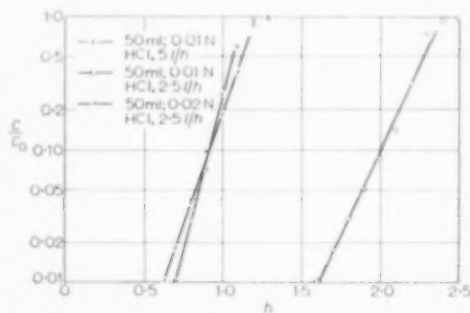


FIG. 5. Kinetic measurements on Permutit ES, plotted on semi-log scale for determining  $k_L$ .

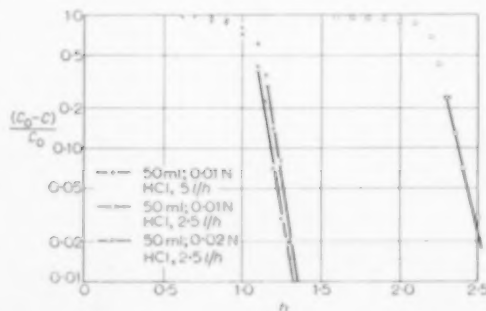


FIG. 6. Kinetic measurement on Permutit ES, plotted on semi-log scale for determining  $k_R$ .

solution concentration on the slope of the straight section is greater than that of the flow rate, whereas in Fig. 6 this effect is not noticeable. It will be shown that film diffusion predominates in Fig. 5 and particle diffusion in Fig. 6.

### 3. DISCUSSION

#### 3.1. Investigation of the stationary character of the curves.

First the question of whether the experimental conditions permitted the formation of a stationary break-through curve will be examined.

The front is stationary, for example, when two break-through curves obtained with different bed depths, but under otherwise identical conditions, run parallel. If  $x_0 < x_r$  (see equation (12), Part I [9]) the difference in time between the two curves then amounts to:

$$t_1 - t_2 = \frac{(x_1 - x_2) \{ a\gamma + S [f(x_0)/x_0] \}}{av} \quad (2)$$

since, according to equation (22), Part IV [7], all concentrations have the same velocity, which is equal to that at instantaneous equilibrium. With  $x_0 > x_r$  ( $x < x_r$ ) the difference becomes:

$$t_1 - t_2 = \frac{(x_1 - x_2) \{ a\gamma + S f'(x_r) \}}{av} \quad (3)$$

The above formulae hold for the  $\text{Na}^+ - \text{H}^+$  exchange on DUSART VKG. In the case of hydrochloric acid adsorption on anion exchangers the following expression is valid:

$$t_1 - t_2 = \frac{(x_1 - x_2) \{ \gamma + S [f(c_0)/c_0] \}}{v} \quad (4)$$

When  $a$  and  $V$  have no effect on the shape of the break-through curve, i.e. in the case of particle diffusion (Part IV [7]), either  $a$  or  $V$  may be varied instead of the bed depth.

The criterion for the stationary character of the measured break-through curve is that the difference in time (which can be determined graphically) at all concentrations be equal to the value found from equation (2), (3) or (4).

Figs. 2, 3 and 4 show that the majority of the experiments were carried out in the stationary region.

With DUSART VKG (Fig. 2) the time difference between the curves for 100 and 200 ml bed volumes (0.01 N sodium chloride ( $x_0 = 1$ ) and 2.5 l/hr flow rate) calculated by means of equation (3) is:

$$t_1' - t_2' = \frac{(x_1 - x_2) S f'(x_r)}{av} \\ = \frac{0.1 \text{ (l)} \times 700 \text{ (mequiv/l)}}{10 \text{ (mequiv/l)} \times 2.5 \text{ (l/hr)}} = 2.8 \text{ hr}$$

The value for  $f'(x_r)$  has been taken from Fig. 4a, Part II [8]. Experiments show (Fig. 2) that the time difference is 2.8 hr with a spread of 1 per cent, the exact value depending on the concentration at which the difference is measured.

With Dowex 3\* (Fig. 3) much longer retention times are required to obtain sharp stationary break-through curves. Moreover they are considerably wider than those required with DUSART VKG and Permutit ES. Using columns of 177 and 88.5 ml bed volume (0.01 N hydrochloric acid and 0.575 l/hr flow rate) the difference in time calculated by means of equation (4) is:

$$t_1' - t_2' = \frac{(x_1 - x_2) S f(c_0)}{c_0 v} \\ = \frac{0.0885 \text{ (l)} \times 2130 \text{ (mequiv/l)}}{10 \text{ (mequiv/l)} \times 0.575 \text{ (l/hr)}} = 32.8 \text{ hr}$$

The difference read from the graph is 32.6 hr with a spread of 0.6 per cent showing that the curves are indeed stationary.

The difference between the curves for 88.5 and 44.3 ml bed volume derived by means of equation (4) is:

$$t_1' - t_2' = \frac{0.0443 \text{ (l)} \times 2130 \text{ (mequiv/l)}}{10 \text{ (mequiv/l)} \times 0.575 \text{ (l/hr)}} = 16.4 \text{ hr}$$

As can be seen from the graph the distance between the curves varies considerably, the average being 14.6 hr with a spread of 7 per cent. It will be clear therefore that the curve for 44.3 ml bed volume is not stationary and is unsuited for further examination.

\*For the curves obtained at 0.575 l/hr flow rate  $S = 2.1 \text{ cm}^2$ .

Permutit ES gives a stationary sharp front rapidly. The time difference between the three curves, obtained at 50, 100 and 200 ml bed volumes (0.01 N hydrochloric acid and 5 l/hr flow rate), are constant. Using equation (4) we find:

$$t_1' - t_2' = \frac{0.1 \text{ (l)} \times 1170 \text{ (mequiv/l)}}{10 \text{ (mequiv/l)} \times 5 \text{ (l/hr)}} = 2.34 \text{ hr}$$

and,

$$t_1' - t_2' = \frac{0.05 \text{ (l)} \times 1170 \text{ (mequiv/l)}}{10 \text{ (mequiv/l)} \times 5 \text{ (l/hr)}} = 1.17 \text{ hr}$$

The differences read from the graph amount to 2.30 hr  $\pm$  1.5 per cent and 1.23 hr  $\pm$  2 per cent respectively.

3.2. *Investigation of the rate of mass transport DUSART VKG (see Fig. 2).* The total ion concentration proves to have an appreciable effect on the shape of the break-through curve, the influence of the flow rate being somewhat less. This dependence of the shape on the variable is characteristic of film diffusion (Part IV [7]). By measuring the slope of the break-through curve and using equation (30) (Part IV [7])  $k_L$  was calculated and the value thus found compared with the one derived from known mass transfer correlations. The following correlations were considered, the first by VAN KREVELEN and KREKELS [10], the second by THOENES [11]:

$$\frac{k_L}{a' D_L} = 0.45 \left( \frac{V \rho}{a' \eta} \right)^{0.5} \left( \frac{\eta}{\rho D_L} \right)^{0.4} \quad (5)$$

$$\frac{\beta k_L d_p}{(1 - \beta) D_L} = 1.0 \left( \frac{V d_p \rho}{(1 - \beta) \eta} \right)^{0.5} \left( \frac{\eta}{\rho D_L} \right)^{0.33} \quad (6)$$

Here  $a'$  = particle area per ml bed volume ( $110 \text{ cm}^2$ ), and

$D_L$  = diffusion coefficient of the  $\text{Na}^+$ -ion (taken at  $1.0 \times 10^{-6} \text{ cm}^2/\text{sec}$  [12]).

The  $k_L$  values calculated by means of equation (30), Part IV [7], (for various equivalent fractions) and equations (5) and (6) are listed in Table 1.

The measured values of  $k_L$  are in good agreement with those found from both equation (5) and (6). Errors of measurement may be due to the following causes:



Table 1. Values of  $k_L$  (Dusarit VKG)

Exchanger volume (ml)	200	200	200	100
Flow rate (l/hr)	2.5	5	2.5	2.5
Initial concentration (N)	0.01	0.01	0.02	0.01
$k_L \times 10^3$ cm/sec	Part IV, equation (30)			
$\alpha = 0.2$	4.8	5.3	3.7	5.6
$\alpha = 0.4$	3.3	4.3	3.4	3.9
$\alpha = 0.6$	3.7	5.3	3.3	3.9
Average	$3.9 \pm 0.6$	$5.0 \pm 0.4$	$3.5 \pm 0.2$	$4.5 \pm 0.8$
According to equation (5)	3.3	4.7	3.3	3.3
According to equation (6)	3.4	4.8	3.4	3.4

A small driving force which consequently cannot be exactly determined.

Non-homogeneous particle size distribution. The impossibility of determining the exact value of  $\beta$ .

In equations (5) and (6) the  $D_L$ -value for sodium chloride was used. According to ADAMSON and GROSSMAN [13] the value of the diffusion coefficient should depend on the relative concentrations and be intermediate between the diffusion coefficients of the participating ions. However, SCHLÖGL and HELFFERICH [14] believe that the effect of the differing ion velocities is counteracted by the formation of a potential gradient in the film layer, which partly represses the effect of the faster ion. The correction suggested by SCHLÖGL and co-workers requires an extra term in Fick's first diffusion law which would render the calculations very complicated. Considering the limited accuracy of our experiments and the relatively small difference between the diffusion coefficients, we believe there is little use in making these corrections; this view is supported by the results published by SELKE *et al.* [15].

Later in Part VI it will be shown that an integration constant  $t'_e$  can be defined by

$$t'_e = \frac{xS}{av} f'(\alpha_e) \quad (7)$$

whose corresponding  $\alpha_e$  value is independent of

the variables. The value of  $t_e$  calculated by means of equation (7) is 2.8 hr for the first three curves of Fig. 2 and 5.6 hr for the fourth.

According to the graph the corresponding value of  $\alpha_e$  is 0.6; however, the curve obtained at a flow rate of 5 l/hr gives a different value. This curve also ought to pass through the intersection of the other two.

Dowex 3 (see Fig. 3)\*. Here again the question arises which mechanism is rate-determining. The fact that the concentration in the inflexion point is relatively low leaves no doubt that particle diffusion will be an important factor. Other workers, having inspected this process (loading of weakly basic anion exchangers with hydrochloric acid solutions) arrived at the same conclusion [16]. A plausible argument can be made however, that particle diffusion need not be the only rate-determining mechanism.

Supposing that both film and particle diffusion play a part, we may write (see equation (1), Part IV [7]):

$$N_A = k_L(c - c_i) = k_R(q_i - q) \quad (8)$$

At first  $c_i$  is either very small or zero (Fig. 10, Part II [8]) and the process may be entirely described as film diffusion. This agrees with the results of batch experiments by KUNIN and MYERS [17] who found that in the early stage of the process the take-up of hydrochloric acid per

\*In all the experiments the particle size of the exchanger was 0.71–0.85 mm.

unit time is directly proportional to  $c$ . Not until a large part of the exchanger surface has been loaded will  $c_i$  adopt a value appreciably larger than zero and will particle diffusion become noticeable.

The values of  $k_L$  and  $k_R$  at 177 ml bed volume (flow rate: 0.575 l/hr; initial concentration: 0.01 N HCl) calculated by means of equations (27), Part IV [7] and (5) ( $D = 2.2 \times 10^{-5}$  cm<sup>2</sup>/sec [12];  $a' = 38.5$  cm<sup>-1</sup>) and equation (25), Part IV [7] respectively have been compiled in Table 2.

As already stated in Part IV a particle diffusion equation as given above is not completely correct. According to GLUECKAUF [18] a better empirical approximation for sharply curved isotherms would be:

$$\left(\frac{\partial q}{\partial t}\right)_s = k_R a' \frac{f^2(c) - q^2}{2q} \quad (9)$$

the best being:

$$\left(\frac{\partial q}{\partial t}\right)_s = k_R a' \frac{(f(c) - q)(3/4 f(c) + 1/4 q)}{q} \quad (10)$$

In both equations

$$k_R a' = \frac{\pi^2 D_R}{r^2} \quad (11)$$

Equation (11) therefore can now be substituted for equation (11), Part IV [7].

The  $k_R$ -values calculated by means of equations (9) and (10) are also given in Table 2.

Table 2 shows that with low effluent concentrations the equation for film diffusion applies whereas at high concentrations the particle diffusion equation is valid. The values obtained

with equations (9) and (10) appear to be more constant than those calculated with equation (25), Part IV [7]; considering that the experiments with this exchanger are well reproducible this conclusion seems permissible.

The value of  $D_R$  derived by means of equations (10) and (11) is  $4.1 \times 10^{-9}$  cm<sup>2</sup>/sec, this being the same value as the one reported by CONWAY *et al.* [19] for the analogous case of neutralization of the weakly basic exchanger Amberlite IRC 50 with sodium hydroxide, viz.  $D_R = 4 \times 10^{-9}$  cm<sup>2</sup>/sec.

To demonstrate whether stationarity of the break-through curve effects the calculated value of the transfer coefficient it should be stated that with  $c = 1$  mequiv/l in the curve for 200 ml bed volume, equation (27), Part IV [7] gives  $k_L = 1.4 \times 10^{-3}$  cm/sec whereas equation (5) yields the much higher value of  $2.8 \times 10^{-3}$  cm/sec.

Strictly speaking, if particle and film diffusion occur side by side, neither of the particle diffusion equations used should be applied since  $q_i \neq f(c)$ . The only way of calculating the  $k_R$  value corresponding with the  $k_L$  value found from equation (5) would then be by trial-and-error; formulating  $k_R$  by means of equation (25), Part IV [7] the driving force may again be determined graphically (see Fig. 7). However, as  $k_R \ll k_L$  the method of calculation used is admissible.

*Permutit ES* (see Figs. 5 and 6). The experiments with Permutit ES proved to be less reproducible than those with Dowex 3. The fairly considerable shrinkage and swelling of the exchanger during loading and regenerating probably plays a part here. It did not seem advisable, therefore, to use a more involved particle diffusion equation than

Table 2. Values of  $k_L$  and  $k_R$  (Dowex 3)

Conc., N · 10 <sup>3</sup>	$k_L \cdot 10^3$ (cm/sec)		$k_R \cdot 10^7$ (cm/sec)		
	Equation (27) Part IV [7]	Equation (5)	Equation (25) Part IV [7]	Equation (9)	Equation (10)
1	1.5	1.4	9.6	2.1	1.5
2	0.95	1.4			
3	0.75	1.4	18	8.7	7.0
4			12	7.9	6.9
5			10	7.8	6.9
6			8.5	7.1	6.6

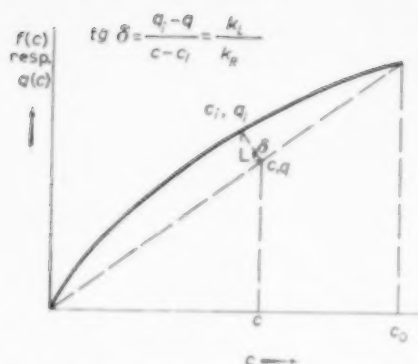


FIG. 7. Driving force in the case of combined film and particle diffusion.

the one suggested in equation (8). From equation (8) and the course of the isotherm it appears that the first part of the process may be described as film diffusion ( $c_i = 0$ ); equation (27), Part IV [7] then becomes:

$$\left(\frac{\partial c}{\partial t}\right)_x = \frac{c_0}{f(c_0)} k_L a' c \quad (12)$$

With  $c_i > 0$ ,  $q_i = f(c_0)$  and the front must satisfy equation (25), Part IV [7].

$$\left(\frac{\partial c}{\partial t}\right)_x = \frac{c_0}{f(c_0)} k_R a' (f(c_0) - q) = k_R a' (c_0 - c) \quad (13)$$

In the former case  $\log c$  is proportional to  $t$  while in the latter case  $\log(c_0 - c)$  is proportional to  $t$ . A few experiments, represented on a logarithmic scale, are shown in Figs. 5 and 6. In the inflexion point of the break-through curve both equations (12) and (13) are applicable and reach their maximum value:

$$\frac{c_0}{f(c_0)} k_L a' c_b = k_R a' (c_0 - c_b) \quad (14)$$

The lines in the figures have been drawn as far as  $c_b$ ;  $k_L$  and  $k_R$  have been derived from the slopes of the lines in Fig. 5 and 6; the  $k_L$  value so found has moreover been compared with  $k_L$  calculated from equation (5) ( $a' = 47 \text{ cm}^{-1}$  and  $D = 2.2 \times 10^{-5} \text{ cm}^2/\text{sec}$  [12]). These values are given in Table 3.

The  $D_R$  calculated from equation (11), Part IV [7] amounts to  $3 \times 10^{-7} \text{ cm}^2/\text{sec}$  this value being approximately equal to that of the self-diffusion

Table 3. Values of  $k_L$  and  $k_R$  (Permutit ES)

Exchanger volume (ml)	50	50	50
Flow rate (l/hr)	5	2.5	2.5
Initial concentration (N)	0.01	0.01	0.02
$k_L$ (Fig. 5) $\times 10^3$ (cm/sec)	4.9 <sup>5</sup>	3.7	3.3 <sup>5</sup>
$k_L$ (equation 5) $\times 10^3$ (cm/sec)	4.5	3.2	3.2
$k_R \times 10^5$ (cm/sec)	10.4	7.1	9.6

coefficient of the  $\text{Cl}^-$  ion in Dowex 2, viz.  $3.54 \times 10^{-7} \text{ cm}^2/\text{sec}$  [20].

### 3.3. Some general conclusions.

It may be observed that the calculated  $k_L$  values agree reasonably with those derived from dimensionless correlations. This supports the view that, in processes where Dumas VKG in the  $\text{H}^+$  form is being loaded with a dilute sodium chloride solution, film diffusion is the rate-determining mechanism. As previously stated the values found for  $D_R$  are of about the same order of magnitude as those determined from similar experiments by other workers. The large difference (factor 100) between the  $D_R$  values for Dowex 3 and Permutit ES remains to be explained; it probably depends on the groups on the exchanger being dissociated or not.

A similar case has been described by VERMEULEN and HUFFMAN [21] who examined the neutralization of Dowex 50 with various amines dissolved in water and in a number of organic solvents. In experiments using the latter the diffusion coefficient was found to decrease with dielectric constant of the solvent, the lowest value being 0.001 of that obtained with the aqueous solution. It may be expected that the degree of dissociation of the exchanger will decrease accordingly.

The comparative measurements by KUNIN and BARRY [22] of the time needed for the  $\text{Ca}^{2+} - \text{Na}^+$  and  $\text{K}^+ - \text{H}^+$  equilibria to become established on weakly acid cation exchangers also furnish an indication that the dissociation of the exchanger plays an important part: the former equilibrium is reached much sooner than the latter.

The difference in  $D_R$  between the two types of anion exchangers may now be qualitatively explained as being due to a difference in the mechanism of particle diffusion. We shall assume to this end that the particle diffusion observed with Permutit ES is a diffusion of hydrochloric

acid through the liquid in the exchanger. Equation (13) then takes the following form:

$$\left(\frac{\partial c}{\partial t}\right)_x = k_R' a' \frac{c_0}{f(c_0)} \Delta c_R \quad (15)$$

where  $c_R$  is the concentration in the gel fluid. From considerations on the Donnan equilibrium it can be derived that  $\Delta c_R$  must be of the order of  $c^2/q$ .

With Permutit ES  $c/q \propto 10^{-2}$  ( $c_0/f(c_0)$ ; see Fig. 10, Part II [8]), in other words (see equations (13) and (15)):

$$k_R' a' \times 10^{-4} c \propto k_R a' (c_0 - c)$$

and, as  $c$  and  $(c_0 - c)$  are of the same order of magnitude,

$$k_R' \times 10^{-4} \propto k_R \quad (16)$$

in analogy to  $k_R a' = 15 D_R/r^2$  (equation (11), Part IV [7]).

We may now write for the diffusion coefficient in the gel liquid:

$$k_R' a' = \frac{15 D_{\text{gel liquid}}}{r^2} \quad (17)$$

and thus:—

$$D_{\text{gel liquid}} \propto 10^4 \times D_R \propto 10^{-3}$$

The  $D_L$ -value thus calculated is 100 times the anticipated  $D$ -value ( $10^{-5}$  cm<sup>2</sup>/sec) showing that the assumed mechanism (diffusion of hydrochloric acid through the fluid in the exchanger) cannot be correct. *This leaves change of position of Cl<sup>-</sup> and OH<sup>-</sup> ions in the well-dissociated exchanger as the only explanation for this rapid transport.*

With Dowex 3 ( $D_R \propto 10^{-9}$ )  $D_{\text{gel fluid}} \propto 10^{-3}$  cm<sup>2</sup>/sec; hence it must be concluded that with this exchanger, which contains practically undissociated amine groups, the normal diffusion of hydrochloric acid through the exchanger fluid is rate-determining.

It will also be clear now why the modified method of determining the equilibrium on Dowex 3 rapidly led to equilibrium conditions (Part II [8]); first, the exchanger was loaded at a high concentration, in consequence the concentration in the gel fluid was also high, causing loading to proceed rapidly.

#### NOTATION

$a$ = total ion concentration in solution	ML <sup>-3</sup>
$a'$ = particle area per unit bed volume	L <sup>-1</sup>
$c$ = concentration in the fluid	ML <sup>-3</sup>
$D$ = diffusion coefficient	L <sup>2</sup> T <sup>-1</sup>
$d_p$ = particle diameter	L
$f(c)$ = concentration in adsorbent at equilibrium	ML <sup>-3</sup>
$k_L$ = coefficient of mass transfer in liquid film	LT <sup>-1</sup>
$k_R$ = coefficient of mass transfer in exchanger	LT <sup>-1</sup>
$k_R'$ = for definition see equation (15)	LT <sup>-1</sup>
$N_A$ = number of ions transported per unit time and per unit particle area	MT <sup>-1</sup> L <sup>-2</sup>
$q$ = concentration in adsorbent	ML <sup>-3</sup>
$r$ = particle radius	L
$S$ = cross-sectional area of the column	L <sup>2</sup>
$t$ = time	T
$t' = t - l_y/v$ = reduced time	T
$V$ = linear velocity	LT <sup>-1</sup>
$v$ = rate of flow	L <sup>3</sup> T <sup>-1</sup>
$x$ = distance to the point where the fluid enters the column	L
$z$ = equivalent fraction of a given ion in solution	
$c_{\text{Na}^+}/z$	
$\beta$ = fractional free space	
$\gamma$ = free space per unit length in column	L <sup>2</sup>
$\eta$ = viscosity	ML <sup>-1</sup> T <sup>-1</sup>
$\rho$ = density	ML <sup>-3</sup>

#### Indices

$b$ = inflexion point
$e$ = integration constant
$i$ = exchanger interface
$L$ = liquid
$R$ = exchanger
$r$ = tangent point (see Part I [9])
$0$ = condition before the liquid enters the column

#### REFERENCES

- [1] BADDOUR R. F. and GILLILAND E. R. *Industr. Engng. Chem. (Industr.)* 1953 **45** 330.
- [2] MICHAELS A. S. *Industr. Engng. Chem. (Industr.)* 1954 **44** 1922.
- [3] HALL R. A. J. *Sci. Instrum.* 1955 **32** 116.
- [4] GLUECKAUF E. and COATES J. J. *J. Chem. Soc.* 1947 1315.
- [5] BADDOUR R. F., GOLDSTEIN D. J. and EPSTEIN P. *Industr. Engng. Chem. (Industr.)* 1954 **46** 2192.
- [6] BYRNE E. B. and LAPIDUS L. *J. Amer. Chem. Soc.* 1955 **77** 6506.

# Studies on ion exchange—V

- [7] KLAMER K., VAN HEERDEN C. and VAN KREVELEN D. W. *Chem. Engng. Sci.* 1958 **9** 1.
- [8] KLAMER K., LINSEN J. C. H. and VAN KREVELEN D. W. *Chem. Engng. Sci.* 1958 **7** 204.
- [9] KLAMER K. and VAN KREVELEN D. W. *Chem. Engng. Sci.* 1958 **7** 197.
- [10] VAN KREVELEN D. W. and KREKELS J. T. C. *Rec. Trav. Chim. Pay-Bas* 1948 **67** 512.
- [11] THOENES D. *Stofoverdracht in een vast bed* Diss., Delft, 1957.
- [12] HODGMAN C. D. *Handbook of Chemistry and Physics* Chemical Rubber Publishing Co., 1948.
- [13] ADAMSON A. W. and GROSSMAN J. J. *J. Chem. Phys.* 1949 **17** 1002.
- [14] SCHLÖGL R. and HELFFERICH F. *J. Chem. Phys.* 1957 **26** 5.
- [15] SELKE W. A., BARD Y., PASTERNAK A. D. and ADITYA S. K. *J. Amer. Inst. Chem. Engrs.* 1956 **2** 468.
- [16] BAUMAN W. C. *Ion Exchange* (Edited by F. C. NACHOD) p. 73. Academic Press, New York 1949.
- [17] KUNIN R. and MYERS R. J. *J. Phys. Chem.* 1947 **51** 1111.
- [18] GLUECKAUF E. *Trans. Faraday Soc.* 1955 **51** 1540.
- [19] CONWAY D. E., GREEN J. H. S. and REICHENBERG D. *Trans. Faraday Soc.* 1954 **50** 521.
- [20] SOLDANO B. A. and BOYD G. E. *J. Amer. Chem. Soc.* 1953 **75** 6099.
- [21] VERMEULEN T. and HUFFMAN E. H. *Ind. Engng. Chem. (Industr.)* 1953 **45** 1658.
- [22] KUNIN R. and BARRY R. E. *Ind. Engng. Chem. (Industr.)* 1949 **41** 1269.



## Studies on ion exchange—VI

### Design and scaling up of ion exchange columns

K. KLAMER and D. W. VAN KREVELEN

Central Laboratory, Staatsmijnen, in Limburg, Geleen, Netherlands

(Received 17 January 1958)

**Abstract**—This final article in our series on the characterization of ion exchangers deals with the design of columns. A comparison between calculated and measured break-through curves is given.

For those processes in which film diffusion is the rate-determining step the correspondence between these two types of curves proves to be very close. In the case of particle diffusion the agreement is less good, although still reasonable if allowance is made for the simplifying assumption used in the calculations.

In the treatment of the scaling-up problem a formula for the kinetic break-through capacity is derived. It is shown in what way laboratory tests have to be carried out if they are to yield results applicable to the design of industrial filters.

**Résumé**—Ce dernier article de cette série sur la caractérisation des échangeurs d'ions se rapporte au calcul des colonnes. Des courbes de traversée calculées sont comparées à celles mesurées.

Pour les processus où la diffusion à travers le film extérieur est déterminante pour la vitesse, la concordance entre ces deux types de courbe s'avère très nette. En cas de diffusion à l'intérieur des grains, la concordance est moins bonne, tout en étant assez raisonnable, vu la supposition simplificatrice pour les calculs.

En traitant le problème de l'agrandissement on dérive une formule pour la capacité de traversée cinétique. On montre de quelle manière les essais de laboratoire devront être effectués si l'on veut obtenir des résultats applicables au calcul des colonnes (filtres) tels qu'utilisés dans l'industrie.

**Zusammenfassung**—Dieser abschliessende Aufsatz in unserer Reihe über die Charakterisierung von Ionen-Austauschern beschäftigt sich mit der Berechnung von Kolonnen. Berechnete und gemessene Durchbruchkurven werden verglichen.

Für Prozesse, bei denen die Filmdiffusion geschwindigkeitsbestimmend ist, gibt es eine sehr gute Übereinstimmung zwischen diesen beiden Kurventypen. Im Falle der Teilchendiffusion ist die Übereinstimmung weniger gut, aber noch befriedigend im Hinblick auf die vereinfachende Annahme in der Berechnung.

Zur Frage der Massstabsvergrößerung wurde eine Gleichung für die kinetische Durchbruchkapazität abgeleitet. Es wird gezeigt, in welcher Weise Laboratoriumsversuche auszuführen sind, um brauchbare Unterlagen für die Berechnung industrieller Kolonnen abzugeben.

In the previous articles it has been shown how it is possible in the case of a stationary sharp front to determine both the driving force (graphically) and the coefficient of mass transfer (Parts IV [1] and V [2]).

The object of this final article is threefold:—

(1) To give a discussion of the design of ion exchange columns and of the calculation of

break-through curves on the basis of the data available.

(2) To compare the calculated with the measured break-through curves.

(3) To establish some generally applicable scaling-up rules.

It is assumed that piston flow occurs. The possibility of a spread in residence times of the

VOL.  
9  
58/59

Table 1. Summary of formulae for the graphic integration

Case		Adsorptive percolation	
		Film diffusion	
$\left(\frac{\partial q}{\partial t}\right)_x$ for stationary front  (equations (1) and (6))	$f'' < 0$	$\left(\frac{\partial c}{\partial t}\right)_x = \frac{c_0}{f(c_0)} k_L a' (c - c_{eq})$	$\left(\frac{\partial c}{\partial t}\right)_x$
	$f'' > 0$	$\left(\frac{\partial c}{\partial t}\right)_x = \frac{1}{f(c_r)} k_L a' (c - c_{eq})$	$\left(\frac{\partial c}{\partial t}\right)_x$
$\left(\frac{\partial q}{\partial t}\right)_x$ integrated  (equations (5) and (10))	$f'' < 0$	$\int_{c_e}^c \frac{dc}{c - c_{eq}} = \frac{c_0}{f(c_0)} k_L a' (t - t_e)$	$\int_{c_e}^c \frac{dc}{f(c)}$
	$f'' > 0$	$\int_{c_e}^c \frac{dc}{c - c_{eq}} = \frac{1}{f(c_r)} k_L a' (t - t_e)$	$\int_{c_e}^c \frac{dc}{f(c)}$
integration constants at $f'' < 0$	time (equation (2))	$t_e = \left\{ t_f + \frac{1}{k_L} \frac{f(c_0)}{c_0} \right\} / v$	
	concentration or equivalent fraction (equation (4))	$\int_0^{c_e} \frac{cdc}{c - c_{eq}} = \int_{c_e}^{c_0} \frac{(c_0 - c) dc}{c - c_{eq}}$	$\int_0^{c_e} \frac{cdc}{f(c)}$
integration constants at $f'' > 0$	time (equation (7))	$t_e = \{ t_f + \frac{1}{k_L} f'(c_r) \} / v$	
	concentration or equivalent fraction (equation (8))	$\int_0^{c_e} \frac{cdc}{c - c_{eq}} = \int_{c_e}^{c_r} \frac{(c_r - c) dc}{c - c_{eq}}$	$\int_0^{c_e} \frac{cdc}{f(c)}$

tion of  $\left(\frac{\partial q}{\partial t}\right)_x = F(c, q)$  in the case of a stationary sharp front

Particle diffusion	Ion exchange	
	Film diffusion	Particle diffusion
$\left(\frac{\partial c}{\partial t}\right)_x = \frac{v_0}{f(c_0)} k_R a' (f(c) - q)$	$\left(\frac{\partial x}{\partial t}\right)_x = \frac{x_0}{f(x_0)} k_L a' a (x - x_{eq})$	$\left(\frac{\partial x}{\partial t}\right)_x = \frac{x_0}{f(x_0)} k_R a' (f(x) - q)$
$\left(\frac{\partial c}{\partial t}\right)_x = \frac{1}{f(c_r)} k_R a' (f(c) - q)$	$\left(\frac{\partial x}{\partial t}\right)_x = \frac{1}{f(x_r)} k_L a' a (x - x_{eq})$	$\left(\frac{\partial x}{\partial t}\right)_x = \frac{1}{f(x_r)} k_R a' (f(x) - q)$
$\frac{dc}{f(c) - q} = \frac{v_0}{f(c_0)} k_R a' (t - t_e)$	$\int_{x_e}^x \frac{dx}{x - x_{eq}} = \frac{x_0}{f(x_0)} k_L a' a (t - t_e)$	$\int_{x_e}^x \frac{dx}{f(x) - q} = \frac{x_0}{f(x_0)} k_R a' (t - t_e)$
$\frac{dc}{f(c) - q} = \frac{1}{f(c_r)} k_R a' (t - t_e)$	$\int_{x_e}^x \frac{dx}{x - x_{eq}} = \frac{1}{f(x_r)} k_L a' a (t - t_e)$	$\int_{x_e}^x \frac{dx}{f(x) - q} = \frac{1}{f(x_r)} k_R a' (t - t_e)$
$\frac{1}{v}$	$t_e = \left\{ a l \gamma + b S \frac{f(x_0)}{x_0} \right\} / a v$	
$\int_0^{x_e} \frac{c dx}{f(c) - q} = \int_{c_e}^{c_0} \frac{(c_0 - c) dc}{f(c) - q}$	$\int_0^{x_e} \frac{x dx}{x - x_{eq}} = \int_{x_e}^{x_0} \frac{(x_0 - x) dx}{x - x_{eq}}$	$\int_0^{x_e} \frac{x dx}{f(x) - q} = \int_{x_e}^{x_0} \frac{(x_0 - x) dx}{f(x) - q}$
$\frac{1}{v}$	$t_e = \{ a l \gamma + b S f'(x_r) \} / a v$	
$\int_0^{x_e} \frac{c dx}{f(c) - q} = \int_{c_e}^{c_r} \frac{(c_0 - c) dc}{f(c) - q}$	$\int_0^{x_e} \frac{x dx}{x - x_{eq}} = \int_{x_e}^{x_r} \frac{(x_0 - x) dx}{x - x_{eq}}$	$\int_0^{x_e} \frac{x dx}{f(x) - q} = \int_{x_e}^{x_r} \frac{(x_0 - x) dx}{f(x) - q}$

VOL  
9  
1958/



liquid in the column owing to channelling has not been included in these considerations because phenomena of this type do not lend themselves to quantitative calculations.

### 1. DESIGN OF ION EXCHANGE COLUMNS

In the case of isotherms with a negative curvature a stationary front will eventually be established; also if the isotherm shows an inflexion point, part of the front will eventually become stationary. These two cases will be dealt with in the order in which they are mentioned here.

(a) *The isotherm has a negative curvature ( $f''(c) < 0$ ).*

In this case the slope of a stationary break-through curve (cf. equation (24), Part IV [1]), is described by

$$\left(\frac{\partial c}{\partial t}\right)_t = \frac{c_0}{f(c_0)} F(c) \quad (1)$$

For the integration of this equation we choose  $c_e$  and  $t_e$  as limits;  $t_e$  is defined by:—

$$t_e = \left( l\gamma + lS \frac{f(c_0)}{c_0} \right) / v \quad (2)$$

This is the time at which—in the case of instantaneous establishment of equilibrium—the

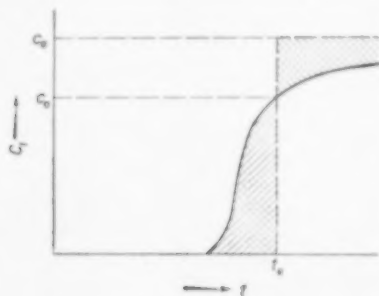


Fig. 1. Stationary sharp front.

discontinuous concentration jump takes place (cf. equation (4), Part I [3]).

The value of  $c_e$  can now be calculated in the following way:—

Assume the break-through curve to have the shape shown in Fig. 1. The two hatched areas must be equal:—

$$\int_0^{t_e} c dt = \int_{c_e}^{c_0} (c_0 - c) dc \quad (3)$$

Substituting  $dt$  from equation (1) in equation (3), we get

$$\int_0^{t_e} \frac{cdc}{F(c)} = \int_{c_e}^{c_0} \frac{(c_0 - c) dc}{F(c)} \quad (4)$$

Both integrals can be calculated as functions of  $c$  by graphic integration of  $c/F(c)$  and  $(c_0 - c)/F(c)$ , respectively.

If the values of these integrals are plotted as functions of  $c_e$  the point of intersection of the resulting curves gives the correct value of  $c_e$ . Integration of equation (1) consequently leads to:

$$\int_{c_e}^{c_0} \frac{dc}{F(c)} = \frac{c_0}{f(c_0)} (t - t_e) \quad (5)$$

From equation (5) the break-through curve may be calculated. Starting from the point  $(c_e, t_e)$ , which is now known, the  $c$  corresponding to every  $t$  can be found by graphic integration of  $1/F(c)$ .

One of the specifications to which a column is designed is a certain concentration in the effluent,  $c_D$ , which may not be reached before a time  $t_D$ , in which  $v_D t_D$  volumes have passed through, has elapsed. Substitution of  $c_D$  and  $t_D$  in equation (5) gives the value of  $t_e$ . The volume of the exchanger,  $lS$ , can simply be calculated from equation (2), provided  $l\gamma/v$  is negligible, which is generally the case. At any rate equation (2) gives a relation between  $l$  and  $S$ .

The forms assumed by equations (1), (4) and (5) in dependence of  $F(c)$  (film or particle diffusion) are shown in Table 1.

(b) *The isotherm shows an inflexion point ( $f''(c) > 0$ ).*

The slope of the break-through curve is now described not by equation (1) but by

$$\left(\frac{\partial c}{\partial t}\right)_t = \frac{1}{f'(c_t)} F(c) \quad (6)$$

while the integration constant  $t_e$  is defined by

$$t_e = \{l \gamma + l S f'(c_r)\} / v \quad (7)$$

and  $c_e$  by

$$\int_0^{c_e} \frac{c dc}{F(c)} = \int_{c_r}^{c_D} \frac{c_D - c}{F(c)} dc \quad (8)$$

Equation (8) can be derived by means of Fig. 2.

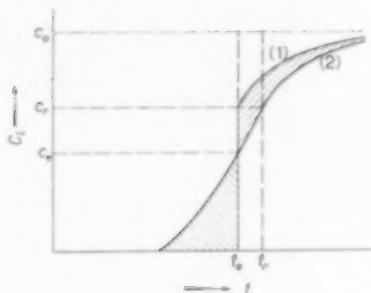


FIG. 2. Equilibrium curve and kinetic break-through curve for an isotherm showing an inflexion point.

Curve (1) represents the break-through curve in the case of an instantaneous establishment of equilibrium, and curve (2) is the stationary break-through curve for the case when  $0 < c < c_r$ . It may be assumed that if  $c > c_r$ , these concentrations travel at the same rate as they do if there is instantaneous establishment of equilibrium. It then follows that if  $c > c_r$  the curves (1) and (2) are parallel and that the area between these curves is equal to the area of the rectangle  $(c_r, t_e) (c_r, t_r) (t_r, c_D) (t_e, c_D)$ . The hatched areas in the figure must then be equal, i.e. :—

$$\int_0^{t_e} c dt = \int_{t_e}^{t_r} (c_1 - c_2) dt = \int_{t_r}^{t_D} (c_D - c_2) dt \quad (9)$$

from which follows — after substitution of  $dt$  from equation (6) in equation (9) — the equation (8).

By the same procedure as described under (a) the determination of  $c_e$  is now carried out.

Integration of equation (6) produces :—

$$\int_{c_e}^c \frac{dc}{F(c)} = \frac{1}{f'(c_r)} (t - t_e) \quad (10)$$

Using equation (10) we can design a column or calculate a break-through curve in the way described in (a) provided that in the effluent  $0 < c_D < c_r$ .

The forms assumed by equations (6), (8) and (10) for film and particle diffusion are shown in Table 1.

The above formulae apply to chromatography in general. For ion exchange analogous equations may be used. A summary of all the formulae is given in the Table.

## 2. COMPARISON OF MEASURED AND CALCULATED BREAK-THROUGH CURVES

An idea of the accuracy of column design may be gained by means of a comparison of calculated and measured break-through curves. In this section some practical cases will be discussed.

### (a) Dusarit VKG

Figure 3 shows the calculated and measured break-through curves for the polyfunctional cation exchanger Dusarit VKG in the  $H^+$  form, loaded with sodium chloride solution.

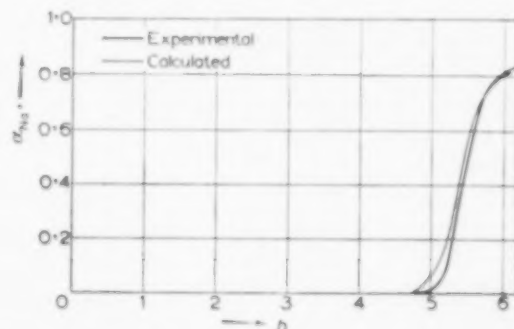


FIG. 3. Calculated and measured stationary break-through curves for Dusarit VKG.

Data : amount of ion exchanger : 200 ml, concentration of sodium chloride : 0.01 N ( $\alpha_0 = 1$ ), space velocity : 2.5 l. per hr, cross-sectional area of column : 4.5 cm<sup>2</sup>, specific surface area : 110 cm<sup>2</sup>, equilibrium curve : cf. Part II [4], mechanism : film diffusion, so that

$$\left( \frac{\partial \alpha}{\partial t} \right)_x = \frac{\alpha_0}{f(\alpha_0)} k_L a' a (\alpha - \alpha_{eq}) \quad (11)$$

$$k_L = 3.0 \times 10^{-3} \text{ cm/sec} \quad (\text{calculated by equation (10)})$$

$$\alpha_e = 0.65 \quad (\text{calculated by means of the equation})$$

$$\int_0^{\alpha_e} \frac{\alpha d\alpha}{\alpha - \alpha_{eq}} = \int_{\alpha_e}^{\alpha_0} \frac{(\alpha_0 - \alpha) d\alpha}{\alpha - \alpha_{eq}} \quad (12)$$

$$t_e = 3.6 h \text{ (calculated by the equation } t_e = \{a l \gamma + l S f'(\alpha_r)/av\}) \quad (13)$$

The agreement between the calculated and the measured break-through curve (as shown in Fig. 3) may be called very good.

(b) *Dowex 3*

Figure 4 shows the calculated and the measured break-through curve for the regenerated weak basic exchanger Dowex 3 loaded with a solution of hydrochloric acid.

As shown previously (Part V [2]), the mechanism of the process in this case depends mainly on

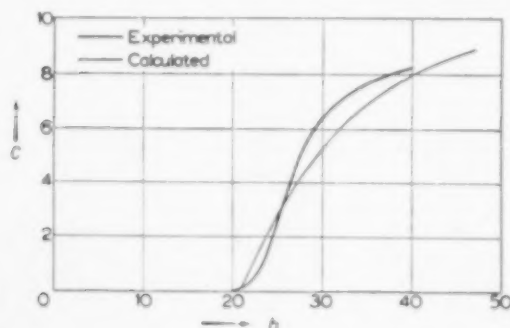


Fig. 4. Calculated and measured stationary break-through curves for Dowex 3.

particle diffusion. In order not to make our calculations too complicated, we shall use the simple equation for particle diffusion, in spite of the fact that at low concentrations the influence of film diffusion is clearly perceptible.

$$\left(\frac{\partial c}{\partial t}\right)_x = \frac{c_0}{f(c_0)} k_R a' (f(c) - q) \quad (14)$$

Data: amount of ion exchanger used: 88.5 ml concentration of hydrochloric acid: 0.01 N, space velocity: 0.575 l. per hr, cross-sectional area of column: 2.1 cm<sup>2</sup>, specific surface area: 38.5 cm<sup>-1</sup>, equilibrium curve: cf. Part II [4]

$$k_R: 6.0 \cdot 10^{-7} \text{ cm/sec}$$

$$c_e: 6.3 \text{ m. eq./l.}$$

(calculated by means of equation (4))

$$t_e: 32.8 \text{ hr (calculated by equation (2))}$$

The agreement between the calculated and the measured break-through curve (Fig. 4) is not as close as in the previous case. This is due to the neglect of the film diffusion and more especially

to the use of a very simple formula for the particle diffusion.

### 3. THE SCALING-UP PROBLEM

Finally we shall consider the scaling up of laboratory columns to large-scale plant apparatus.

Especially the break-through capacity will be considered. The kinetic break-through capacity  $\psi_v(x_D)$  is the number of milli-equivalents of a given ion taken up per litre of exchanger until the moment when a certain (low) concentration  $x_D a$  of the ion is observed in the effluent; it is defined by:—

$$\psi_v(x_D) = \frac{x_0 a v}{l S} \left( t_D - \frac{l \gamma}{v} \right) \quad (15)$$

From a technical point of view only the break-through capacity on loading is of interest. Technical loading is carried out nearly exclusively in the case of isotherms having a negative curvature. If the break-through curve is stationary,  $\psi_v$  is to be written — after substitution of equation (15) in the pertinent formulae of the Table — as:—

$$\int_{x_e}^{x_D} \frac{dx}{x - x_{eq}} = \frac{k_L a' l S}{f(x_0) v} \{ \psi_v(x_D) - f(x_0) \} \quad (16)$$

and

$$\int_{x_e}^{x_D} \frac{dx}{f(x) - q} = \frac{k_R a' l S}{f(x_0) a v} \{ \psi_v(x_D) - f(x_0) \} \quad (17)$$

In the case of particle diffusion as a rate determining factor a technical-scale filter will give the same result as a laboratory filter, provided the group:—

$$a' l S / a v = a' l / a V \quad (18)$$

is the same for the two columns. It is essential that in the laboratory experiment the break-through curve is stationary.

Bearing in mind that the integral in equation (17) has a negative value, we see from this equation that the break-through capacity decreases in proportion to the increase of the concentration in solution and of the space velocity (number of unit volumes of liquid transferred per unit time and per unit volume of exchanger,  $v/lS$ ).

McGARVEY and THOMPSON [5] found this relation to apply to the break-through capacity of Amberlite IRC 50 in the case of calcium bicarbonate solutions. We may,

therefore, conclude that in this process *particle diffusion* is the rate-determining step.

With *film diffusion* as a rate determining factor the matter is different. We may assume that for Reynolds numbers below 10 :—

$$\frac{k_L}{a' D} = 0.45 \left( \frac{V \rho}{a' \eta} \right)^{0.5} \left( \frac{\eta}{\rho D} \right)^{0.4} \quad (19)$$

and hence

$$k_L = \epsilon_1 \cdot V^{1/2} \cdot a'^{1/2} \quad (20)$$

If the Reynolds number is greater than 50 we get [6]

$$\frac{k_L}{a' D} = 0.15 \left( \frac{V \rho}{a' \eta} \right)^{0.8} \left( \frac{\eta}{\rho D} \right)^{0.4} \quad (21)$$

so that

$$k_L = \epsilon_2 \cdot V^{0.8} \cdot a'^{0.2} \quad (22)$$

Similarity may be expected in the case of film diffusion for  $Re < 10$  if

$$a'^{1.5} \cdot l \cdot V^{0.5} = \text{constant} \quad (23)$$

and for  $Re > 50$  if

$$a'^{1.2} \cdot l \cdot V^{0.2} = \text{constant} \quad (24)$$

Not only from the point of view of loading (break-through capacity), but also with regard to regeneration (percentage of exchanger regenerated and regeneration efficiency) the scaling up problem is interesting.

Naturally, we are here concerned with a case in which the isotherm has a positive curvature. Mathematically, the kinetics here present a very difficult problem. It may be recalled however that in various instances (cf. Part IV [1]), the  $c_f(t)$  curve of the effluent was found to look as if instantaneous establishment of equilibrium had

taken place in the column. Therefore, it is generally permissible in dealing with these cases to use the equilibrium methods described earlier (Part III [7]).

#### NOTATION

$a$ = total ion concentration in solution	$ML^{-3}$
$a'$ = particle surface area per unit of bed volume	$L^{-1}$
$c$ = concentration in the liquid	$ML^{-3}$
$D$ = diffusion coefficient	$L^2 T^{-1}$
$F(c)$ = as defined by equation (1)	$ML^{-3} T^{-1}$
$f(c)$ = concentration in the adsorbent at equilibrium	$ML^{-3}$
$f(x)$ = concentration in the ion exchanger at equilibrium	$ML^{-3}$
$k_R$ = coefficient of mass transfer in the particle	$LT^{-1}$
$k_L$ = coefficient of mass transfer in the liquid film	$LT^{-1}$
$l$ = length of column	$L$
$q$ = concentration in the adsorbent	$ML^{-3}$
$S$ = cross-sectional area of column	$L^2$
$t$ = time	$T$
$V$ = linear velocity of liquid	$LT^{-1}$
$v$ = rate of flow of liquid	$L^3 T^{-1}$
$x$ = distance to the point where the liquid enters the column	$L$
$\alpha$ = equivalent fraction of a given ion in solution = $c_{Na^+}/a$	
$\gamma$ = free space per unit length in the column	$L^2$
$\eta$ = viscosity	$ML^{-1} T^{-1}$
$\rho$ = density	$ML^{-3}$
$\psi_c(z_D)$ = kinetic break-through capacity	$ML^{-3}$

#### Indices

$D$ = break-through
$e$ = discontinuous break-through
$eq$ = equilibrium
$r$ = tangent point
$0$ = condition before the liquid enters the column

#### REFERENCES

- [1] KLAMER K., VAN HEERDEN C. and VAN KREVELEN D. W. Part IV, *Chem. Engng. Sci.* 1958 9 1.
- [2] KLAMER K., LINSSSEN J. CHR. H. and VAN KREVELEN D. W. Part V, *Chem. Engng. Sci.* 1958 9 10.
- [3] KLAMER K. and VAN KREVELEN D. W. Part I, *Chem. Engng. Sci.* 1958 7 197.
- [4] KLAMER K., LINSSSEN J. CHR. H. and VAN KREVELEN D. W. Part II, *Chem. Engng. Sci.* 1958 7 204.
- [5] MCGARVEY F. X. and THOMSON J. *Ind. Engng. Chem.* 1951 43 741.
- [6] VAN KREVELEN D. W. and KREKELS J. TH. C. *Rec. Trav. Chim.* 1948 67 512.
- [7] KLAMER K. and VAN KREVELEN D. W. Part III, *Chem. Engng. Sci.* 1958 8 216.

## Perforated-plate performance

R. A. McALLISTER\*, P. H. McGINNIS, JR. and C. A. PLANK†

North Carolina State College, Raleigh, N.C.

(Received 2 August 1957)

**Abstract**—The effect of the ratio of plate thickness,  $T$ , to hole diameter,  $D_h$ , on dry-plate pressure drop has been correlated over a wide range of column size, hole area, and Reynolds number through the holes. New data are presented showing the effect of  $T/D_h$  on the wet-plate pressure-drop characteristics (for the air-water system) of perforated plates in a 15-in. diameter column having a tray spacing of 18 in. An oscillating region, where the aerated liquid mass on the tray moves back and forth perpendicularly to the direction of liquid flow, is reported. The mass flow rate of gas at which oscillation begins (the oscillation point) has been correlated with the height of clear liquid on the operating tray. In every case the oscillation point occurred well before flooding. The data presented here agree with the weepage correlation of HUGHMARK and O'CONNELL [1].

**Résumé**—L'effet du rapport épaisseur du plateau,  $T$ , au diamètre du trou,  $D_h$ , a été relié à la chute de pression à travers chaque plateau sec dans un champ étendu de dimension de colonne, de surface de trou, et de nombre de Reynolds à travers les trous. Pour une colonne aux plateaux mouillés (système air-eau) les nouveaux résultats présentés montrent l'effet du rapport  $T/D_h$  sur la chute de pression à travers chaque plateau. La colonne utilisée avait 15 pouces de diamètre et les plateaux perforés étaient séparés par une distance de 18 pouces. Il a été montré que dans une certaine région le liquide ventilé sur les plateaux vibrait perpendiculairement à la direction de flux. Le flux massique de gaz pour lequel les oscillations commencent (le point d'oscillation) a été relié à la hauteur de clair liquide sur le plateau opérant. Dans tous les cas le point d'oscillation apparaît bien avant que le plateau soit submergé. Les résultats présentés ici sont en accord avec corrélation de HUGHMARK et O'CONNELL [1] qui permet de déterminer le flux de gaz pour lequel le liquide est retenu sur les plateaux.

**Zusammenfassung**—Die Wirkung des Quotienten aus Plattendicke  $T$  zu Lochdurchmesser  $D_h$  wurde in Beziehung zum Druckabfall der trockenen Platte innerhalb eines weiten Bereiches der Kolonnengrösse, der Lochfläche und der Reynoldszahl in den Löchern. Für eine Kolonne von 38 cm Durchmesser mit perforierten Platten bei 46 cm Bodenabstand werden neue Werte mitgeteilt, die den Einfluss von  $T/D_h$  auf den Druckabfall der benetzten Platte beim System Luft-Wasser zeigen. Es wurde gefunden, dass in einem bestimmten Bereich die belüftete Flüssigkeitsmasse auf dem Boden senkrecht zur Strömungsrichtung ins Schwingen gerät. Der Massenstrom des Gases, bei dem die Schwingung beginnt (der Schwingungspunkt), wurde in Beziehung gesetzt zu der Flüssigkeitshöhe über dem arbeitenden Boden. In allen Fällen wurde der Schwingungspunkt vor dem Fluten erreicht. Die hier mitgeteilten Daten stimmen mit der Beziehung von Hughmark und O'Connell [1] überein, mit der sich jener Gasstrom berechnen lässt, bei dem die Flüssigkeit auf dem Boden zurückgehalten wird (weep point).

THE number of technical papers appearing in the last decade or so [1-20] concerned with perforated-plate column performance is indicative of a lively interest in this type of counter-current liquid-vapour contactor. The investigations have shown that in addition to stable operation, these plates

have many distinct advantages over conventional bubble-cap plates. They are easy to fabricate and are more economical than bubble-cap plates. MAYFIELD, CHURCH, GREEN, LEE and RASMUSSEN [16] and JONES and PYLE [8] found that perforated-plate efficiencies were greater than those for

\*Present address : Lamar State College of Technology, Beaumont, Texas.

†Present address : University of Louisville, Louisville, Ky.



bubble-cap plates under similar conditions. KELLY [13] and ZENZ [20] indicated that perforated-plate columns had greater capacities than those containing bubble caps. In addition, hydraulic gradient [6, 16], entrainment [8, 12], and pressure-drop [8] characteristics for sieve plates are, in general, superior to those for bubble-cap plates.

The purpose of the work reported here was to obtain new operating data with special attention focused on the effect of the plate thickness to hole diameter ratio ( $T/D_h$ ), and on the oscillating region reported by McALLISTER and PLANK [17].

The dry-plate pressure drop using plates having various values of  $T/D_h$  was first studied extensively by KAMEI *et al.* [10, 11]. Their results, and those of other investigators, indicate that for a given plate thickness, free space, and mass flow rate of air, as the hole diameter is decreased the pressure drop decreases until a value of  $T/D_h \approx 2.3$  is reached. Further decrease of the hole diameter (increase in the value of  $T/D_h$ ) causes the pressure drop to increase.

It is shown in this paper that the increased dry-plate pressure drop for values of  $T/D_h > 2.3$  results from hole friction and can be calculated accurately using the usual Fanning friction factor for smooth pipes [22]. Below  $T/D_h = 2.0$  the friction term becomes negligible and the pressure drop is a function primarily of the contraction and expansion losses when the gas passes through the holes as indicated by HUNT, HANSON and WILKE [5]. All available dry-plate data ( $T/D_h$  ranging from 0.08 to 7.9) including the additional results presented here [ $T/D_h$  ranging from 0.116 to 5.333] correlate well.

Studies of pressure drop as a function of vapour rate indicate several regions displaying different types of operation. The three types of curves encountered in this work are shown in Fig. 1. The curve of Type I, Fig. 1, is that for the dry-plate runs. No liquid was flowing in the column, and the pressure drop versus flow rate curve was linear on log-log graph paper, and had a slope of approximately 2.0.

By far the most common type of curve with liquid running in the column is labelled Type III in Fig. 1. The column behaviour with this type

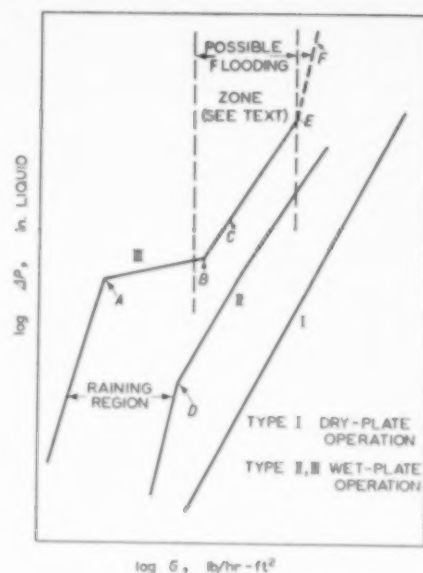


FIG. 1. Characteristic operating curves for perforated plates.

of curve is discussed in detail by ARNOLD, PLANK and SCHOENBORN [2], and may be described briefly as follows. Below point A the liquid drains freely through the plates—the liquid “rains.” Above point A, bubbling of gas through the liquid occurs at some of the perforations. At other perforations the liquid “weeps” through the holes. Point B is called the weep point. At point B, all the holes are bubbling, and above this point has been considered to be the normal operating region of sieve-tray columns.

The curve shown as Type II generally occurs only at low liquid rates (less than 350 lb. liquid/hr ft<sup>2</sup> of column) and then only with certain plates. In the work reported here only Insert IV, operating at a liquid mass flow rate of 350 lb/hr ft<sup>2</sup>, showed a curve of Type II. ARNOLD *et al.* [2] reported data from a different plate (with 0.376-in. holes, 11.5 per cent free space, 0.029-in. plate thickness, 270 lb/hr ft<sup>2</sup> liquid flow rate) which operated in this manner. Below point D, Curve II, Fig. 1, liquid is draining through the perforations in the plate and no bubbling occurs. At point D, which might be called a weep point, the gas flow begins to support liquid on the tray and bubbling begins in some of the perforations.



The other perforations sometimes weep and sometimes bubble. At still higher gas rates, weeping appears visually to stop. However, there is no break in the performance curve. One other observation over the range of gas flow rates noted here, and by ARNOLD *et al.* [2], was that oscillation never occurred with a system having a Type II performance curve.

The oscillation behaviour in perforated-plate columns was described first by PLANK [21], and more recently by McALLISTER and PLANK [17]. The latter showed that the effect of the oscillation increased the plate efficiency, since it decreased back-mixing on the tray. However, indications are that a detrimental effect may result due to possible flooding in the oscillating region. This latter effect is discussed more fully below. When oscillation occurs the whole liquid and frothing mass on the tray moves back and forth perpendicularly to the direction of flow of liquid. That is, if the net liquid flow is from left to right, the surging is established from front to back.

For plates and liquid flow rates having performance curves of Type III, oscillation either began at point *B*, or at a point such as *C*. In this work in general for the thick plates, over  $\frac{1}{16}$  in. thick, oscillation began at point *B*, while for the thin plates, 0.029 in. thick, oscillation began at point *C*. For the latter plates it is significant to emphasize that no additional break in the performance curve occurred at the oscillation point. In all cases where oscillation occurred there was periodic "dumping" of the liquid through the plates on the same side of the plate as the crest of the wave. The holes on this side of the plate momentarily ceased to bubble as the wave reached its peak, and then liquid discharged through the holes as the wave began to fall.

"Flooding" in a perforated plate column can result from several causes and hence is shown as a zone of broken lines in Fig. 1. Flooding can result from (1) backing up of liquid in the downcomer, (2) expansion of the froth into the tray above, (3) splashing of the liquid into the tray above due to oscillations, (4) complete lifting of the liquid from the tray floor, (5) carry-over of all the liquid on the tray as entrainment and,

(6) perhaps other possibilities. Types 1 and 2 are quite common, and result in a vertical  $\Delta P$  line at the flooding velocity. Depending on the tray spacing and physical properties of the system, especially the frothing characteristics, flooding of this type might occur at any point between *A* and *E*. Type 3 is usually only a partial flooding. Once the oscillation point is reached, further increase in the gas rate at a given liquid rate only increases the violence and amplitude of the oscillations. In this study the splashing was quite often vigorous enough to carry liquid up into the tray above, even though an "average" froth height of only  $\frac{1}{2}$  to  $\frac{3}{4}$  of the tray spacing was observed. PLANK [21] noted action of Type 4, where all the liquid was lifted off the tray and hung as suspended drops between the plates accompanied by heavy entrainment. Whether or not this tray action can be considered to be a type of flooding is largely a matter of definition. This type of flooding is quite unstable and very easily changes to flooding of Type 5. Still further increase in the gas velocity would inevitably result in complete carry-over of the liquid in the form of entrainment (Type 5) possibly giving a curve such as *F* in Fig. 1. There may be combinations of more than one type of flooding simultaneously, or in all likelihood other mechanisms which result in flooding. In the work reported here flooding of Type 3 only was observed.

#### EQUIPMENT

The perforated-plate column used here was the same one used by ARNOLD *et al.* [2]. Many of the details of construction, including some photographs, are given in the above reference. A summary of some of the pertinent dimensions of the column is given in Table 1.

Table 1. Perforated-plate column dimensions

Number of plates	3
Inside column diameter	15 in.
Tray spacing	18 in.
Inlet weir height	$\frac{1}{2}$ in.
Outlet weir height	2 in.
Height of splash baffle (outlet side)	8 in.
Clearance between outlet weir and splash baffle	$\frac{3}{4}$ in.
Clearance under baffle, from floor of tray	$\frac{1}{2}$ in.

Table 2. Plate insert dimensions

Plate insert	Plate thickness $T$ , (in.)	Hole diam. $D_h$ , (in.)	Pitch $p$ , (in.)	$T/D_h$	Number of holes	Free space,* (FA) per cent
I	$\frac{1}{16}$	$\frac{3}{16}$	27/64	0.333	545	8.52
II	$\frac{1}{8}$	$\frac{1}{4}$	1-13/64	1.000	77	8.55
III	$\frac{1}{8}$	$\frac{1}{4}$	19/32	2.000	312	8.65
IV	$\frac{1}{8}$	$\frac{5}{16}$	27/64	2.667	545	8.52
V	$\frac{1}{8}$	3/32	14/64	5.333	2180	8.47
VI†	0.029	$\frac{1}{4}$	0.87	0.116	160	4.43
VII†	0.029	$\frac{5}{16}$	1 $\frac{1}{4}$	0.093	90	3.92

\*Based on column area.

†Inserts 1-4 and 1-5, respectively, used by ARNOLD, PLANK and SCHOENBORN [2].

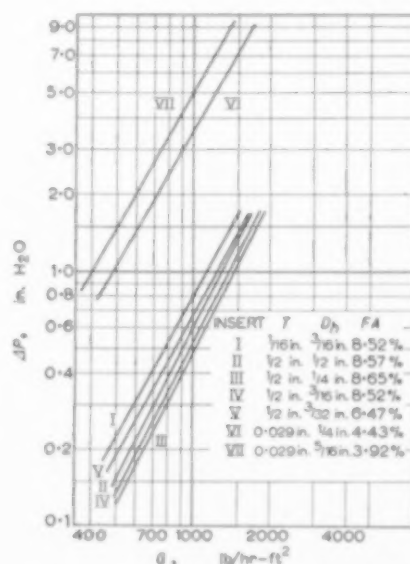
The perforated plates in this column were removable inserts for ease in changing plate thickness ( $T$ ), hole diameter ( $D_h$ ), and distance between holes ( $p$ ). The dimensions of the inserts are given in Table 2.

All the holes were drilled or punched on a triangular pattern. It is important to note that there were no holes closer than about 1 $\frac{1}{8}$  in. downstream of the inlet weir, or closer than 1 $\frac{1}{8}$  in. upstream of the outlet weir. It was noted in this investigation, and in others [2, 14-16], that if the perforations are too close to either the inlet or the outlet weir these holes will weep continually. Also, if the holes are too close to the outlet weir, excessive froth passes under the splash baffle and over the outlet weir. Inserts I-V were made of Plexiglas, whereas Inserts VI and VII were made of stainless steel. For the Plexiglas plates, holes were drilled and the burrs were carefully removed. The stainless steel plates were punched.

## RESULTS

**Dry-plate pressure drop.** The dry-plate pressure drop as a function of the mass flow rate of air is shown in Fig. 2 for Inserts I-VII. The pressure loss as gas passes through a dry perforated plate results from (1) a contraction loss, (2) a friction loss in the hole, and (3) an expansion loss. HUNT, HANSON and WILKE [5] at a  $T/D_h$  ratio of 1.0 correlated their results, considering only the contraction and expansion losses. For thicker

plates,  $T/D_h \approx 2.3$ , the magnitude of the friction through the holes themselves becomes important, requiring a term for the pressure loss due to friction of the Fanning type.

FIG. 2. Dry-plate  $\Delta P$  as a function of  $G$ .

Following the approach of HUNT *et al.* sudden contraction losses in pipes [22] can be expressed as:—

$$h_c = 0.4 \left( 1.25 - \frac{A_2}{A_1} \right) \frac{V_2^2}{2g} \quad (1)$$

For expansion,

$$h_e = \left(1 - \frac{A_2}{A_1}\right)^2 \frac{V_2^2}{2g} \quad (2)$$

The corresponding equation for friction losses is:-

$$h_f = \frac{4f l V_2^2}{2g d_2} \quad (3)$$

Combining these three losses for a perforated plate, and substituting plate thickness  $T$  for  $l$  in equation (3) results in the following relation for a single plate:-

$$h = k \left[ 0.4 \left( 1.25 - \frac{A_h}{A_c} \right) + 4f \left( \frac{T}{D_h} \right) + \left( 1 - \frac{A_h}{A_c} \right)^2 \right] \frac{V_h^2}{2g} \quad (4)$$

The factor  $k$  has been added in the formulation of equation (4) since equations (1), (2) and (3) were derived for a single hole (a pipe) and not an array of parallel paths. Presumably coefficient  $k$  can take care of interference between adjacent jets, and the Couette correction and velocity-gradient irregularities within the holes. For each insert used here,  $k$  was plotted against the quantity  $[0.4(1.25 - A_h/A_c) + 4f(T/D_h) + (1 - A_h/A_c)^2] V_h^2/2g$ . In each case a straight line resulted having a slope of  $k$ . Likewise data from all other readily available sources were treated in the same manner. Fig. 3 shows the calculated  $k$  values as a function of  $T/D_h$ . The agreement of the points with the line is remarkable in view of the range of  $T/D_h$ , column diameter, free space, and hole velocity represented in Fig. 3.

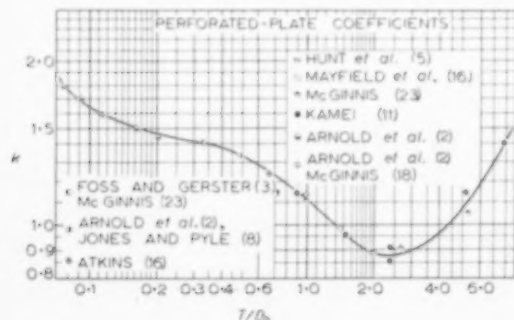


FIG. 3. Dry-plate coefficient  $k$  as a function of  $T/D_h$ .

Figure 4 shows a comparison of pressure drops calculated by the use of equation 4 and Figure 3, and experimentally determined pressure drops. The average deviation of the points from the line of equality in Fig. 4 is small.

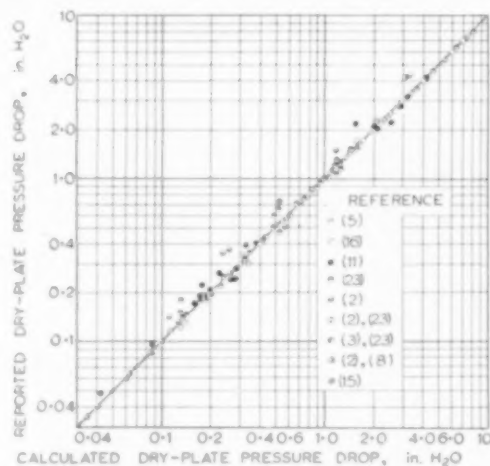


FIG. 4. Comparison of calculated and reported dry-plate pressure drop.

**Wet-plate pressure drop.** Figs. 5-11 show the performance curves of all the inserts used here. The wet-plate pressure drop is given for the indicated liquid rates as a function of the mass

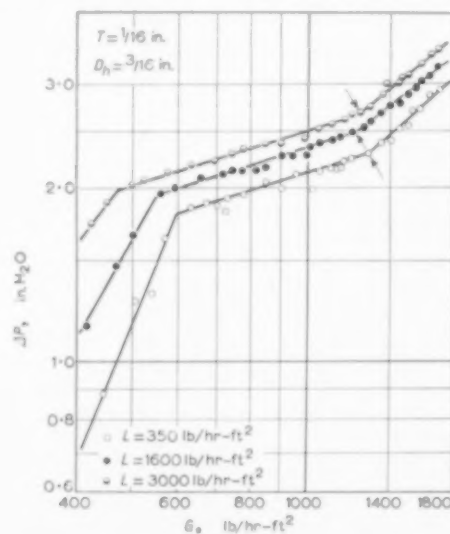
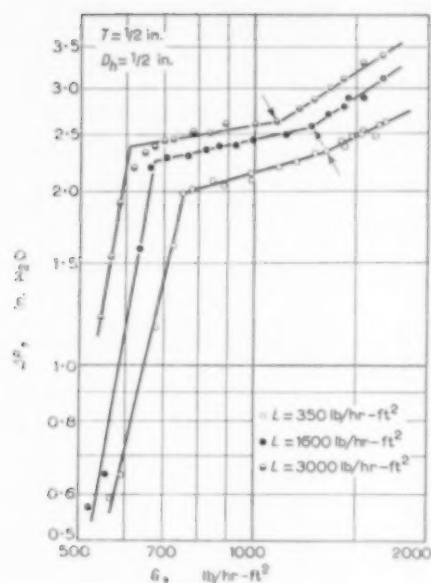
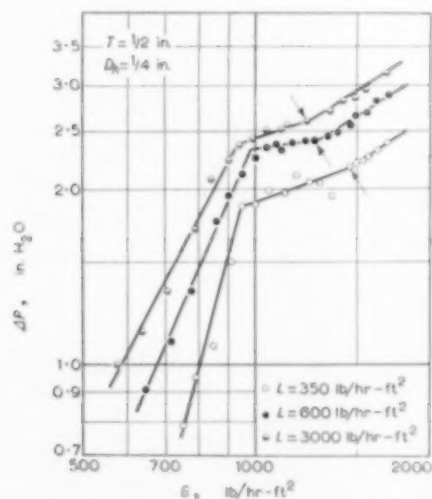
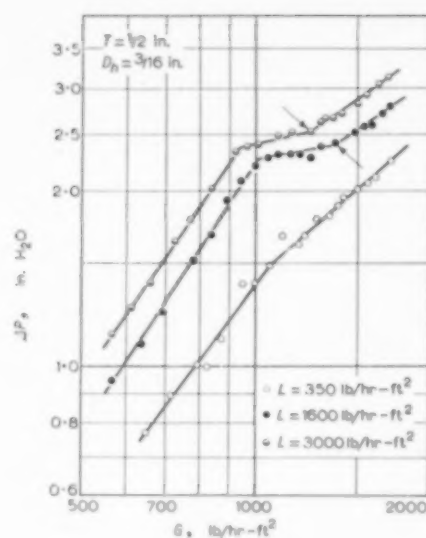


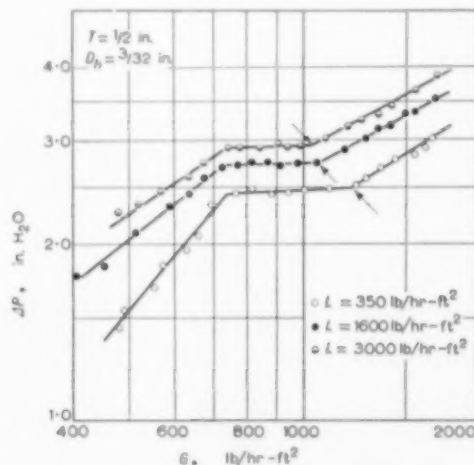
FIG. 5.  $\Delta P$  as a function of  $G$  - Plate insert I.

FIG. 6.  $\Delta P$  as a function of  $G$  - Plate insert II.

flow-rate of air,  $G$ , in lb air/hr-ft<sup>2</sup> of column cross-sectional area. All of the curves are of the Type III shown in Fig. 1 with the exception that in Fig. 7 for a liquid mass flow-rate of 350 lb water/hr-ft<sup>2</sup>. This curve is of Type II. The oscillation points are indicated in Fig. 4-10 as the small arrows.

FIG. 7.  $\Delta P$  as a function of  $G$  - Plate insert III.FIG. 8.  $\Delta P$  as a function of  $G$  - Plate insert IV.

In Fig. 12 and 13 total pressure drop minus the clear liquid head, as a function of the mass flow-rate for Inserts V and VI respectively, has been plotted. The solid line shown in these Figures is the dry-plate pressure drop. The vertical distance from the line to-the wet-plate data points is known as the "residual" pressure [5]. Fig. 14 shows the residual pressure drop as a function of  $T/D_h$  at a single mass flow-rate

FIG. 9.  $\Delta P$  as a function of  $G$  - Plate insert V.

# Perforated-plate performance

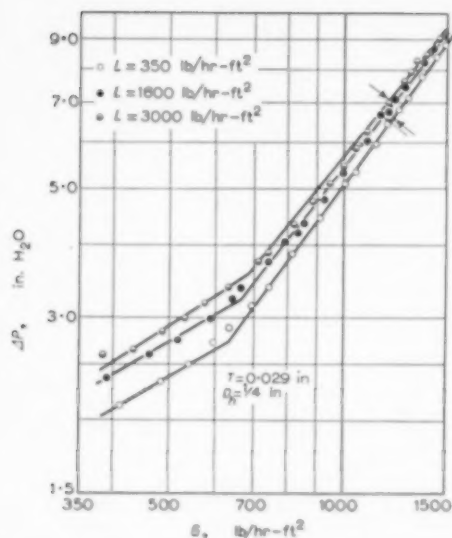


FIG. 10.  $\Delta P$  as a function of  $G$  - Plate insert VI.

of air. At other values of  $G$ , the residual pressure drop increases with increasing  $G$ . The data in Figs. 12, 13 and 14 show the residual pressure drop to be a function of  $T/D_h$ ,  $L$  and  $G$ . An increase of  $L$ , for thick plates, results in an increase of  $R$ . Likewise  $R$  increases as  $T/D_h$  increases for constant values of  $L$ . No general correlation was made, but these data were given to indicate the general trends.

The results of this investigation and those obtained by ARNOLD *et al.* [2] show that for thin

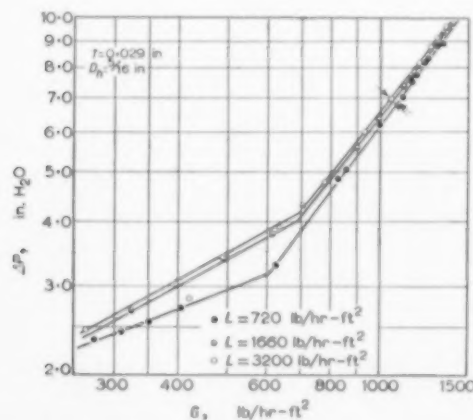


FIG. 11.  $\Delta P$  as a function of  $G$  - Plate insert VII.

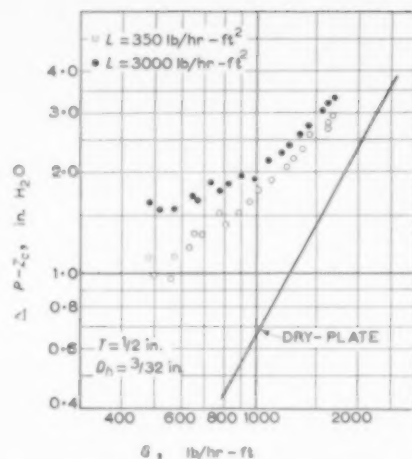


FIG. 12. Total pressure drop minus the clear liquid head as a function of  $G$  - Plate insert V.

plates the residual pressure drop is affected little by changes in liquid flow-rate. The ratio of the residual pressure drop to the dry-plate pressure drop remains about constant for the thin plates. Thus the data lie above and in a line parallel to the dry-plate curve in Fig. 13. Fig. 24 of ref. [2] shows the same trend for the thin plates

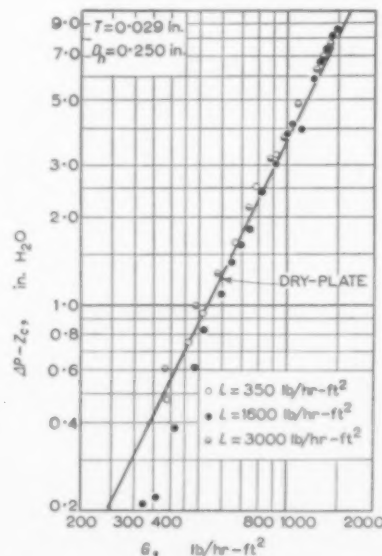


FIG. 13. Total pressure drop minus clear liquid head as a function of  $G$  - Plate insert VI.



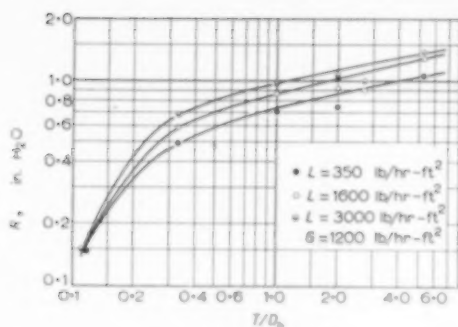


FIG. 14. Residual pressure drop as a function of  $T/D_h$  and  $L$ .

used by ARNOLD *et al.* [2]. For the thicker plates, however, the residual pressure drop increases with an increase of liquid flow-rate. The ratio of residual pressure drop to dry-plate pressure drop decreases with increasing gas flow-rate.

The complete set of data for Inserts I-VI giving total pressure drop, clear liquid height, froth height, gas and liquid flow-rate, etc. has been tabulated by MCGINNIS [23].

**Weepage correlation.** Fig. 15 shows the total pressure drop plotted as a function of the vapour  $F$ -factor through the holes at the weep point. The vapour  $F$ -factor is the square root of kinetic

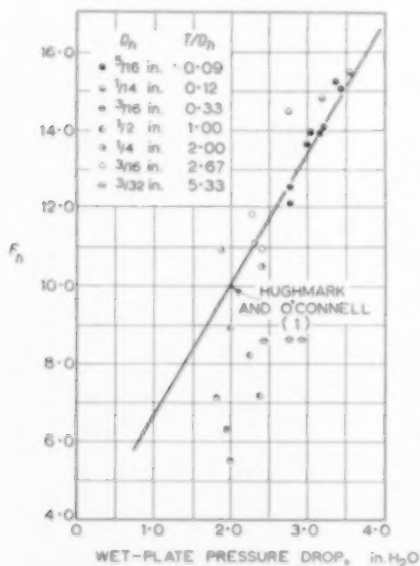


FIG. 15. Weep-point correlation.

Table 3. Weep points

Plate insert No.	$L$ (lb H <sub>2</sub> O/hr ft <sup>2</sup> )	$\Delta P$ (in. H <sub>2</sub> O)	$G$ (lb air/hr ft <sup>2</sup> )	$F_h$
I	350	1.82	610	7.07
	1600	1.96	555	6.43
	3000	2.00	470	5.45
II	350	2.00	770	8.94
	1600	2.26	710	8.23
	3000	2.37	620	7.18
III	350	1.87	940	10.88
	1600	2.32	960	11.11
	3000	2.40	910	10.54
IV	350	—	—	—
	1600	2.28	1020	11.83
	3000	2.40	945	10.96
V	350	2.44	740	8.57
	1600	2.75	740	8.57
	3000	2.92	740	8.57
VI	350	2.75	640	14.40
	1600	3.20	665	14.97
	3000	3.55	695	15.62
VII	450	3.74	645	16.4
	720	3.68	630	16.1
	960	4.06	691	17.7
	1380	3.46	586	15.0
	1660	3.86	645	16.4
	2020	4.14	688	17.5
	2450	3.46	574	14.6
	2610	3.90	649	16.5

energy of the gas per unit volume. Table 3 presents the weep-point data of this investigation. The solid line in Fig. 15 is the weepage correlation proposed by HUGHMARK and O'CONNELL [1]. The data of the present investigation agree reasonably well with the correlation. However, some of the data points shown in Fig. 15 are not in the range of hole diameters included in HUGHMARK and O'CONNELL's correlation; thus the weep-points for the  $\frac{1}{2}$  in. holes are out of the range of the correlation and do not agree with it. Also the data for the  $\frac{3}{32}$  in. holes ( $T/D_h = 5.33$ ) do not agree with the correlation. It is felt that there is a surface tension effect which should



Table 4. Oscillation points

Plate insert No.	$L$ (lb $H_2O$ /hr $ft^2$ )	$G$ (lb air/hr $ft^2$ )	$\Delta P$ (in. $H_2O$ )	$Z_c$ (in. $H_2O$ )
I	350	1220	2.22	0.68
	1600	1160	2.42	0.91
	3000	1150	2.60	1.00
II	350	1330	2.33	0.60
	1600	1260	2.56	0.78
	3000	1100	2.65	1.06
III	350	1470	2.18	0.34
	1600	1280	2.43	0.72
	3000	1220	2.61	0.92
IV	1600	1375	2.40	0.51
	3000	1240	2.53	0.79
V	350	1200	2.50	0.46
	1600	1050	2.76	0.82
	3000	1030	2.95	0.98
VI	350	1238	6.81	0.83
	1600	1187	6.74	0.91
	3000	1306	7.95	0.95
VII	450	1223	7.99	0.57
	720	1220	7.64	0.83
	960	1211	7.87	0.91
	1380	1200	7.83	0.87
	1660	1191	7.13	0.71
	2020	1182	7.40	1.14
	2450	1170	8.00	0.95
	2610	1166	8.03	1.06
	3200	1148	7.51	1.30

be included in the correlation, and that this effect may be magnified by the high  $T/D_h$  ratio.

**Oscillation-point correlation.** Table 4 presents the oscillation point data of this investigation, and Fig. 16 presents the air mass flow-rate as a function of the clear liquid height, both at the oscillation point. The agreement is quite satisfactory except for Insert V ( $\frac{1}{2}$  in. thick,  $\frac{3}{32}$  in. holes). It should be noticed that the weep-point correlation for this particular insert was also unsatisfactory. Possibly some surface tension effect incorporated into both correlations would improve the agreement of the data for Insert V with that of the other inserts. It is interesting

to note that the oscillation-point correlation was based on the column mass flow-rate whereas the weepage correlation required the hole velocity to bring the data into the proper order.

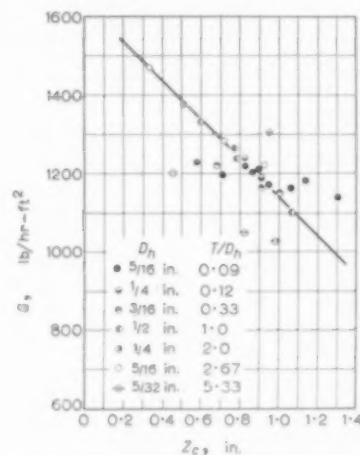


FIG. 16. Oscillation-point correlation.

The clear liquid height,  $Z_c$ , at the centre of the operating tray was used in the oscillation-point correlation, and was measured with a manometer. One leg of the manometer was inserted through the plate from beneath and was made flush with the top surface of the plate. The other leg of the manometer was mounted in the vapour space above the plate. The manometer reading itself was considered to be the clear liquid height, measured in inches or centimetres of liquid. It represents the hydraulic pressure of the liquid and froth on the plate in terms of clear liquid head. The clear liquid height, along with the froth height has been shown by PLANK [24] to be an important quantity in characterizing aeration on the tray. Aeration in turn is one of the factors which affects mass-transfer efficiency in liquid-phase controlling systems [24].

The clear liquid height is a difficult quantity to measure accurately. It fluctuates constantly, especially in the oscillation region described above, and is often less than 1 in. in magnitude, even with a 2-in. weir. The clear liquid height and the froth height undoubtedly hold many of

the keys to a complete understanding of tray hydraulics, as well as mass-transfer efficiency on perforated-plate trays, bubble-cap trays, and the like.

### CONCLUSIONS

- (1) The dry-plate pressure drop for perforated plates is described well by equation (4) and Fig. 3.
- (2) At constant hole diameter and free area, dry-plate pressure drop decreases with increasing plate thickness (i.e.  $T/D_h$  increases) until hole friction becomes appreciable (at  $T/D_h \cong 2.3$ ); then a reversal of this trend occurs.
- (3) Four distinct types of plate action were encountered in this study—raining, weeping, stable operation, and oscillation.
- (4) Periodic liquid and froth surges or oscillations can occur at high gas rates and is accompanied by periodic liquid dumping through the perforations near the column walls.
- (5) For thin plates, residual pressure drop is shown not to be a function of the liquid flow-rate, it increases with increasing gas flow-rate, but the ratio of residual pressure drop to dry-plate pressure drop is essentially constant. For thick plates the residual pressure drop is a function of  $T/D_h$ ,  $G$  and  $L$ .
- (6) The results of the investigation are in agreement with the weepage correlation of HUGHMARK and O'CONNELL [1].
- (7) The mass flow-rate,  $G$ , lb air/hr ft<sup>2</sup> of column area, at which oscillation begins is shown

to be a linear function of the clear liquid height at the oscillation point.

### NOTATION

- $A_1$  = cross-sectional area of the larger pipe, ft<sup>2</sup>  
 $A_2$  = cross-sectional area of the smaller pipe, ft<sup>2</sup>.  
 $A_c$  = column cross-sectional area, ft<sup>2</sup>.  
 $A_h$  = total perforation area, ft<sup>2</sup>.  
 $D_h$  = diameter of the perforations, in.  
 $D_2$  = diameter of the smaller pipe, ft.  
 $\Delta P$  = pressure drop across a plate, in. of fluid.  
 $f$  = Fanning friction factor for smooth pipes, ref. [20]  
 $FA$  = total perforation area-to-column area ratio, per cent.  
 $F_h$  =  $F$ -factor through the holes,  $V_h \sqrt{\rho_g}$ , where  $\rho_g$  = gas density, lb/ft<sup>3</sup>.  
 $g$  = acceleration of gravity, ft/sec<sup>2</sup>.  
 $G$  = mass flow-rate of gas, lb gas/hr ft<sup>2</sup> of total column cross-sectional area.  
 $h$  = head loss across a dry perforated plate, ft of gas flowing.  
 $h_c$  = head or pressure loss due to contraction, ft of fluid.  
 $h_e$  = head or pressure loss due to expansion, ft of fluid.  
 $h_f$  = head or pressure loss due to friction, ft of fluid.  
 $k$  = a dimensionless coefficient.  
 $l$  = length of pipe, ft.  
 $L$  = mass flow rate of liquid, lb liquid/hr ft<sup>2</sup> of total column cross-sectional area.  
 $p$  = pitch, the centre-to-centre distance between the perforations, in.  
 $R$  = residual pressure loss (total pressure loss minus dry plate loss minus  $Z_c$ ).  
 $T$  = plate thickness, in.  
 $V_2$  = average velocity in the smaller pipe, ft/sec.  
 $V_h$  = average velocity in a perforation, ft/sec.  
 $Z_c$  = clear liquid height, in.

### REFERENCES

- [1] HUGHMARK G. A. and O'CONNELL H. E. *Chem. Engng. Progr.* 1957 **53** 127M.
- [2] ARNOLD D. S., PLANK C. A. and SCHOENBORN E. M. *Chem. Engng. Prog.* 1952 **48** 633.
- [3] FOSS A. S. and GERSTER J. A. *Performance of Sieve Trays for Extractive Distillation Columns*, Report RuR SR No. 281, University of Delaware, 1954.
- [4] GUNNESS R. C. and BAKER J. G. *Industr. Engng. Chem. (Industr.)* 1938 **30** 1394.
- [5] HUNT C. d'A., HANSON D. N. and WILKE C. R. *Amer. Inst. Chem. Engrs. J.* 1955 **1** 441.
- [6] HUTCHINSON M. H., BURON A. G. and MILLER B. P. *Aerated Flow Principle Applied to Sieve Plates*, Paper presented at Los Angeles Meeting of the Amer. Inst. Chem. Engrs. 1949.
- [7] JOHNSON A. I., Kwei T. K. and LAVERGNE E. A. L. *Chem. Can.* 1955 **37** 32.
- [8] JONES J. B. and PYLE C. *Chem. Engng. Progr.* 1955 **51** 424.
- [9] JONES P. D. and VAN WINKLE M. *Industr. Engng. Chem. (Industr.)* 1957 **49** 232.
- [10] KAMEI S., TAKAMATSU T., GOTO K. and KOMETANI A. *Chem. Engng. (Japan)* 1954 **18** 307.
- [11] KAMEI S., TAKAMATSU T., MIZUNO S. and TOMIZAWA Y. *Chem. Engng. (Japan)* 1954 **18** 108.

# Perforated-plate performance

- [12] KAMEI S., TAKAMATSU T., UMESHITA I., OKAWA H. and OZU T. *Chem. Engng. (Japan)* 1951 **15** 19.
- [13] KELLY R. E. *Petrol. Refin.* 1955 **34** 188.
- [14] LEE D. C. *Chem. Engng.* 1954 **61** 179.
- [15] LEIBSON I., KELLY R. E. and BULLINGTON L. A. *Petrol. Refin.* 1957 **36** 127.
- [16] MAYFIELD F. D., CHURCH W. L., GREEN A. C., LEE D. C. and RASMUSSEN R. W. *Industr. Engng. Chem. (Industr.)* 1952 **44** 2238.
- [17] McALLISTER R. A. and PLANK C. A. *Amer. Inst. Chem. Engrs. J.*, In press.
- [18] NANDI S. K. and KARIM B. J. *Indian Chem. Soc. (Industr. News Ed.)* 1948 **11** 3.
- [19] UMHOLTZ C. L. and VAN WINKLE M. *Industr. Engng. Chem. (Industr.)* 1957 **49** 226.
- [20] ZENZ F. A. *Petrol. Refin.* 1954 **33** 99.
- [21] PLANK C. A., M.S. *Thesis in Chemical Engineering*, N. C. State College, 1951.
- [22] PERRY J. H. (Editor) *Chemical Engineers' Handbook* (3rd Ed.) McGraw-Hill, New York, 1950.
- [23] MCGINNIS P. H. JR. *M. S. Thesis in Chemical Engineering*, N. C. State College 1957.
- [24] PLANK C. A., Ph.D. *Thesis in Chemical Engineering* N. C. State College, 1957.

## Adiabatic convection batch drying with recirculation of air

D. A. VAN MEEL

Central Technical Institute T.N.O., Koningskade 5, The Hague, Netherlands

(Received 30 October 1957)

**Abstract**—In batchwise drying the moisture content of the material that is to be dried is a function of the drying time as well as of the location of the material in the drier. Using dimensionless parameters, and based on some simplifying assumptions, a method of calculation is given for this method of drying which permits prediction of the distribution of the moisture content of the material and of the drying potential of the air. This is possible regardless of the shape of the curve which relates rate of drying to moisture content, as obtained from laboratory drying tests under constant drying conditions.

**Résumé**—Dans le séchage par charge le teneur en eau du matériel à sécher est une fonction de la durée de séchage de même que de la position du matériel dans le séchoir. En se servant de paramètres sans dimensions, et partant de quelques suppositions simplifiantes, une méthode de calcul est présentée qui permet de prédire la distribution du teneur en eau du matériel et de la force de séchage de l'air. Cette méthode est possible sans compter la forme de la curve qui lie la vitesse de séchage au teneur en eau, résultant des expériences de séchage laboratoires dans des conditions de séchage invariables.

**Zusammenfassung**—Beim chargenweisen Trocknen ist der Feuchtigkeitsgehalt des Trockengutes eine Funktion der Trocknungszeit und des Ortes innerhalb des Trockners. Unter Verwendung dimensionsloser Parameter und mit einigen vereinfachenden Annahmen wird für diese Trocknungsart eine Berechnungsmethode mitgeteilt, die die Verteilung des Feuchtigkeitsgehalts und die trocknende Wirkung der Luft voraussagen gestattet. Diese Voraussage ist möglich ohne Rücksicht auf die Kurvenform der Beziehung zwischen der Trocknungsgeschwindigkeit und dem Feuchtigkeitsgehalt, wie sie aus Laboratoriumsversuchen unter konstanten Trocknungsbedingungen erhalten wird.

In convection batch driers drying is achieved by forced convection of air across or through a stationary arrangement of wet solid material. Examples are tray and compartment driers as used in the heavy brick and clay industry, tray and truck driers for drying wood, sieve tray driers for drying thick beds of various granular materials.

In connexion with this method of drying two main problems arise, both relating to the uniformity of the moisture content of the products. One of them is, how to obtain a uniform distribution of the air across or through the stock. This problem is an aerodynamical one and, though sometimes difficult, a satisfactory solution can be found in most cases, e.g., by flow experiments on small-scale models to determine the appropriate dimensions and arrangements.

However even if a uniform distribution of the air can be realized there remains the non-uniformity of the moisture content of the materials that is inherent in this method of drying. It is caused by the increasing humidity of the air on its way through the drier and by the fact that the rate of drying depends on the moisture content of the material. Since the moisture content of the material is a function of drying time and of location with reference to the entrance of the air, the situation is more complicated than in the case of continuous driers; so far we know of no general calculation methods, as are available for continuous driers. This is perhaps one of the reasons why the use of batch driers is generally avoided if possible.

However for materials which require a long drying time, such as green brick and wood, batch

driers must be used. The problem arises of predicting the drying conditions and calculating the drying time required to keep the moisture content of the product between given and generally rather close limits. Also certain combinations of moisture content, humidity and temperature conditions of the air which would cause deterioration in the material must be avoided.

This paper gives a method for calculating the moisture content of the material and the humidity of the air as functions of drying time and location, some idealizing assumptions being made.

Rate of drying *v*, moisture content curves determined under constant conditions by laboratory drying experiments are assumed to be available. It is assumed that the adiabatic saturation temperature of the air remains constant. In case of recirculation, the time required to return air from the exit to the entrance is neglected. Furthermore the assumption is made that a one-dimensional treatment is possible. In many driers of the batch-type the actual configuration can be arranged so that the same conditions for the material and for the air can be expected in cross-sections normal to the direction of the air flow.

Another assumption is discussed in the derivation of the differential water balance, i.e. the rate of change of the water vapour content of the air in the drier is neglected with respect to the net rate of water-vapour transport by forced convection.

Two cases of initial moisture distribution that are believed to cover most practical cases are treated in this paper. Mathematical details not directly needed for understanding the calculations are omitted to reduce the size of the paper. We intend to check the validity of the calculations by experiments, but present sufficient data are not yet available for insertion in this paper.

#### THE EQUATION FOR THE RATE OF DRYING

The rate of drying of a wet solid in flowing air depends on drying conditions in a complicated way. For most engineering purposes, however, it can be described with reasonable accuracy by the equation:

$$-\frac{\partial F}{\partial t} = k \cdot V \cdot g(F) \quad (1)$$

As a first approximation the various factors in this equation are separated into three independent groups: the mass transfer coefficient *k* which depends on the air flow conditions, the driving force or drying potential *V* which is a function of temperature and humidity of the air and finally the dimensionless function *g*(*F*) of the mean water content which takes into account the physical properties of the material to be dried. In most cases the functions *k* and *g*(*F*) must be obtained from laboratory drying experiments under conditions approaching as closely as possible the actual conditions in a drier.

If, as is often the case, the critical moisture content *F<sub>c</sub>* and the equilibrium moisture content *F<sub>e</sub>* can be assumed to be constants it is more convenient to write *g*(*F*) = *f*(*F* - *F<sub>e</sub>*/(*F<sub>c</sub>* - *F<sub>e</sub>*)), this function *f* having the value 1 for *F* ≥ *F<sub>c</sub>* and 0 for *F* = *F<sub>e</sub>*.

For low temperature and humidity *V* equals (*H<sub>s</sub>* - *H*). The formula

$$V = 0.622 \ln \frac{P - p_1}{P - p_0} \quad (2)$$

has a more extended range of applicability.

By converting partial pressures into specific humidities:

$$V = 0.662 \ln \frac{0.662 + H_s}{0.662 + H} \quad (3)$$

If a correction factor *b* is introduced:

$$V = \frac{0.622}{0.622 + H_s} \cdot b \cdot (H_s - H) = \beta (H_s - H) \quad (4)$$

If adiabatic saturation of the air is assumed *H<sub>s</sub>* is a constant. For the temperature ranges occurring in practice *b* will only vary slightly. It appears therefore that in cases of high temperature and humidity drying can be approximately described by applying a constant correction factor *β* to the drying potential (*H<sub>s</sub>* - *H*). Hence equation (1) can be written as:

$$-\frac{\partial F}{\partial t} = k \cdot \beta \cdot (H_s - H) f\left(\frac{F - F_e}{F_c - F_e}\right) \quad (5)$$

#### THE DIFFERENTIAL WATER BALANCE

In this paper tray and compartment driers are treated which, for purposes of calculation, can



be represented, at least sectionally, by the mathematical model shown in Fig. 1. Of course the possibility of doing this requires an equal distribution of the air through the actual drier. For the model of Fig. 1 a one-dimensional treatment is assumed to be applicable.

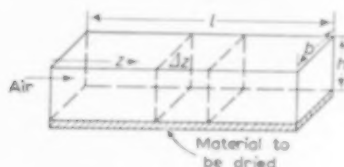


FIG. 1. Mathematical model of drier.

Considering an element of volume between cross-sections at  $z$  and  $z + \Delta z$  during a time interval  $\Delta t$ , a water balance can be written by equalizing the amount of water vaporized from the wet solid to the sum of the net amount of water vapour transported by convection and the increase of the water vapour content of the air in this element. If a factor  $b \cdot \Delta z \cdot \Delta t$  is dropped, the following equation is obtained:

$$-\frac{1}{Q} \frac{\partial F}{\partial t} = h \frac{\partial H}{\partial z} + \frac{h}{Q} \frac{\partial}{\partial t} \left( \frac{P}{47.1T - 0.622} + H \right) \quad (6)$$

The last term of this equation can be approximated by  $(h\gamma_a/Q) \partial H/\partial t$  if  $\gamma_a$  is the specific weight of dry air at the adiabatic saturation temperature. Now in the equation:

$$-\frac{1}{Q} \frac{\partial F}{\partial t} = h \frac{\partial H}{\partial z} + \frac{h\gamma_a}{Q} \frac{\partial H}{\partial t} \quad (6a)$$

the ratio of the coefficients of the second and third term is approximately equal to the linear air velocity on a dry air basis. Under conditions generally occurring in practice the rate of change of the water-vapour content of a given element of the drier will be small in comparison with the net rate of vapour transport from the element by forced convection. For most practical cases it can therefore be expected that a good approximation is still obtained if the last term of equation (6a) is neglected and the calculations are based on the approximate water-balance:

$$-\frac{1}{Q} \frac{\partial F}{\partial t} = h \frac{\partial H}{\partial z} \quad (7)$$

#### Dimensionless equations

Equations (5) and (7) can be made dimensionless by introducing the parameters:

$$\phi = \frac{F - F_c}{F_c - F_c}; \quad \tau = \frac{\beta kt}{F_c - F_c};$$

$$\zeta = \frac{\beta kz}{hQ}; \quad \pi = \frac{V}{\beta} = H_s - H \quad (8)$$

Equation (5) transforms into

$$-\frac{\partial \phi}{\partial \tau} = \pi f(\phi) \quad (9)$$

and equation (7) into

$$\frac{\partial \phi}{\partial \tau} = \frac{\partial \pi}{\partial \zeta} \quad (10)$$

The parameter  $\pi$  can be eliminated from (9) and (10) giving:

$$\frac{\partial^2 \phi}{\partial \tau \partial \zeta} - \frac{1}{f(\phi)} \frac{df(\phi)}{d\phi} \frac{\partial \phi}{\partial \tau} \frac{\partial \phi}{\partial \zeta} + f(\phi) \frac{\partial \phi}{\partial \tau} = 0 \quad (11)$$

With an arbitrary function  $P(\zeta)$  an intermediate integral of (11) is:

$$\frac{1}{f(\phi)} \frac{\partial \phi}{\partial \zeta} + \phi = P(\zeta) \quad (12)$$

Another equation that is needed gives the drying potential of the air entering the drier as a function of the drying potential of the fresh air and the recirculation ratio. Again it is assumed that the adiabatic saturation temperature is a constant. Furthermore the time needed to transport the air leaving the drier back to the entrance, where it is mixed with fresh air, is neglected:

$$V_s = (1 - a)V_0 + aV_L \quad (13)$$

Here  $V_s$ ,  $V_0$  and  $V_L$  respectively represent the values of  $V$  at the entrance of the drier, of the fresh air and of the air at the exit of the drier.

#### CALCULATION OF THE DRYING PROCESS

##### Initial moisture content above the critical moisture content

Now the case is considered when drying starts with the moisture content greater than  $F_c$  at all points in the drier. Three periods can be distinguished:



First period : Everywhere  $F > F_c$ . Drying rate independent of  $F$ . A moisture gradient develops through the drier. This period terminates when  $F = F_c$  at the entrance.

Second period : Moisture contents both higher and lower than  $F_c$  are present. The critical moisture content moves through the drier.

Third period :  $F < F_c$  everywhere in the drier.

#### First period

In general the initial moisture distribution will be uniform :  $F = F_0$ . Sometimes, however, after the period of heating up a non-uniform distribution is caused by condensation of water-vapour on the wet material at the moment at which drying really starts. In order to include such a case a more general initial distribution is assumed :—

$$\phi(\zeta, 0) = \phi_0 + \phi_1 e^{-\zeta} \quad (14)$$

in which  $\phi_1$  can be positive, negative or zero as long as  $\phi(\zeta, 0) \geq 1$  for  $0 \leq \zeta \leq \lambda$ . During this first period we can take  $f(\phi) = 1$ . Then equation (12) takes the form :

$$\frac{\partial \phi}{\partial \zeta} + \phi = \phi_0 \quad (15)$$

From equations (9), (10) and (13) :

$$\pi(\zeta, \tau) = \frac{(1-a)\pi_0}{1-ae^{-\lambda}} e^{-\zeta} \quad (16)$$

and with equation (14) :—

$$\phi(\zeta, \tau) = \phi_0 + \phi_1 e^{-\zeta} - \frac{(1-a)\pi_0}{1-ae^{-\lambda}} e^{-\zeta} \tau \quad (17)$$

Of course  $\pi$  appears to be independent of  $\tau$  and for a given  $\zeta$ ,  $\phi$  decreases linearly with  $\tau$ . It is further noted that a time  $\tau$  can always be found for which  $\phi = \phi_0$ . With (16) and (17) the first period is fully described.

The second period starts at  $\tau = \tau_1$  for which  $\phi(0, \tau_1) = 1$ . It follows that :

$$\tau_1 = (\phi_0 + \phi_1 - 1) \frac{1 - ae^{-\lambda}}{(1-a)\pi_0} \quad (18)$$

and the distribution of the moisture content at this moment is given by :—

$$\phi(\zeta, \tau_1) = \phi_0 - (\phi_0 - 1) e^{-\zeta} \quad (19)$$

This distribution is independent of  $\phi_1$ ,  $a$ ,  $\pi_0$  and  $\lambda$ .

#### Second period

From the initial distribution for this period and from equation (12) it follows that :

$$\frac{1}{f(\phi)} \frac{\partial \phi}{\partial \zeta} + \phi = \phi_0 \quad (20)$$

in which again  $f(\phi) = 1$  for  $\phi \geq 1$ , whereas for  $0 \leq \phi \leq 1$ , the function  $f(\phi)$  has an arbitrary shape which is known from drying experiments.

By integration of (20) :

$$\int_{\phi}^1 \frac{ds}{(\phi_0 - s)f(s)} = M(\tau) - \zeta \quad (21)$$

If the critical moisture content  $\phi = 1$  is situated at  $\zeta_c$ , it is easily derived from (21) :  $M(\tau) = \zeta_c$ , so :

$$\int_{\phi}^1 \frac{ds}{(\phi_0 - s)f(s)} = \zeta_c - \zeta \quad (22)$$

It is noted that  $\phi$  depends on  $\zeta_c - \zeta$ . The distribution for  $\zeta > \zeta_c$  is given by :

$$\int_1^{\phi} \frac{ds}{\phi_0 - s} = \zeta - \zeta_c \text{ or } \phi = \phi_0 - (\phi_0 - 1) e^{(\zeta_c - \zeta)} \quad (22a)$$

The value of  $\pi$  is calculated from equations (9) and (22) to be :

$$\pi = (\phi_0 - \phi) \frac{d\zeta_c}{d\tau} \quad (23)$$

in which  $d\zeta_c/d\tau$  is the dimensionless velocity of the critical moisture content. This velocity is calculated from the recirculation equation (13) by substitution of  $\pi$  from equation (23) for  $\zeta = 0$  and  $\zeta = \lambda$  :

$$\frac{d\zeta_c}{d\tau} = \frac{(1-a)\pi_0}{\phi_0 - \phi(0, \tau) - a\{\phi_0 - \phi(\lambda, \tau)\}} \quad (24)$$

The values of  $\phi(0, \tau)$  and  $\phi(\lambda, \tau)$  are found as functions of  $\zeta_c$  from equation (22).

Equation (24) can be substituted in (23) to give :

$$\frac{\pi}{\pi_0} = (1-a) \frac{\phi_0 - \phi}{\phi_0 - \phi(0, \tau) - a\{\phi_0 - \phi(\lambda, \tau)\}} \quad (23a)$$

The value of  $\zeta_c$  as a function of  $\tau$  is easily calculated afterwards by graphical integration of  $d\tau/d\zeta$  with respect to  $\zeta_c$ .

### Third period

If for  $\tau = \tau_2$ ,  $\zeta_c$  has reached the value  $\lambda$ , the third period begins. It is clear, however, that the calculations for this period follow exactly the same lines as those for the second period. If a physical meaning is no longer attached to  $\zeta_c$  there is no necessity to treat this period as a separate one.

Some remarks can be made that considerably reduce the amount of work for calculation of the distributions. From equation (22) it follows that the distributions  $\phi$  during the second and the third period follow from the parallel shift of a single curve lying between  $\phi = 0$  and  $\phi = \phi_0$  and approaching these limits asymptotically for  $-\infty$  and  $+\infty$ .

For the second period the distributions for  $\phi > 1$  are found by parallel shift of the distribution given by equation (19). The easiest way to complete these distributions for the second period is by calculation of the distribution for  $\zeta_c = \lambda$  from equation (22) and shifting this until it fits into the given value of  $\zeta_c$ .

The distribution of  $\pi$  is found from equation (23a) or, according to equation (24), by deriving the value of  $d\zeta_c/d\tau$  from the graph of moisture distributions and multiplication with  $\phi_0 - \phi$  as obtained from the same graph.

If for values of  $\phi$  close to zero the graphical integration of equation (22) becomes difficult on account of the great values of the integrand, the function  $f(\phi)$  can be approximated in this range by a linear function permitting analytical integration.

### Linear falling rate section: $f(\phi) = \phi$

In the falling rate section we can put for many materials as a good approximation  $f(\phi) = \phi$ . In this case the graphical integration can be replaced by an analytical one and some formulae can be derived.

Of course for the first period the formulae given before remain unchanged.

For the second period integration gives:

$$0 \leq \phi \leq 1 \quad \phi(\zeta, \tau) = \frac{\phi_0}{(\phi_0 - 1)e^{\phi_0(\zeta_c - \zeta)} + 1} \quad (25)$$

$$\phi \geq 1 \quad \phi(\zeta, \tau) = \phi_0 - (\phi_0 - 1)e^{\zeta_c - \zeta}$$

To determine  $\pi(\zeta, \tau)$  from equation (23)  $d\zeta_c/d\tau$  must be calculated from equation (13):

$$\frac{d\zeta_c}{d\tau} \left[ \frac{\phi_0}{\phi_0 - 1 + e^{-\phi_0\zeta_c}} - ae^{\zeta_c - \lambda} \right] = \frac{(1-a)\pi_0}{\phi_0 - 1} \quad (26)$$

Integration gives  $\tau$  as a function of  $\zeta_c$ :

$$(1-a)\pi_0(\tau - \tau_1) = \ln \frac{(\phi_0 - 1)e^{\phi_0\zeta_c} + 1}{\phi_0} - a(\phi_0 - 1)e^{-\lambda}(e^{\zeta_c} - 1) \quad (27)$$

The following observation can be useful. For some materials it is necessary, in order to avoid deleterious effects, to keep the driving force  $V$  below a certain value as long as the moisture content is above  $F_c$ . If this maximum allowable value is applied at the beginning of the second period it can be shown that, for high values of the recirculation ratio, there is danger that after some time the drying potential at  $\zeta_c$  rises above this value. If no recirculation is applied, the value of  $\pi$  at  $\zeta = \zeta_c$  is given by:

$$\pi(\zeta_c, \tau) = \frac{\pi_0}{\phi_0} (\phi_0 - 1 + e^{-\phi_0\zeta_c}) \quad (28)$$

and there is no risk since this is a monotonic decreasing function of  $\zeta_c$  which tends to the limit:

$$\pi = \pi_0 \frac{\phi_0 - 1}{\phi_0}$$

In fact this allows a further raising of  $\pi_0$  after some time with nearly a factor  $\phi_0/\phi_0 - 1$ .

For the third period formulae (26) and (27) become:

$$\begin{aligned} \frac{d\zeta_c}{d\tau} \left[ \frac{1}{\phi_0 - 1 + e^{-\phi_0\zeta_c}} - \frac{a}{\phi_0 - 1 + e^{-\phi_0(\zeta_c - \lambda)}} \right] &= \frac{(1-a)\pi_0}{\phi_0(\phi_0 - 1)} \quad (29) \end{aligned}$$

and

$$(1-a)\pi_0(\tau-\tau_2) = \ln \frac{(\phi_0-1)e^{\phi_0\zeta} + 1}{(\phi_0-1)e^{\phi_0\lambda} + 1} - a \ln \frac{(\phi_0-1)e^{\phi_0(\zeta-\lambda)} + 1}{\phi_0} \quad (30)$$

A simple formula for the total drying time  $\tau_3$ , needed to obtain a value  $\phi_2 < 1$  at  $\zeta = \lambda$  for drying under constant conditions can be derived from equations (18), (27) and (30):

$$(1-a)\pi_0\tau_3 = (1-a)(\phi_0-1) + \phi_1(1-ae^{-\lambda}) + a \ln \phi_2 + \ln \frac{1 + \left(\frac{\phi_0-1}{\phi_2}\right)e^{\phi_0\lambda}}{\phi_0} \quad (31)$$

If  $\phi_2 < \phi_0$ , this can be simplified to:

$$\pi_0\tau_3 = \phi_0 - 1 - \ln \phi_2 + \frac{\phi_0\lambda}{1-a} + \phi_1 \frac{1-ae^{-\lambda}}{1-a} \quad (32)$$

#### Homogeneous initial distribution below the critical moisture content

If the initial distribution is denoted by  $\phi_0 (< 1)$ , equation (20) can be used again. A treatment slightly differing from the foregoing one is given below. Equation (20) is now integrated to:

$$\int_{\phi_1}^{\phi} \frac{ds}{(\phi_0-s)f(s)} = \zeta \quad (33)$$

with  $\phi_1 = \phi(0, \tau)$ .

Taking an arbitrary value of  $\phi_1 (\leq \phi_0)$  the distribution is easily completed by graphical integration of equation (33). In this way a complete set of distribution curves can be obtained. The drying time  $\tau$  can be calculated as follows. From equations (9) and (33):

$$\frac{1}{(\phi_0-\phi)f(\phi)} \frac{\partial \phi}{\partial \tau} = \frac{1}{(\phi_0-\phi_1)f(\phi_1)} \frac{d\phi_1}{d\tau} \quad (34)$$

From (34) and (13), if  $\phi_\lambda = \phi(\lambda, \tau)$ :

$$\frac{1}{f(\phi_1)} \cdot \frac{d\phi_1}{d\tau} \cdot \left[ a \frac{\phi_0 - \phi_\lambda}{\phi_0 - \phi_1} - 1 \right] = (1-a)\pi_0 \quad (35)$$

(If  $\tau = 0$ ,  $\phi_1 = \phi_\lambda = \phi_0$  and  $\frac{\phi_0 - \phi_\lambda}{\phi_0 - \phi_1} = 1$ ).

Since  $\phi_\lambda$  is known from the distribution  $\phi$

calculated before as a function of  $\phi_1$ , equation (35) can be integrated to give  $\phi_1$  as a function of  $\tau$ :

$$\int_{\phi_1}^{\phi_0} \frac{1}{f(s)} \left[ 1 - a \frac{\phi_0 - \phi_\lambda(s)}{\phi_0 - s} \right] ds = (1-a)\pi_0\tau \quad (36)$$

The calculation of  $\pi$  proceeds as follows: From equations (9) and (34):

$$\pi = - \frac{\phi_0 - \phi_1}{\phi_0 - \phi_1} \cdot \frac{1}{f(\phi_1)} \frac{d\phi_1}{d\tau} \quad (37)$$

hence with (35):

$$\frac{\pi}{\pi_0} = \frac{\phi_0 - \phi}{\phi_0 - \phi_1 - a(\phi_0 - \phi_\lambda)} (1-a) \quad (38)$$

which formula is the same as (23a);  $\pi$  can now be calculated from the set of distributions  $\phi$ .

#### Linear falling rate curve

In case of  $f(s) = s$ , the formulae given in this section can be integrated directly. Formula (33) gives:

$$\phi = \frac{\phi_0\phi_1 e^{\phi_0\zeta}}{\phi_0 - \phi_1 + \phi_1 e^{\phi_0\zeta}} \quad (39)$$

From this equation  $\pi$  is easily found by means of equation (38).

For  $f(s) = s$  formula (36) integrates to:

$$\begin{aligned} \pi_0\tau &= \ln \frac{\phi_0}{\phi_1} \\ &+ \frac{a}{1-a} (e^{\phi_0\lambda} - 1) \ln \frac{\phi_0 e^{\phi_0\lambda}}{\phi_0 - \phi_1 + \phi_1 e^{\phi_0\lambda}} = \\ &= \ln \frac{\phi_0}{\phi_1} + \frac{a}{1-a} (e^{\phi_0\lambda} - 1) \ln \frac{\phi_\lambda}{\phi_1} \quad (40) \end{aligned}$$

#### CHANGE OF DRYING CONDITIONS

According to equation (22) the drying potential  $V$  and the recirculation ratio  $a$  do not affect the shape of the moisture distribution  $\phi$ , as long as the air velocity  $Q$  remains unchanged. Formula (24) shows that drying time is inversely proportional to  $V_0$  as is to be expected from equation (1); so the effect of changing this parameter can easily be taken into account. As mentioned earlier  $\phi(0, \tau)$  and  $\phi(\lambda, \tau)$  can be regarded as functions of  $\zeta_c$ . In case of a recirculation ratio  $a$  being a function of time, integration of equation (24)

remains possible in principle, resulting in the drying time  $\tau$  corresponding to a given value of  $\zeta_c$ . However, in case of stepwise variation of  $a$ , the new drying time can more easily be determined from repeated graphical integration of equation (24).

In case of varying air velocity  $Q$  the situation becomes somewhat more difficult since in general the mass transfer coefficient  $k$  will vary too. As  $Q$  and  $k$  enter into the equations (8) for  $\tau$  and  $\zeta$ , both the drying time and the distributions of the water content will be changed. However, for high air velocities  $k$  will vary approximately as  $Q^{0.8}$  and therefore the effect of varying  $Q$  on  $k/Q$  in

$$\zeta = \frac{\beta z}{h} \cdot \frac{k}{Q}$$

will be rather small. As a first approximation the distributions of the water content can be assumed to be independent of  $Q$  under these conditions.

#### EXAMPLE

Suppose that the actual drier can be reduced to the simple shape of Fig. 1 for purposes of calculation. The following data are given:  $L = 10$  m;  $h = 0.1$  m;  $F_0 = 7.25$  kg/m<sup>2</sup>;  $F_c = 3.62$  kg/m<sup>2</sup>;  $F_e = 0.72$  kg/m<sup>2</sup>;  $Q = 10,000$  kg/m<sup>2</sup>h, corresponding with a linear air velocity of about 3 m/sec.;  $k = 200$  kg/m<sup>2</sup>h,  $V = 1$ .

Air conditions: fresh air supply at 105°C; ad.sat.temp. 80°C;

$$H_s = 0.5511; \pi_0 = 0.063$$

$$b = 1, \text{ so } \beta = \frac{0.622}{0.622 + 0.5511} = 0.53; \quad V = 0.53 \pi.$$

The dimensionless parameters are:

$$\phi = \frac{F - 0.72}{2.90}; \quad \tau = \frac{0.53 \times 200}{2.9} t = 36.55 t;$$

$$\zeta = \frac{0.1 \times 10,000}{0.53 \times 200} z = 0.106 z; \quad \lambda = 0.106 \times 10 = 1.06.$$

Drying is assumed to start from a homogeneous initial distribution  $F = F_0$  or

$$\phi_0 = \frac{7.25 - 0.72}{2.90} = 2.25.$$

Recirculation ratio  $a = 5/6$ .

The case of drying under constant inlet conditions, as given above will now be treated. The rate curve  $f(\phi)$  is supposed to have the shape given in Fig. 2 as determined by laboratory experiments.

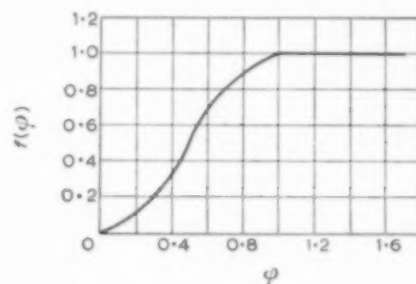


FIG. 2. Dimensionless rate curve.

#### First period

At the end of this period the distribution of the water content follows from equation (19):

$$\phi(\zeta, \tau) = 2.25 - 1.25 e^{-\zeta}.$$

Drying time according to equation (18):

$$\tau_1 = 1.25 \frac{1 - \frac{5}{6} e^{-1.06}}{\frac{1}{6} \times 0.063} = 84.68 \text{ or } t_1 = 2.32 \text{ h.}$$

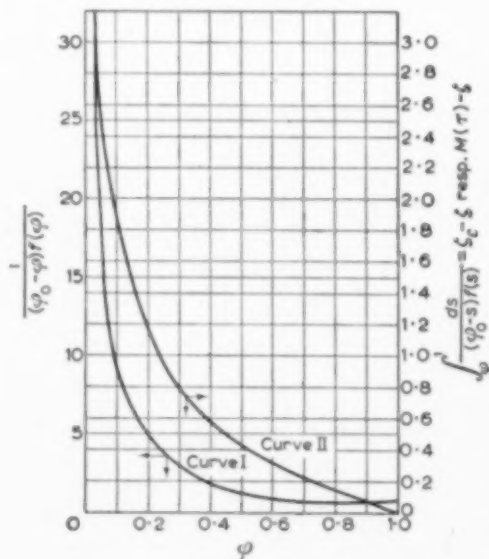


FIG. 3.

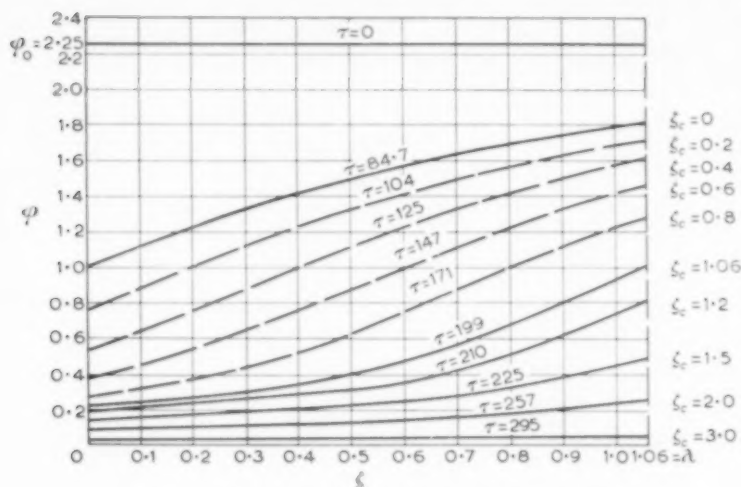


FIG. 4. Dimensionless distribution of water content.

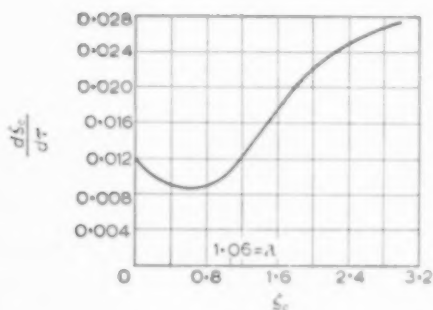


FIG. 5.

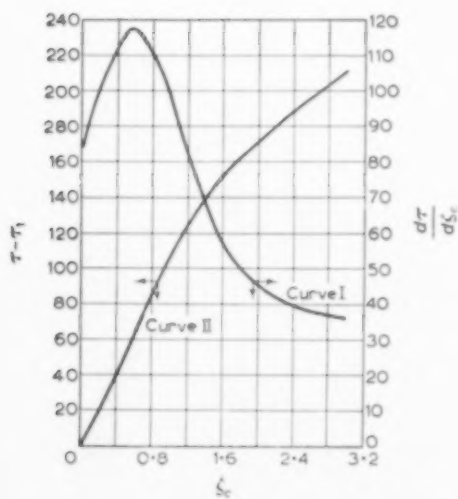


FIG. 6.

From equation (16):  $\pi = 0.01476e^{-\xi}$  or  $V = 0.0078 e^{-\xi}$ . If no recirculation is applied the drying time will be  $\tau_1 = 19.84$  or  $t_1 = 0.54$  h.

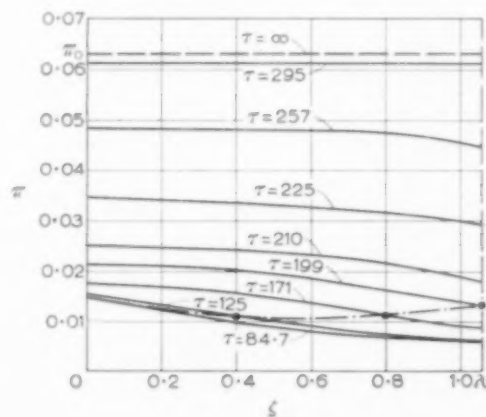


FIG. 7.

### Second and third period

From  $f(\phi)$  as given by Fig. 2 the function

$$\frac{1}{(\phi_0 - \phi)f(\phi)}$$

is plotted as curve 1 in Fig. 3. By integration the function

$$\int_0^1 \frac{ds}{(\phi_0 - s)f(s)}$$

is derived from this curve as shown by curve 2 in Fig. 3. This curve forms the basis of the distributions  $\phi$ , if  $\phi < 1$ .

At the end of the second period  $\zeta_c = \lambda$ . From equation (22) it follows that curve 2 (Fig. 3) gives the desired value of  $\phi$  at a given value of  $\zeta$ . In Fig. 4 the distribution for  $\zeta_c = 0$  and for  $\zeta_c = 1.06$  are plotted first. By parallel shift of the first one to the right and of the second one to the left, the intermediate distributions for  $\zeta_c = 0.2; 0.4; 0.6; 0.8$  are found. From curve 2 (Fig. 3) distributions for the third period are found by inserting  $\zeta_c = 1.2; 1.5; 2$  and  $3$ . These distributions can partially be found by parallel shift. Once Fig. 4 being completed the values of  $\phi_0 - \phi(0, \tau)$  and of  $\phi_0 - \phi(\lambda, \tau)$  can be obtained from this graph. This enables us to calculate  $d\zeta_c/d\tau$  as a function of  $\zeta_c$  as shown in Fig. 5. According to equation (23) the distribution of the drying potential is found by multiplication of  $\phi_0 - \phi$  as taken from Fig. 4, with the corresponding value of  $d\zeta_c/d\tau$  as read from Fig. 5. The result is given in Fig. 7. As mentioned before, the recirculation causes a steady increase of  $\pi$  at  $\zeta_c$  after some time. The calculations are completed by integration of

$$d\tau/d\zeta \text{ (curve 1, Fig. 6),}$$

giving the time  $\tau - \tau_1$  belonging to a given value of  $\zeta_c$ .

#### FINAL REMARKS

Starting with the equations (9) to (12) more general cases could be treated. For a rate of drying curve possessing a linear falling rate

section, calculations have been made by the author for the general case of an arbitrary initial distribution. In general, however, there will be no need for this, and sufficient information will be given by a study of the two cases described above.

It will be observed that, by means of some obvious modifications, cases such as the drying of thick beds of granular material by means of through circulation can be treated along the same lines.

#### NOTATION

- $a$  = recirculation ratio: part of the mass rate of flow through the drier that is recirculated; dimensionless.
- $b$  = correction factor, dimensionless.
- $F$  = moisture content, kg/m<sup>2</sup> of exposed surface.
- $F_0$  = initial value of  $F$ .
- $F_c$  = critical moisture content.
- $F_e$  = equilibrium moisture content.
- $h$  = height of drier, m.
- $H$  = specific humidity, kg H<sub>2</sub>O/kg of dry air.
- $H_s$  = specific humidity at saturation.
- $k$  = mass transfer coefficient, kg/m<sup>2</sup>h,  $V = 1$ .
- $L$  = length of drier, m.
- $P$  = total pressure, kg/m<sup>2</sup>.
- $p_1$  = partial H<sub>2</sub>O-pressure in bulk of air, kg/m<sup>2</sup>.
- $p_0$  = partial H<sub>2</sub>O-pressure at wet surface, kg/m<sup>2</sup>.
- $Q$  = dry-air mass-velocity, kg/m<sup>2</sup>h.
- $T$  = absolute temperature, K.
- $V$  = drying potential, dimensionless.
- $V_0$  = drying potential of fresh air.
- $V_L$  = drying potential of recirculated air.
- $z$  = co-ordinate, m.
- $\beta$  = correction factor, dimensionless.
- $\gamma_a$  = specific weight of dry air, kg/m<sup>3</sup>.
- $\tau$  = dimensionless parameters.
- $\zeta$  = defined by equation (8).
- $\pi$  = defined by equation (8).
- $\phi$  = value of  $\zeta$  at  $z = L$ .



## Diffusion in binary mixtures

C. O. BENNETT

Purdue University, West Lafayette, Indiana, U.S.A.

(Received 6 May 1957; in revised form 1 November 1957)

**Abstract**—The effect on the ordinary coefficient of diffusion of the mobilities of two interdiffusing, non-ionic components is evaluated by a straightforward application of the equations of irreversible thermodynamics along the lines suggested by DE GROOT [1]. The form of the resultant equations for the diffusion coefficient indicates that this approach does not agree with experiment so well as that of considering the effect of the different mobilities according to the equations proposed by DARKEN [2] and others. The analysis given in the text indicates that a binary diffusion coefficient is best calculated from the measured rates of diffusion of radio-active tracers by the equations of DARKEN [2].

**Résumé**—L'effet de la mobilité de deux composés non-ioniques, diffusant réciproquement, sur le coefficient ordinaire de diffusion, est évalué par une application directe des équations de thermodynamique irréversible, en accord avec les suggestions de DE GROOT [7]. La forme des équations, du coefficient de diffusion, qui en découlent, montre que cette approche du problème ne concorde pas aussi bien que l'expérience, que celle qui consiste à considérer l'action des différentes mobilités d'après les équations proposées par DARKEN [4] etc... L'analyse reproduite dans ce texte indique qu'il est préférable de calculer le coefficient binaire de diffusion à partir des mesures de vitesses de diffusion de traceurs radioactifs, d'après les équations de DARKEN [4].

**Zusammenfassung**—Die Wirkung der Beweglichkeiten von zwei ineinander diffundierenden, nicht ionisierten Komponenten auf den gewöhnlichen Diffusionskoeffizienten wird durch direkte Anwendung der Gleichungen der irreversiblen Thermodynamik gemäss den Überlegungen von DE GROOT [7] berechnet. Die Form der Endgleichungen für den Diffusionskoeffizienten zeigt, dass dieses Ergebnis nicht so gut mit dem Experiment übereinstimmt als die Betrachtung der Wirkung der verschiedenen Beweglichkeiten gemäss den Vorschlägen von DARKEN [4] und anderen. Die im Text mitgeteilte Untersuchung zeigt, dass ein binärer Diffusionskoeffizient am besten aus den gemessenen Diffusionsgeschwindigkeiten radioaktiver Indikatoren durch die Gleichungen von DARKEN [4] berechnet werden kann.

In common with many other natural processes, diffusion can be studied by postulating a mechanism and attempting to relate the observed rate of diffusion and the coefficient of diffusivity derived therefrom to the basic, known parameters for the molecules or atoms involved. On the other hand, the diffusion can be described from the macroscopic point of view by the use of the thermodynamics of irreversible processes. Whereas the former procedure is probably more fruitful for the relatively simple cases for which the theory is satisfactory, at present it is necessary to be satisfied with the phenomenological description in many non-ideal situations.

Radio-active tracers have proved very useful in measuring self-diffusion coefficients and have

also been used to some extent for measuring diffusion in binary mixtures. It is with particular regard to this latter situation that the equations to follow have been developed. Although developed in connexion with the measurements of gaseous diffusion at high pressure, because of their general thermodynamic nature, the relations hold also for liquids and in certain cases for solids.

The coefficient of diffusion of "1" in a mixture of "1" and "2,"  $D_{12}$ , will be defined for a non-ionic system by the equation:—

$$J_1 = - D_{12} (dc_1/dr) \quad (1)$$

for flow in one dimension at constant temperature and density with no driving forces present except the concentration gradient.  $J_1$  is the flux in

g moles/cm<sup>2</sup> sec relative to the molar average velocity. For the case where  $\rho$  is not independent of  $x$  (i.e. of  $y_1$ )  $D_{12}$  may conveniently be defined by:—

$$J_1 = -\rho D_{12} (dy_1/dx) \quad (2)$$

For flow relative to a stationary set of axes, define a flux  $N_1$  by

$$N_1 = J_1 + (N_1 + N_2) y_1 \quad (3)$$

Also, for the other component,

$$N_2 = J_2 + (N_1 + N_2) y_2 \quad (4)$$

and

$$J_2 = -\rho D_{21} (dy_2/dx) \quad (5)$$

In addition,

$$J_1 + J_2 = 0 \quad (6)$$

and, since  $y_1 + y_2 = 1.0$ ,  $D_{21}$  and  $D_{12}$  are identical; there is only one diffusion coefficient of the type defined by equation (1) needed for a binary mixture. The above results are well known, but they are presented here again in order to make the basis of the following discussion clear. The need for a careful definition of the basic factors in a diffusion problem has been emphasized at some length by BIRD [3].

Note that if the density were a function of  $y_1$ , equation (1) would give:—

$$J_1 = -D_{12} \left( \rho + y_1 \frac{d\rho}{dy_1} \right) \frac{dy_1}{dx} \quad (7)$$

and many equations in the subsequent development would be complicated by the appearance of the term involving  $d\rho/dy_1$ . Therefore it is convenient to define  $D_{12}$  by equation (2) for the unusual case of a variable density.

The introduction of equations (3) and (4) is consistent with equation (6), which is true in general. By the use of radio-active tracers to measure self-diffusion in either a pure component or a uniform mixture, experimental conditions are obtained for which  $N_1 = -N_2$ , and so  $N_i = J_i$ . The measured flux of the tracer can thus be simply related to the determination of  $D_{12}$ . Note that if there is no tracer, and a gradient is introduced into the same system as previously used with the tracer so that ordinary "chemical" diffusion results,  $N_1$  does not necessarily any

longer equal  $-N_2$ . The actual relation between  $N_1$  and  $N_2$  will depend upon the geometry of the diffusion-measuring system and the way in which  $\rho$  is related to the composition. Problems involving the evaluation of  $N_1$  and  $N_2$  have been discussed by BIRD [3]. JOST ([4], page 441) applies equations (3) and (4) to solvents evaporating through a capillary or to the slow dissolution of a salt in a similar geometrical arrangement. The relation between  $N_1$  and  $N_2$  will be determined by the change in volume of the salt as it dissolves and diffuses out, for example.

After this preliminary discussion, let us turn to the relation between  $D_{12}$  in a binary mixture and the measured rates of diffusion of radio-active tracers through the otherwise homogeneous mixture; that is, a mixture with no concentration gradient except that due to the radio-active tracer. We shall not here be concerned with the mathematics involved in obtaining a diffusion coefficient from measured concentration gradients in an unsteady-state experiment. This topic is well covered for many situations in the book by CRANK [5], for example.

Let us first see what understanding of the problem can be obtained from the thermodynamics of irreversible processes. For a mixture of 1 and 2, ([1], pages 100-104):—

$$J_1 = L_{11} \frac{d\mu_1}{dx} + L_{12} \frac{d\mu_2}{dx} \quad (8)$$

$$J_2 = L_{21} \frac{d\mu_1}{dx} + L_{22} \frac{d\mu_2}{dx} \quad (9)$$

Since it might be argued that there is no coupling effect in ordinary binary diffusion [6], one might set  $L_{12}$  in equation (8) equal to zero. For example, doing so and considering an ideal gas leads to the equation:—

$$\frac{L_{11}}{c_1} = \frac{-D_{12}}{RT} \quad (10)$$

For an ideal gas  $D_{12}$  is independent of concentration to a first approximation [7], and in many other cases  $D_{12}$  does not vary greatly with concentration. Therefore, it seems reasonable to define a new quantity,  $G_1$ , by:—

$$G_1 = L_{11}/c_1 \quad (11)$$

and also,

$$G_2 = L_{22}/c_2 \quad (12)$$

Although it will be seen below that equations (13) and (16) to be obtained from equations (8) and (9) with  $L_{12} = 0$  are not correct, the simple definitions of  $G_1$  and  $G_2$  given by equations (11) and (12) are generally useful and will be retained from here on. For an ideal gas, with  $L_{12}$  zero,

$$G_1 = G_2 = -D_{12}/RT \quad (13)$$

For a real solution, not necessarily gaseous,

$$d\mu_1 = RT d \ln a_1 \quad (14)$$

and  $a_1$  is conveniently defined as:—

$$a_1 = \frac{\gamma_1 c_1}{\rho} = \gamma_1 y_1 \quad (15)$$

so that,

$$D_{12} = -G_1 RT \left( 1 + y_1 \frac{\partial \ln \gamma_1}{\partial y_1} \right) = -G_1 \psi_1 RT \quad (16)$$

for  $L_{12} = 0$ .

Before considering the case where  $L_{12} \neq 0$ , let us consider another approach ([8], [9], [10]). If  $d\mu_1/dx$  is viewed as a "virtual force," a mobility  $G_1'$ , can be defined as the average molecular velocity in the  $x$ -direction under unit force. Then the number of molecules passing a unit area per second is:—

$$c_1 G_1' (d\mu_1/dx)$$

and so a flux in terms of moles is

$$\frac{c_1 G_1'}{N} \frac{d\mu_1}{dx} = \phi_1 \quad (17)$$

where  $N$  is Avogadro's number. The coefficient  $G_1$  already introduced is merely  $G_1'/N$ . The mobility may be regarded as defining a flux of molecules of one component relative to a set of axes fixed in the bulk of the fluid. Because of the obvious differences in mobilities of the molecules of the components of a gaseous or liquid mixture, and the existence of the KIRKENDALL effect ([11], [12]) equation (16) cannot be expected to hold. Since using a tracer is really a direct way (see below) of measuring the mobility, and since the mobilities found by using first active "1" and then active "2" as tracers are different, equation (16) would have

the impossible result of giving two values of  $D_{12}$  for the same conditions.

Let us now reconsider equations (8) and (9) with  $L_{12} \neq 0$  and see whether the term involving  $L_{12}$  can account for the observed differences in mobility. Using equation (11), the Gibbs-Duhem equation,  $L_{12} = L_{21}$ , and the fact that  $J_1$  must equal  $-J_2$ , there follows:—

$$G_1 - G_2 = \frac{L_{12}}{\rho} \left( \frac{1}{y_2} - \frac{1}{y_1} \right) \quad (18)$$

By combining (8) and (18),

$$J_1 = (G_2 y_1 - G_1 y_2) \rho \frac{y_1}{y_1 - y_2} \frac{d\mu_1}{dx} \quad (19)$$

For this case:—

$$D_{12} = RT \frac{(G_1 y_2 - G_2 y_1)}{y_1 - y_2} \psi_1 \quad (20)$$

where,

$$\psi_1 = \left( \frac{\partial \ln \gamma_1}{\partial \ln y_1} + 1 \right)$$

and so:—

$$\frac{d\mu_1}{dx} = \frac{RT}{y_1} \psi_1 \frac{dy_1}{dx} \quad (21)$$

According to DE GROOT [1] and also, for example, JOST ([4], page 498) or ordinary binary diffusion  $L_{11} = -L_{12} = L_{22}$  so that:—

$$y_1 G_1 = -L_{12}/\rho = y_2 G_2 \quad (22)$$

and equation (20) reduces to,

$$D_{12} = RT \psi_1 G_1/y_2 = -RT \psi_1 G_2/y_1 \quad (23)$$

Equation (22) follows from a mathematical treatment of the equations of irreversible thermodynamics ([1], pages 101-104). It is shown that if  $d\mu_1/dx$  is set equal to  $d\mu_2/dx$ ,  $L_{11}$  equals  $-L_{12}$ , and since the  $L$ 's are not functions of the driving forces ( $d\mu_1/dx$  and  $d\mu_2/dx$ ),  $L_{11}$  should equal  $L_{12}$  for other values of the driving forces. Two facts lead one to question the applicability of this reasoning to ordinary binary diffusion. First, no physical situation exists for which  $d\mu_1/dx$  equals  $d\mu_2/dx$  except the trivial case where both equal zero. Second, in order to change the relative magnitudes of  $d\mu_1/dx$  and  $d\mu_2/dx$  (i.e., make them unequal) the concentration must be varied. Thus, in order to retain  $L_{11} = -L_{12}$  it would

be necessary for the  $L$ 's to be independent of concentration in addition to driving force.

For the special case of measurements using a tracer "2" in a bulk of normal "1" of the same chemical species,  $y_2 \approx 0$ , and  $\psi_1$  and  $\psi_2$  both equal unity, so according to equation (20) :—

$$D_{12} = -RT G_2 = -RT G_1 = D_1^* \quad (24)$$

and  $L_{12}$  is rigorously zero.  $D_{12}$  is the coefficient of self-diffusion in this case; let us call it  $D_1^*$ . This is a quite reasonable result. However, given the physically reasonable assumption that  $G_1$  essentially equals  $G_2$  for this case, equation (22) is not satisfied, casting further doubt on the statement that :—

$$L_{11} = L_{22} = -L_{12}$$

In a ternary mixture we write down :—

$$\left. \begin{aligned} J_1 &= G_1 y_1 \rho \frac{d\mu_1}{dx} + L_{12} \frac{d\mu_2}{dx} + L_{13} \frac{d\mu_3}{dx} \\ J_2 &= L_{12} \frac{d\mu_1}{dx} + G_2 y_2 \rho \frac{d\mu_2}{dx} + L_{23} \frac{d\mu_3}{dx} \\ J_3 &= L_{13} \frac{d\mu_1}{dx} + L_{23} \frac{d\mu_2}{dx} + G_3 y_3 \rho \frac{d\mu_3}{dx} \end{aligned} \right\} \quad (25)$$

This case is of interest in the present discussion if one of the components ("2") is a tracer of the same chemical species as the normal "1"; "3" represents the normal second chemical species. If the tracer is introduced into an otherwise homogeneous mixture of "1" and "3," there results  $J_1 = -J_2$  and  $J_3 = 0$ . Also  $d\mu_3/dx = 0$ . Therefore the equations (25) give once more equation (19), with the added requirement that :—

$$y_1 L_{23} = y_2 L_{13} \quad (26)$$

Since  $y_2 \approx 0$ ,  $L_{23}$  is zero;  $L_{13}$  is not necessarily zero. Indeed, since  $L_{13}$  is actually the same as the cross coefficient for the two normal species, it should not be zero. In addition, equation (19) for  $y_2 \approx 0$  reduces to :—

$$J_1 = G_2 \rho y_1 (d\mu_1/dx) = -J_2$$

and,

$$J_2 = G_2 \rho y_2 (d\mu_2/dx) = G_2 RT (dc_2/dx) \quad (27)$$

Equation (27) shows that the rate of diffusion of a tracer in an otherwise homogeneous binary mixture gives a direct measurement of  $G_1$ , and by using a tracer of the other component  $G_3$  can be obtained. The ordinary diffusivity is then calculated from :—

$$D_{13} = RT \frac{(G_1 y_3 - G_3 y_1)}{y_1 - y_3} \psi_1 \quad (28)$$

and,

$$L_{13} = (G_1 - G_3) \frac{\rho y_3 y_1}{y_1 - y_3} \quad (29)$$

The equations developed require a somewhat surprising variation in  $G_1$  and  $G_3$  with  $y_1$ . In particular, at  $y_1 = 0.5$ ,  $G_1 = G_3$ ; the behaviour is not in accord with measurements on the diffusion of active silver and active gold in a 50 per cent Ag-Au alloy ([2], [12]). The equations to be given below describe this case more adequately and permit  $G_1$  to differ from  $G_3$  at  $y_1 = 0.5$ , as is observed experimentally. A possible variation of the various coefficients as a function of  $y_1$  required by equation (28) is given in Fig. 1.

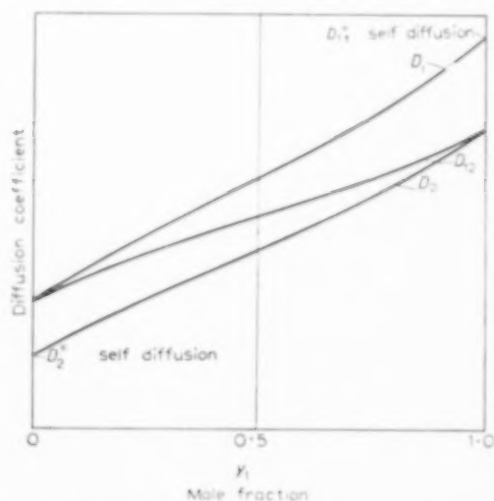


FIG. 1. Schematic curves of the variation of various coefficients according to equation (28).

It seems correct to state that irreversible thermodynamics as applied here do not give a reasonable interpretation of the situation, although there are at present few data on which to base conclusions.

Now consider the case of the chemical diffusion of "1" through "3" where there is a known portion of active "1" present, which we shall call "2." In this case all three of the equations (25) are needed, and  $d\mu_3/dx \neq 0$ .

However,  $y_1/y_2$  is a constant, so that:—

$$\frac{dy_1}{y_1 dx} = \frac{dy_2}{y_2 dx}$$

Also,

$$\frac{d\mu_2}{dx} = \frac{RT}{y_2} \psi_1 \frac{dy_2}{dx}$$

and,

$$\frac{d\mu_1}{dx} = RT \frac{\psi_1}{y_1} \frac{dy_1}{dx} \text{ where } \psi_1 \neq 1.0$$

Thus:—

$$\frac{d\mu_1}{dx} = \frac{RT}{y_2} \psi_1 \frac{dy_2}{dx} = \frac{d\mu_2}{dx} \quad (30)$$

and from equation (25):—

$$J_1 = \left( G_1 y_1 \rho + L_{12} - L_{13} \frac{y_1}{y_3} \right) \frac{RT}{y_1} \psi_1 \frac{dy_1}{dx} \quad (31)$$

$$J_2 = \left( L_{12} + G_2 y_2 \rho - L_{23} \frac{y_1}{y_3} \right) \frac{RT}{y_1} \psi_1 \frac{dy_1}{dx} \quad (32)$$

$$J_3 = (L_{13} + L_{23} - G_3 \rho y_1) \frac{RT}{y_1} \psi_1 \frac{dy_1}{dx} \quad (33)$$

If, as postulated in irreversible thermodynamics, the coefficients  $L$  depend on the composition and not on the value of the driving forces, for a mixture having the same composition as that considered in the previous section it is permissible to use the values of  $L$  already determined. From the previous results,  $L_{23} = 0$  and  $L_{13}$  is given by equation (29). Thus:—

$$J_1 = RT \psi_1 \left[ \left( \frac{G_3 y_1 - G_1 y_3}{y_1 - y_3} \right) + \frac{L_{12}}{\rho y_1} \right] \rho \frac{dy_1}{dx} \quad (34)$$

and,

$$D_{13} = RT \frac{G_1 y_3 - G_3 y_1}{y_1 - y_3} \psi_1 - \frac{L_{12}}{\rho y_1} \psi_1 \quad (35)$$

The value of  $D_{13}$  obtained from equation (28) and from equation (35) would be the same only if  $L_{12}/\rho y_1$  is negligible, but since "1" and "2" are chemically identical and have been assumed to diffuse at the same relative rates, it may be that the term actually is negligible.

Alternatively ([1], [2], [5], [13]) the whole problem can be treated by leaving out any cross coefficients such as  $L_{12}$ , etc. A flux  $\phi_1$ , relative to an axis moving at the molar average velocity can be defined as:—

$$\phi_1 = -D_1 \rho (dy_1/dx) \quad (36)$$

and, noting that  $\phi_i$  and  $J_i$  are referred to the same axis,

$$J_1 = \phi_1 - (\phi_1 + \phi_2) y_1 \quad (37)$$

$$J_2 = \phi_2 - (\phi_1 + \phi_2) y_2 \quad (38)$$

in a binary system, where  $\phi_1$  is positive in the positive  $x$ -direction and  $J_1 = -J_2$ . Notice that the term  $(\phi_1 + \phi_2) y_1$  arises from the difference of the molecular mobilities; it has nothing to do with whether  $N_1 = -N_2$  or not.  $J_1$  may be viewed as the sum of  $\phi_1$ , the basic diffusion flux arising from the gradient of chemical potential, and  $-(\phi_1 + \phi_2) y_1$ , a flux caused by displacement to satisfy  $J_1 = -J_2$ . In addition,

$$N_1 = \phi_1 - (\phi_1 + \phi_2) y_1 + (N_1 + N_2) y_1 \quad (39)$$

The term  $N_1 + N_2$  results from the bulk, hydrodynamic flow of the system in which diffusion is taking place; it is influenced by the geometry of the apparatus and the way in which the density of the mixture varies with composition. The term  $-(\phi_1 + \phi_2)$  represents a flow on a molecular scale relative to an axis fixed at the "centre of moles" of the fluid, i.e., an axis moving with a velocity related to the flux  $N_1 + N_2$ . The magnitude of  $-(\phi_1 + \phi_2)$  is fixed by the mobilities of the diffusing molecules—i.e. by the state of the system, and it is not influenced by the external arrangements which cause hydrodynamic flow. Possible relative magnitudes of these quantities are illustrated in Fig. 2. The arrows are vectors for the one-dimensional case being considered. For the case of diffusion in a solid, the movement of inert markers is related to the flux  $(N_1 + N_2 - \phi_1 - \phi_2)$ .

By combining equations (1), (36) and (37) one obtains:—

$$J_1 = \phi_1 y_2 - \phi_2 y_1 - D_{12} \frac{dy_1}{dx} = -y_2 D_1 \frac{dy_1}{dx} - y_1 D_2 \frac{dy_1}{dx} \quad (40)$$



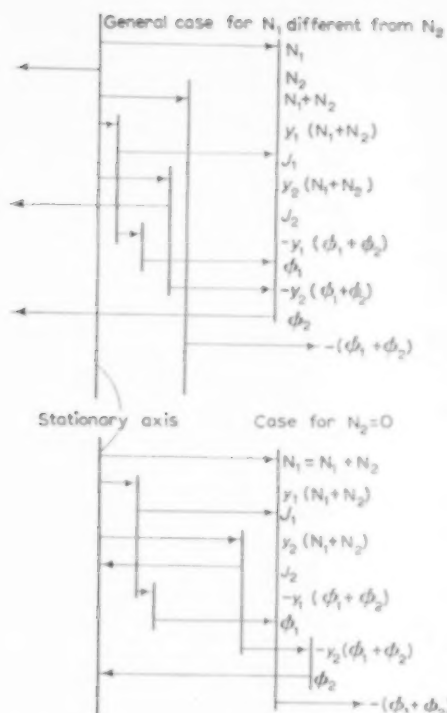


FIG. 2. Vectors representing the relative magnitudes of the various fluxes at a point at which  $y_1 = 0.2$  and  $|\phi_2| > |\phi_1|$ .

and,

$$D_{12} = y_2 D_1 + y_1 D_2 \quad (41)$$

If the flux  $\phi_1$  is given by:—

$$\phi_1 = G_1 c_1 d\mu_1/dx \quad (42)$$

as suggested by the discussion leading to equation (17), the quantities  $G_1$  and  $G_2$  can be determined by measurements with tracers of "1" and "2" in an otherwise homogeneous mixture. From (36) and (42),

$$D_1 = -RT G_1 \psi_1 \quad (43)$$

and,

$$D_2 = -RT G_2 \psi_1 \quad (44)$$

Thus:—

$$D_{12} = -RT (y_2 G_1 + y_1 G_2) \left( 1 + \frac{d \ln y_1}{d \ln y_1} \right) \quad (45)$$

In contrast to equation (20), equations (41) and (45) certainly seem to require a variation of the various

coefficients with concentration which appears intuitively satisfactory, and moreover which is in accord with available data ([14], [15]). A sketch of these curves is given in Fig. 3.

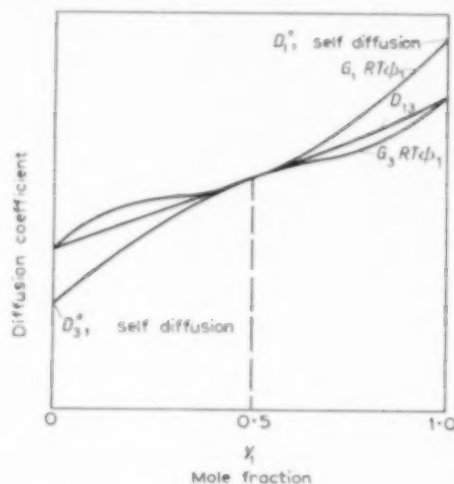


FIG. 3. Schematic curves of the variation of the various coefficients with concentration according to equation (37).

## CONCLUSION

The equations proposed for steady-state, one-dimensional diffusion in a binary mixture are:—

$$N_1 = J_1 + (N_1 + N_2) y_1 \quad (3)$$

$$J_1 = -D_{12} \rho (dy_1/dx) \quad (1)$$

$$D_{12} = -RT (y_2 G_1 + y_1 G_2) \psi_1 \quad (45)$$

where the mobilities  $G_1$  and  $G_2$  can be obtained from measurements on the rate of diffusion of tracers of 1 and 2 in otherwise homogeneous mixtures. These equations are essentially those of DARKEN [2].

The basic diffusion equations involved in the above relations are obtained from equations (40) and (42), giving:—

$$J_1 = G_1 c_1 y_2 (d\mu_1/dx) - G_2 c_2 y_1 (d\mu_2/dx) \quad (46)$$

On the other hand, equations (8) and (9) from irreversible thermodynamics lead to:—

$$J_1 = G_1 c_1 \frac{d\mu_1}{dx} + L_{12} \frac{d\mu_2}{dx} \quad (47)$$

or, using equation (18),

$$J_1 = G_1 c_1 \frac{d\mu_1}{dx} + \left[ \frac{G_1 c_1 y_2 - G_2 c_2 y_1}{y_1 - y_2} \right] \frac{d\mu_2}{dx} \quad (48)$$

If DE GROOT's assertion that  $G_1 c_1 = G_2 c_2$  is accepted, equation (48) becomes:—

$$J_1 = G_1 c_1 \left( \frac{d\mu_1}{dx} - \frac{d\mu_2}{dx} \right) \quad (49)$$

Although equation (46) seems to be in reasonable accord with experimental results ((14) and (15), for example), neither equation (48) nor (49) appear to be in accord with the results obtained in binary systems involving ordinary diffusion.

The conclusions which may be drawn from the above remarks may be summarized as follows:—

1. Although equations (28), (48) and (49) are not in agreement with experimental data, only limited conclusions should be drawn from this point. The Onsager relations and equations (8) and (9) have proven their validity in many other cases, such as the treatment of thermal diffusion, to name only one.
2. Equation (45) and the related equations certainly can be viewed as owing much in their derivation to one of the basic ideas of irreversible thermodynamics, namely, that in diffusion there is a linear relation between the flux and the gradient of chemical potential. This idea is at least as attractive as that of a "virtual force."

*Acknowledgement*—The financial support of the office of Ordnance Research is gratefully acknowledged. Experimental measurements using  $A^{37}$  and  $C^{14}O_2$  are presently being carried out in this laboratory.

#### NOTATION

- $D_{ik}$  = coefficient of diffusion,  $\text{cm}^2/\text{sec}$ , defined by the equation  $J_i = -D_{ik} \rho (dy_i/dx)$
- $D_i$  = coefficient of diffusion,  $\text{cm}^2/\text{sec}$ , defined by the equation  $\phi_i = -D_i \rho \frac{dy_i}{dx}$ .
- $G_i$  = mobility,  $\text{g mole cm/sec-dyn}$ , defined by the equation  $\phi_i = G_i c_i \frac{d\mu_i}{dx}$ .
- $J_i$  = flux relative to an axis across which  $J_i = -J_k$ ,  $\text{g mole/cm}^2 \text{ sec}$  i.e., an axis moving at molar average velocity
- $L_{ik}$  = coefficient in Onsager's equations,  $(\text{g mole})^2/\text{sec-dyn-cm}^2$
- $N_i$  = flux relative to a stationary axis,  $\text{g. mole/cm}^2 \text{ sec}$
- $R$  = gas constant,  $\text{dyn-cm/g mole}^\circ\text{K}$
- $T$  = absolute temperature,  $^\circ\text{K}$
- $a_i$  = activity
- $c_i$  = concentration,  $\text{g mole/cm}^3$
- $x$  = distance,  $\text{cm}$
- $y_i$  = mole fraction
- $\gamma_i$  = activity coefficient
- $\mu_i$  = chemical potential,  $\text{dyn-cm/g mole}$
- $\phi_i$  = flux relative to an axis moving at the molar average velocity and related to the molecular mobility by  $\phi_i = G_i c_i (d\mu_i/dx)$ ,  $\text{g mole/cm}^2 \text{ sec}$ . It accounts for only part of  $J_i$ , to which it is related by equation (40).
- $\phi_i = 1 + \frac{\partial \ln \gamma_i}{\partial \ln y_i}$
- $\rho$  = density,  $\text{g mole/cm}^3$

#### BIBLIOGRAPHY

- [1] DE GROOT S. R. *Thermodynamics of Irreversible Processes* Interscience. New York 1951.
- [2] DARKEN L. S. *Trans. Amer. Inst. Min. (Metall.) Engrs.* 1948 **175** 184-94.
- [3] BIRD R. B. *Advances in Chemical Engineering* pp. 156-239. Academic Press, New York 1956.
- [4] JOST W. *Diffusion in Solids, Liquids, Gases.* Academic Press, New York 1952.
- [5] CRANK J. *The Mathematics of Diffusion.* Oxford 1956.
- [6] DENBIGH K. G. *Thermodynamics of the Steady State.* Methuen, London, 1951.
- [7] CHAPMAN S. and COWLING T. G. *Mathematical Theory of Non-uniform Gases.* Cambridge University Press 1939.
- [8] ONSAGER L. and FUOSS R. M. *J. Phys. Chem.* 1932 **36** 2689-2778.
- [9] LECCLAIRE A. D. *Progress in Metal Physics* vol. 1, pp. 306-79. Interscience, New York 1949.
- [10] EINSTEIN A. *Ann. Phys., hpc.* 1905 **17** 549; *Ibid.* 1906 **19** 18.
- [11] SMIGELSKAS A. D. and KIRKENDALL E. O. *Trans. Amer. Inst. Min. (Metall.) Engrs.* 1947 **171** 120-35.
- [12] HARTLEY G. S. *Trans. Faraday Soc.* 1946 **42 B** 6.
- [13] MATANO C. *Jap. J. Phys.* 1923 **8** 100-13.
- [14] JOHNSON W. A. *Trans. Amer. Inst. Min. (Metall.) Engrs.* 1942 **147** 331-47.
- [15] REYNOLDS J. E., AVERBACH B. L. and COHEN M. *Acta (Met.)* 1957 **5** 29-40.

## Heat transfer between a fluidized bed and a horizontal tube

H. A. VREEDENBERG

Koninklijke/Shell-Laboratorium, Amsterdam

(Received 1 November 1957)

**Abstract**—Measurements of coefficients of heat transfer from fluidized beds to horizontal water-cooled tubes are discussed. The bed diameter was 0.565 m. The following quantities were varied: (1) bed temperature; (2) mass velocity of the fluidizing air; (3) mean particle diameter; (4) particle shape; (5) particle density; (6) water-tube diameter. The second, third and fifth quantities were varied down to much lower values than before [1]; the sixth quantity had not previously been varied.

The results of old and new experiments are correlated by two different formulae, one for the range where the viscous forces on the particles are predominant and an analogy between the fluidized bed and a flowing gas or liquid is assumed, and another for the range of coarser and heavier particles where inertia effects prevail. The distinction between the two ranges is characterized by the value of a Reynolds group. The limitations of the applicability of the correlations are discussed.

**Résumé**—L'auteur discute des mesures des coefficients du transfert de chaleur à partir de lits fluidisés vers des tubes refroidis à l'eau. Le diamètre du lit était de 0.565 m. On a fait varier les facteurs suivants: (1) température du lit; (2) vitesse massique de l'air fluidisant; (3) diamètre moyen des particules; (4) forme des particules; (5) densité des particules; (6) diamètre des tubes à eau. Les facteurs sous (2), (3) et (5) ont été variés jusqu'à des valeurs beaucoup plus basses qu'auparavant [1]. Le facteur sous (6) n'avait pas été varié avant.

Les résultats des expériences antérieures et présentes sont mis en corrélation à l'aide de deux formules différentes, une pour l'intervalle où dominent les forces visqueuses agissant sur les particules et où l'on admet qu'il existe une analogie entre le lit fluidisé et un courant de gaz ou de liquide, et une autre pour l'intervalle des particules plus grossières et plus lourdes où agissent des effets d'inertie. La distinction entre les deux est caractérisée par la valeur d'un groupe Reynolds. On discute les limitations de l'applicabilité des corrélations.

**Zusammenfassung**—Messungen der Koeffizienten der Wärmeübertragung von Fließbetten an waagerechte wassergekühlte Rohre werden besprochen. Der Bett-Durchmesser betrug 0.565 m. Folgende Folgende Grossen wurden verändert: (1) Bett-Temperatur, (2) Luftgeschwindigkeit, (3) Mittlere Teilchendurchmesser, (4) Teilchenform, (5) Teilchendichte, (6) Durchmesser des Wasserrohres.

Die zweite, dritte und fünfte Grösse wurden bis zu viel kleineren Grossen variiert als bisher [1]; die sechste Grösse wurde bisher nicht geändert.

Die Ergebnisse der alten und neuen Versuche wurden durch zwei verschiedene Gleichungen korreliert, eine für jenen Bereich, in dem die Zähigkeitskräfte an den Teilchen vorherrschen und eine Analogie zwischen dem Fließbett und einem strömenden Gas oder einer Flüssigkeit angenommen werden kann, und eine andere für den Bereich gröberer und schwererer Teilchen, in dem die Trägheitswirkungen vorherrschen. Die Unterscheidung zwischen den beiden Bereichen ist durch den Wert einer Reynolds-Zahl gekennzeichnet. Die Grenze der Anwendbarkeit der Beziehungen werden besprochen.

## 1. INTRODUCTION

A FEW years ago, the results of some measurements of the coefficient of heat transfer from a large-scale fluidized bed to a horizontal water-cooled tube were presented [1]. Beds consisting of various kinds of coarse sand and iron ore were

investigated. The diameter of the tube was not varied. Many data were obtained on the influence of bed temperature and mass velocity of the fluidizing air. It was found that the heat-transfer coefficient was independent of the air pressure when the linear velocity of the air in the bed remained

Table 1. Experiments with a horizontal tube 0.85 m above the sieve plate. The height of the bed was 1.2 m in the non-fluidized state; the bed diameter was 0.565 m

Material	Mean volume-surface particle diameter [3]	Weight-mean diameter [3]	Particle density	Minimum value of product of mass velocity and kinematic viscosity at which fluidization was observed	Particle shape	Outer diameter of tube	Mass velocity of air	Curve in Figs. 1, 2, 3, 5, and 6
	$D_p$		$\rho_s$			$D_t$	$G$	
	(m $\times 10^{-6}$ )	(m $\times 10^{-6}$ )	(kg/m <sup>3</sup> $\times 10^3$ )	(kg/sec <sup>2</sup> $\times 10^{-6}$ )		(m)	(kg/m <sup>2</sup> sec)	
Regenerated cracking catalyst	63.5	68	1.60	0.065	Sharp	0.0169	0.0103	G ---- G
						0.0169	0.0152	H ---- H
						0.0169	0.0642	I ---- I
						0.0169	0.097	J ---- J
						0.0336	0.0103	G ---- G
						0.0336	0.0153	H ---- H
						0.0336	0.0636	I ---- I
						0.0336	0.097	J ---- J
						0.0336	0.149	K ---- K
						0.0510	0.0155	H ---- H
Sand used for sand-blasting	136	187	2.66	0.42	Sharp	0.0169	0.0457	T ---- T
						0.0169	0.0771	U ---- U
						0.0336	0.0459	T ---- T
						0.0336	0.0773	U ---- U
						0.0510	0.0460	T ---- T
						0.0510	0.0753	U ---- U
Dune sand	213	230	2.66	0.65	Round	0.0169	0.0555	A ---- A
						0.0169	0.095	B ---- B
						0.0336	0.0562	A ---- A
						0.0336	0.096	B ---- B
New type of Maas sand	316	393	2.66	1.09	Sharp	0.0169	0.099	C ---- C
						0.0169	0.161	D ---- D
						0.0331	0.102	C ---- C
						0.0331	0.163	D ---- D
						0.0336	0.100	C ---- C
						0.0336	0.159	D ---- D
						0.0510	0.099	C ---- C
						0.0510	0.160	D ---- D

constant. The influences of bed-height and location of the diametrical tube were smaller than 20 per cent.

Since then some complementary measurements with much finer and lighter particles have been made, and stainless-steel tubes with various diameters have been applied. The bed temperature and the mass velocity of the air were varied in the same way as before. The air pressure, the bed height, and the position of the tube were kept constant.

In what follows old and new results will be correlated by two different formulae, one for the

range of fine and light particles, and another for the range of coarse and heavy particles. The transition between the ranges of validity of the two expressions will be discussed.

In a subsequent publication similar correlations for heat transfer between a fluidized bed and a vertical tube will be derived from the data already published by us [2] and those of other investigators.

## 2. HEAT-TRANSFER MEASUREMENTS

The experimental setup, the test procedure, and the method of dealing with the data have

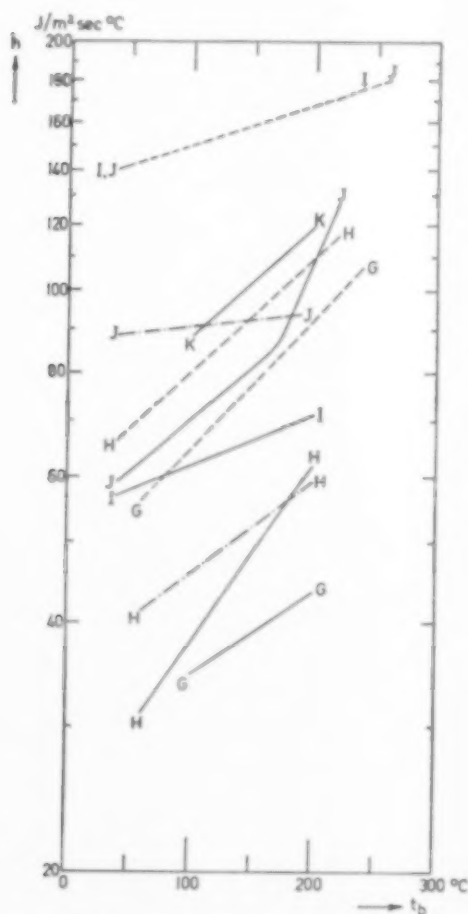


FIG. 1. Coefficients of heat transfer  $h$  from beds of catalyst at various mass velocities to horizontal tubes with different diameters, as functions of the bed temperature  $t_b$  (see Table 1).

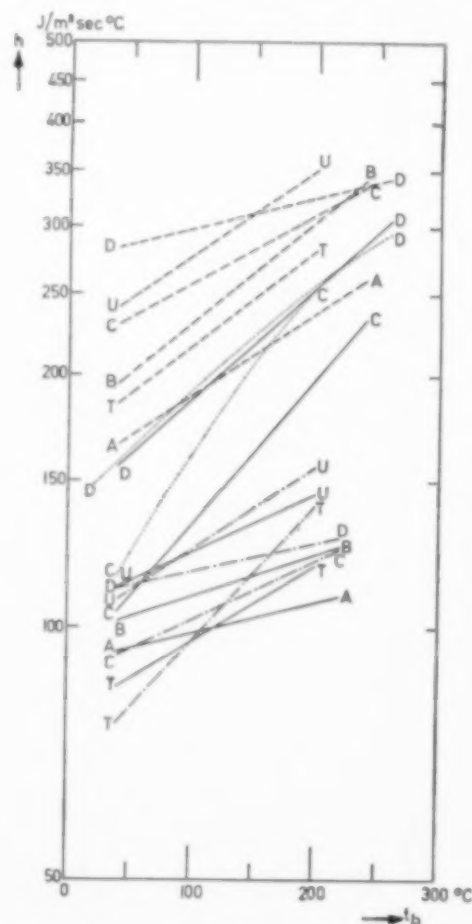


FIG. 2. Coefficients of heat transfer  $h$  from beds of sand at various mass velocities to horizontal tubes with different diameters, as functions of the bed temperature  $t_b$  (see Table 1).

been described previously [1]. Table 1 summarizes the new series of experiments, the results being shown in Figs. 1 and 2. The increase in the heat-transfer coefficient  $h$  with increasing bed temperature or mass velocity has already been discussed [1]. A similar increase is found at constant mass velocity, when the tube diameter is decreased; this effect is analogous to the well-known increase in the coefficient of heat transfer between a tube and a fluid flowing normally to that tube with decreasing tube diameter.

### 3. PRESSURE MEASUREMENTS

Pressure measurements were made in the same way as previously described [2]. The results obtained with the four different horizontal tubes did not appear to differ.

With all kinds of sand the pressure drop per unit length proved to be independent of the location in the bed, and the porosity  $\epsilon$  could be derived from it in the same way as before [2]. This procedure was justified because the total pressure drop was equal to the total weight of the bed per unit of area. Some results are given in Fig. 3.

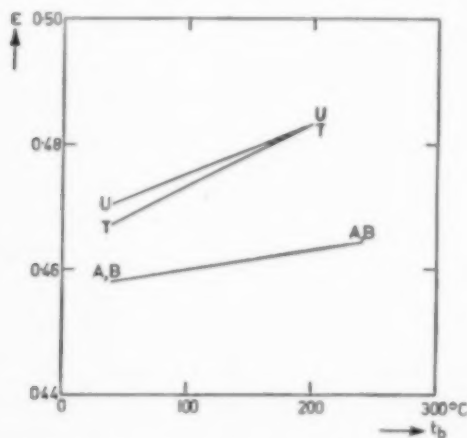


Fig. 3. The porosities  $\epsilon$  of beds of sand at various mass velocities, as functions of the bed temperature  $t_b$  (see Table 1).

The absence of any measurable difference between the two curves observed with dune sand may be owing to experimental error.

With catalyst the pressure drop per unit length was by no means independent of the location in

the bed. The results obtained in the upper part of the bed agreed in some measure with those obtained with sand, but in the lower part some remarkable features were observed. The apparent values  $\epsilon_1$  of the porosity, derived in the usual way from the pressure measurements in the lower part of the bed, decreased with increasing mass velocity  $G$  and, at low values of  $G$ , also with rising bed temperature. It was concluded that  $\epsilon_1$  did not represent the true porosity  $\epsilon$ , the pressure drop being unequal to the weight of the bed per unit of area. All these anomalies could be ascribed to a combination of two phenomena:—

Segregation of the catalyst particles, so that the majority of the coarser particles will move to the lower part of the bed, and the majority of the finer particles to the upper part. This effect will cause the porosities  $\epsilon$  and  $\epsilon_1$  to be higher in the upper part of the bed than in the lower part; the difference will decrease with increasing mass velocity  $G$  owing to better mixing of all particles throughout the bed. It was found, however, still to exist even at the highest values of  $G$  applied in the present investigation.

Channelling is an effect which has been described by various authors [4, 5]. LEVA [4] states that it is promoted by low mass velocities and low mean particle diameters, by large bed diameters, and by the presence of moisture. All but the last of these factors are favourable to the occurrence of channelling in our experiments with catalyst. It causes a decrease in the pressure drop, which becomes lower than the weight of the bed per unit of area [4, 5]; differences up to 28 per cent were observed. Accordingly,  $\epsilon_1$  will become higher than  $\epsilon$ . The main reason is that a great part of the particles are supported by the sieve plate instead of being borne by the flow of fluidizing gas. It follows that the effect is most important in the lower part of the bed, and that it decreases with increasing mass velocity  $G$ . At the highest value of  $G$  applied it was absent even in the lower part of the bed, since the total pressure drop was found to be equal to the total weight of the bed per unit of area.



The distance between the sieve plate and the horizontal tube was so large that channelling did not occur at the location of the tube. Therefore, the local value of  $\epsilon$  could be derived in the usual way from pressure measurements in the upper part of the bed. Results are given in Fig. 4. No

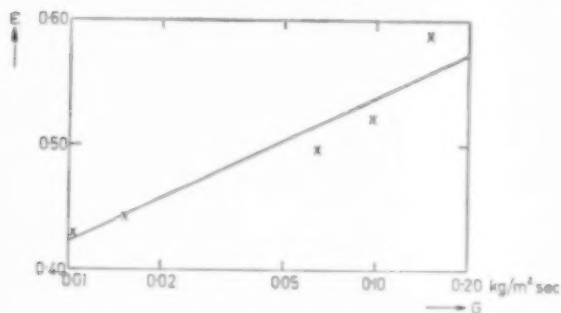


FIG. 4. The porosity  $\epsilon$  of the upper part of a bed of catalyst as a function of the mass velocity  $G$ .

systematic influence of the bed temperature on  $\epsilon$  was observed, possibly because the normal increase in  $\epsilon$  with increasing bed temperature compensated for a decrease in the effect of segregation. The large influence of the mass velocity is due to the wide range of values of  $G$  covered in the experiments with catalyst.

#### 4. CORRELATION FORMULAE

Since the experimental data obtained with fine particles, such as catalyst, and with tubes of various diameters, cannot be represented by an expression as simple as the correlation of previous results [1], a discussion of new correlation formulae covering old and new data will follow.

It has proved to be worth while to describe the new results with fine and light particles, namely catalyst, sand used for sand-blasting, and dune sand, separately from those with coarser and heavier materials. This distinction between two groups of particles may be connected with a difference in the nature of their motion in the gas currents, and the assumption will be made that the fine and light particles will almost exactly follow the paths of the gas, whereas the coarser and heavier particles, owing to their inertia, will have a motion that is less dependent on these paths. Of course, such an assumption may over-

simplify the picture, but a reasonable description of the experimental results obtained with fine and light particles may be derived from it.

If the paths of the fine and light particles do not differ from those of the gas, the mixture of gas and particles can be considered as one fluid moving in the same way as the fluidizing gas. This cannot be true throughout the bed, but the greater part of the horizontal water tube will be in the inner zone of the bed where both the particles and the gas are moving upward [2], so that there it may be correct to consider the mixture as one fluid.

Coefficients of heat transfer between a tube and a gas or liquid flowing normally to that tube can be represented by plotting the Nusselt group divided by  $Pr_{0.3}$  as a function of the Reynolds group [6]. Therefore the assumed analogy between a fluidized bed of fine and light particles and a fluid could be checked by attempting to represent the experimental results obtained with these particles by a relationship between:—

$$\frac{hD_t k}{(c\mu/k)^{0.33}} \text{ and } \frac{GD_t \rho_s (1 - \epsilon)}{\rho \mu \epsilon}$$

The Reynolds group  $GD_t \rho_s (1 - \epsilon) / \rho \mu \epsilon$  contains the bed density which, since the contribution  $\rho \epsilon$  of the gas is negligible as compared with the contribution  $\rho_s (1 - \epsilon)$  of the particles, is equal to the latter contribution, and the interstitial gas velocity  $G / \rho \epsilon$  which has to be used since, in general, the particle velocity in a fluidized bed is unknown. Similar arguments apply to the other quantities occurring in the Reynolds group, the Nusselt group  $hD_t / k$ , and the Prandtl group  $c\mu / k$ .

Fig. 5 proves that it is indeed possible to give, by means of a relation between the two groups considered, a fair representation of the results of all the measurements with fine and light particles specified in Table 1. The experimental curves do not deviate by more than 42 per cent from the straight line:—

$$\frac{hD_t / k}{(c\mu/k)^{0.33}} = 0.66 \left( \frac{GD_t \rho_s (1 - \epsilon)}{\rho \mu \epsilon} \right)^{0.44}$$

A good correlation of all the data for coarse and heavy particles, namely the new type of Maas sand

# Heat transfer between a fluidized bed and a horizontal tube

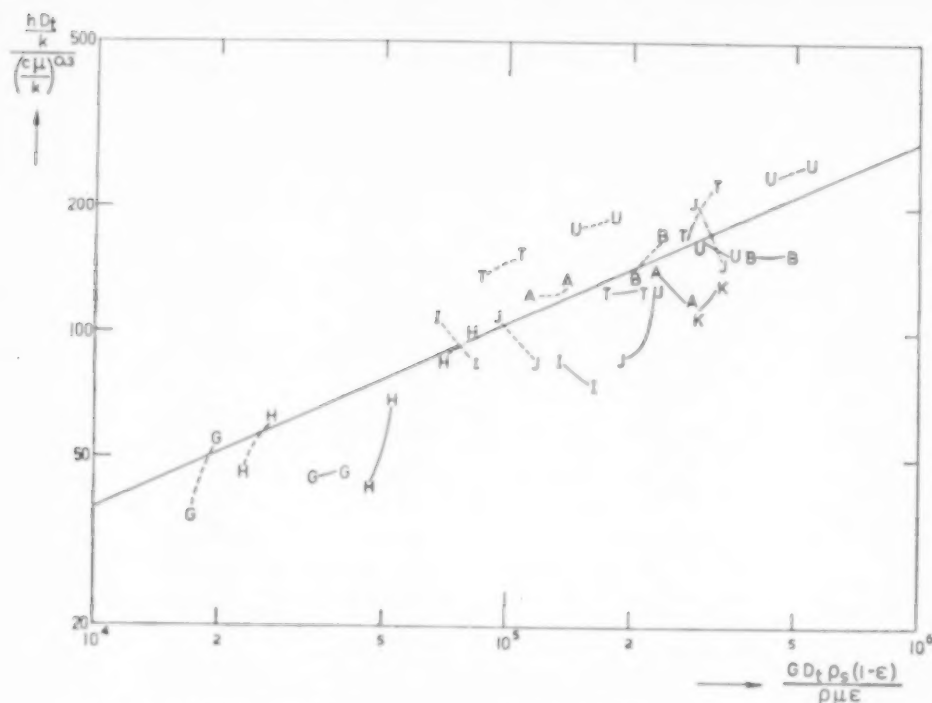


FIG. 5. Correlation of results of experiments with fine and light particles (see Table 1).

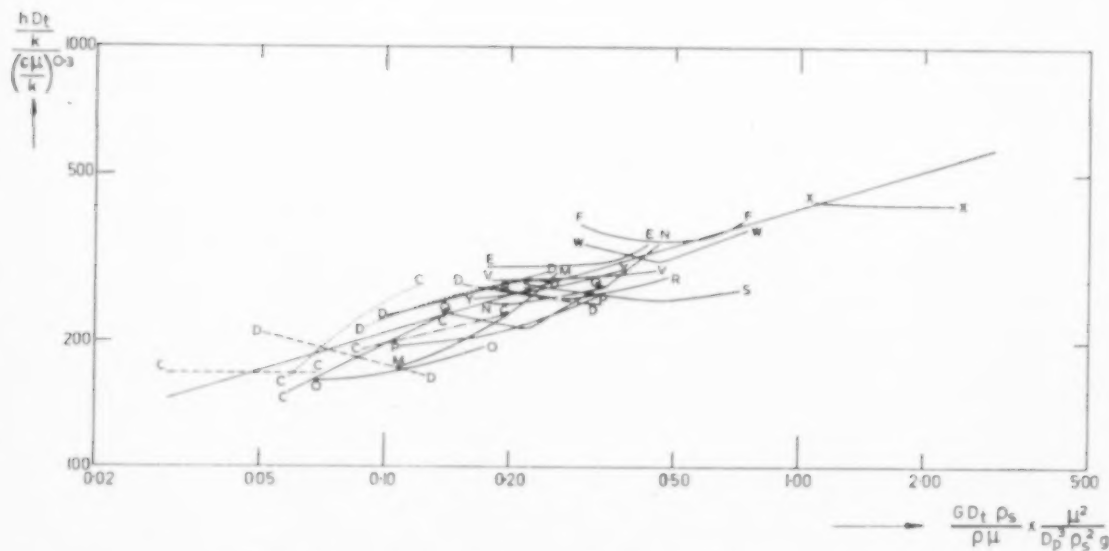


FIG. 6. Correlation of results of experiments with coarse and heavy particles (see Table 1 and Ref. [1], or Table 2).

and the materials previously specified [1], was obtained by adding the dimensionless group:—

$$\frac{\mu^2}{D_p^3 \rho_s^2 g}$$

to the two groups mentioned above. This group will be discussed further in the next section. It might be argued that a porosity term like  $(1 - \epsilon)/\epsilon^3$  should be added, but it was found that the introduction of a porosity term into the correlation did not improve the description of the experimental data for coarse and heavy particles. It was therefore omitted from the third group, and also from the Reynolds group. The representation of the results of all the measurements with coarse and heavy particles by means of a simple relationship between the three groups thus obtained, is given in Fig. 6. The curves do not deviate by more than 29 per cent from the straight line:—

$$\frac{h D_p / k}{(c \mu / k)^{0.3}} = 420 \left( \frac{G D_p \rho_s}{\rho \mu} \times \frac{\mu^2}{D_p^3 \rho_s^2 g} \right)^{0.3}$$

If the mean particle diameter  $D_p$  is increased and it is required to maintain the same bed temperature, the same mass velocity  $G$ , the same tube diameter  $D_t$ , the same particle density  $\rho_s$ , the same specific heat of the particles  $c$ , a similar particle shape, and a similar particle size distribution, there will be a decrease in the porosity  $\epsilon$ : hence the correlation for fine and light particles predicts an increase in the heat-transfer coefficient  $h$ . According to the correlation for coarse and heavy particles, however, the heat-transfer coefficient  $h$  is proportional to  $D_p^{-0.9}$  so that it should decrease.

When  $D_p$  is increased and the degree of fluidization\* is to be kept constant while the same bed temperature, the same tube diameter, the same particle density, the same specific heat, a similar particle shape and a similar particle size distribution are maintained, it will be necessary to increase the mass velocity  $G$ . At the same time, the increase in  $D_p$  will cause a small decrease in

the porosity  $\epsilon$ . For these two reasons the correlation for fine and light particles again predicts an increase in  $h$ . However, since the effect of the increase in  $D_p^3$  will exceed the effect of the increase in  $G$ , the correlation for coarse and heavy particles again predicts a decrease in  $h$ .

When the particle density  $\rho_s$  is increased and the other properties of the particles, the bed temperature, the mass velocity, and the tube diameter are kept constant, there will be a decrease in the porosity  $\epsilon$  because of the decreasing degree of fluidization. For fine and light particles, both the increase in  $\rho_s$  and the decrease in  $\epsilon$  will cause an increase in  $h$ . For coarse and heavy particles, however, the heat-transfer coefficient is proportional to  $\rho_s^{-0.3}$ , so that it will decrease.

When  $\rho_s$  is increased and the other particle properties, the degree of fluidization, the bed temperature, and the tube diameter are to be kept constant, it will be necessary to increase  $G$  proportionally to  $\rho_s - \rho$  [4, 7, 8]. Since  $\rho$  is negligible as compared with  $\rho_s$ , this means that for fine and light particles the heat-transfer coefficient is proportional to  $\rho_s^{0.88}$ , so that it will increase. For coarse and heavy particles, however, no change in  $h$  is to be expected.

It should be borne in mind that the effects of an increase in  $D_p$  or  $\rho_s$  on  $h$  were derived on the assumption that the increase would not involve a transition from the range of fine and light particles to that of coarse and heavy materials. This limitation will be discussed in the next section. It follows from the above that under definite conditions maximum heat-transfer coefficients can be obtained by choosing values of  $D_p$  and  $\rho_s$  that belong to the transition between the two ranges.

Similar statements about the effects of other quantities contained in the correlation formulae can easily be derived.

## 5. RANGE OF VALIDITY OF THE CORRELATIONS

After a collision between two particles, the resulting velocities may be in any direction. When external forces are absent, they will retain their directions up to the next collision. When, however, the ambient gas moves relatively to

\* The degree of fluidization can be defined as the ratio of the product of mass velocity and kinematic viscosity of the fluidizing gas to the minimum value of this product at which fluidization can occur [1].

the particle, a force will be exerted on the particle owing to the viscosity of the gas and it will bend the path of the particle towards the direction of the gas flow. This force acts on the particle along a distance which, on an average, is equal to the mean path between two successive collisions. The corresponding work is proportional to the product of this path and the force and, if it is assumed that the particle velocity is proportional to the interstitial gas velocity  $G/\rho\epsilon$ , the ratio between the kinetic energy of the particle and this amount of work can be shown to be proportional to  $GD_p\rho_s/\rho\mu$ . The porosity  $\epsilon$  does not occur in this ratio.

Since the Reynolds group  $GD_p\rho_s/\rho\mu$  is a measure of the ratio between the actions of inertia and the viscous forces, the latter will be predominant for low values of the group, and the inertia effects for high values. Thus for low

values the paths of the particles will be bent towards the direction of the gas flow, and the assumption under which the correlation for fine and light particles has been derived may be expected to be valid. This conception is compatible with the mechanism of heat transfer proposed by MICKLEY and FAIRBANKS [9] and KRAMERS [10]. For high values of the Reynolds group the correlation for coarse and heavy particles may apply; it would appear that in this case the group  $\mu^2/D_p^3\rho_s^2g$  affects the stirring factor introduced by MICKLEY and FAIRBANKS [9]. The group  $\mu^2/D_p^3\rho_s^2g$  is the ratio between the Froude group  $G^2/D_p\rho_s^2g$  [11] and the square of the Reynolds group  $GD_p\rho_s/\rho\mu$ .

The range of the values of the Reynolds group pertaining to all the relevant experiments is given in Table 2. A survey of these values leads to the conclusion that the correlation in Fig. 5

Table 2. Applicability of the two correlations

Material	Mean volume-surface particle diameter [3]	Particle density	Range of max velocity $G$	Range of bed temperature $t_b$	Range of Reynolds group $\frac{GD_p\rho_s}{\rho\mu}$	Results in Fig. or in Ref. no.	Curves in relevant figures	Correlation in Fig. no.
	$D_p$	$\rho_s$						
	(m $\times 10^{-6}$ )	(kg/m <sup>3</sup> $\times 10^3$ )	(kg/m <sup>2</sup> sec)	(°C)				
Regenerated catalyst	64	1.60	0.010-0.149	40-260	40-740	Fig. 1	G, H, I, J, K	5
Sand used for sand-blasting	136	2.66	0.046-0.077	40-200	670-1200	Fig. 2	T, U	5
Dune sand	213	2.66	0.056-0.096	40-240	1270-2550	Fig. 2	A, B	5
New type of Maas sand	316	2.66	0.099-0.163	20-260	3300-6610	Fig. 2	C, D	6
Sharp silver sand	215	2.66	0.089-0.151	40-260	2050-4060	Ref. [1]	E, F, V, W	6
Old type of Maas sand	353	2.66	0.148-0.242	40-320	5620-10900	Ref. [1]	O, P	6
Mixture of silver and old type of Maas sand	260	2.66	0.118-0.198	40-340	3270-6600	Ref. [1]	Q, R, S	6
Round silver sand	259	2.66	0.091-0.150	40-280	2520-5500	Ref. [1]	M, N	6
Ground iron ore, wide sieve fraction	130	5.15	0.234	40-220	6160-7250	Ref. [1]	X	6
Ground iron ore, more homogeneous fraction	247	5.15	0.239	40-240	12900-15100	Ref. [1]	Y	6

is applicable when the value is lower than 2050, and that the correlation in Fig. 6 applies when it is higher than 2550. Values of the Reynolds group between 2050 and 2550 are included in both correlations. For this transitional range it is recommended that the average of the amounts given by the two correlations be considered a good prediction of the heat-transfer coefficient  $h$ .

Since  $D_p$  and  $\rho_s$  occur in the numerator of the Reynolds group, it is obvious that the criterion given can be considered as a distinction between fine and light particles on the one hand, and coarse and heavy particles on the other. However, this conception is too crude because, for instance, even with catalyst the value of the group may exceed 2050 if extremely high values of  $G$  or low values of  $\rho$  are applied. In these cases the same procedure should be followed as with coarser and heavier particles, since it is not permissible to neglect inertia effects.

Since the correlation in Fig. 5 has been derived from an assumed analogy between the fluidized bed and a flowing gas or liquid, it is recommended that it be applied in all cases where a coefficient of heat transfer between a fluidized bed and a diametrically inserted tube has to be calculated, so long as the value of the Reynolds group is less than 2050. When the bed diameter is greater than 0.2 m the value of  $\epsilon$  occurring in the correlation can be derived from the data given in Figs. 3 and 4. LEVA [7, 12, 13, 14] presents data

for bed diameters smaller than 0.2 m. The influence of the bed diameter on the porosity has already been discussed [2, 15].

The dimensionless group  $\mu^2/D_p^3 \rho_s^2 g$  has been introduced into the correlation in Fig. 6 only because a good description of the experimental data could thus be obtained. The use of this correlation can therefore safely be recommended only when the value of the Reynolds group is higher than 2550 and when, moreover, all the variables are within or nearly within the range covered by the experiments.

#### NOTATION

$c$	= specific heat of particles at bed temperature (J/kg°C)
$D_p$	= mean volume-surface particle diameter [3] (m)
$D_t$	= outer diameter of tube (m)
$G$	= mass velocity of fluidizing gas (kg/m <sup>2</sup> sec)
$g$	= acceleration of gravity (m/sec <sup>2</sup> )
$h$	= coefficient of heat transfer between bed and tube (J/m <sup>2</sup> sec°C)
$k$	= thermal conductivity of gas at bed temperature (J/sec m°C)
$Pr$	= prandtl group
$t_b$	= mean bed temperature (°C)
$\epsilon$	= fraction of voids (in the absence of channelling $\epsilon = \epsilon_1$ )
$\epsilon_1$	= apparent fraction of voids, derived from pressure drop
$\mu$	= dynamic viscosity of gas at bed temperature (kg/sec m)
$\rho$	= density of gas at bed temperature (kg/m <sup>3</sup> )
$\rho_s$	= density of particles (kg/m <sup>3</sup> )

#### REFERENCES

- [1] VREEDENBERG H. A. *Proceedings of the General Discussion on Heat Transfer, London, 1951*, pp.373, 389. Institution of Mechanical Engineers 1951.
- [2] VREEDENBERG H. A. *J. Appl. Chem.* 1952 **2** S26.
- [3] DALLAVALLE J. M. *Micromeritics*. London 1948.
- [4] LEVA M., GRUMMER M., WEINTRAUB M. and POLLCHIK M. *Chem. Engng. Progr.* 1948 **44** 511.
- [5] AGARWAL O. P. and STORROW J. A. *Chem. & Ind.* 1951 278.
- [6] McADAMS W. H. *Heat Transmission*. New York 1954.
- [7] LEVA M., GRUMMER M., WEINTRAUB M. and POLLCHIK M. *Chem. Engng. Progr.* 1948 **44** 619.
- [8] VAN HEERDEN C., NOBEL A. P. P. and VAN KREVELEN D. W. *Chem. Engng. Sci.* 1951 **1** 37.
- [9] MICKLEY H. S. and FAIRBANKS D. F. *Amer. Inst. Chem. Engrs. J.* 1955 **1** 374.
- [10] KRAMERS H. *Chemical Reaction Engineering*, (Edited by K. Rietema) p. 45. Pergamon Press, London 1957.
- [11] WILHELM R. H. and KWAUK M. *Chem. Engng. Progr.* 1948 **44** 201.
- [12] LEVA M., WEINTRAUB M., GRUMMER M. and POLLCHIK M. *Industr. Engng. Chem.* 1949 **41** 1206.
- [13] LEVA M., SHIRAI T. and CHIN-YUNG WEN *Génie Chim.* 1956 **75** 33.
- [14] CHIN-YUNG WEN and LEVA M. *Amer. Inst. Chem. Engrs. J.* 1956 **2** 482.
- [15] VREEDENBERG H. A. *Proceedings of the General Discussion on Heat Transfer, London, 1951*. p. 487. Institution of Mechanical Engineers 1951.



## A statistical analysis of certain mixing problems

S. KATZ

American Cyanamid Company, 30 Rockefeller Plaza, New York 20, N.Y.

(Received 5 June 1957)

**Abstract**—The problem of smoothing out concentration fluctuations by passage through cascades of stirred mixers is formulated from the point of view of probability. The formulation is in terms of the theory of random processes, and techniques based on covariance functions are introduced side by side with spectral techniques. The two methods are illustrated by application to various particular problems, some of which have previously been treated by DANCKWERTS ([4], [5]) and others.

**Résumé**—Les problème de la répartition uniforme des fluctuations de concentration, par passage à travers une série de mélangeurs agités, est formulé du point de vue de la probabilité. La formule est établie à partir de la théorie des répartitions désordonnées. Des techniques ayant pour base les fonctions covariantes sont présentées en relation avec des techniques spectrales. Les deux méthodes sont illustrées par leur application à divers problèmes; certains d'entre eux ayant déjà été discutés par DANCKWERTS [4], [5] et d'autres auteurs.

**Zusammenfassung**—Das Problem, Konzentrationsschwankungen beim Durchgang durch Rührkesselskaskaden auszugleichen, wird vom Standpunkt der Wahrscheinlichkeit formuliert. Es wird die Theorie der Zufallsprozesse herangezogen und Rechenmethoden, die auf kovarianten Funktionen beruhen, werden zusammen mit Spektralmethoden angewandt. Diese beiden Methoden werden an verschiedenen Anwendungsfällen demonstriert, von denen einige bereits durch Danckwerts ([4], [5]) und andere behandelt worden sind.

### I. STATISTICAL INTRODUCTION

THIS paper studies the performance of cascades of stirred tanks designed to smooth out random concentration fluctuations in a continuous process stream. The point of view adopted is statistical in the following sense: the concentration history of some material in a stream is considered not as a single function of the time  $t$ , but rather as an ensemble of such functions indexed by a parameter  $\alpha$ . Such an ensemble of time histories is called a random process. The ensemble index  $\alpha$  may be thought of as ranging over duplicate pieces of equipment operating under the same statistical conditions.

The statistics arise in establishing probability distributions over the ensemble index  $\alpha$ . Thus, for an ensemble of concentration histories  $c(t, \alpha)$ , one has the univariate probability density  $P_c$

$P_c(x; t) dx$  = the probability that  $x < c(t, \alpha) < x + dx$

= the fraction of all possible  $\alpha$  for which  $x < c(t, \alpha) < x + dx$

the bivariate probability density  $Q_c$ ,

$Q_c(x, y; \tau, t) dx dy$  = the probability that  $x < c(t, \alpha) < x + dx$  and  $y < c(t + \tau, \alpha) < y + dy$  simultaneously

= the fraction of all possible  $\alpha$  for which  $x < c(t, \alpha) < x + dx$  and  $y < c(t + \tau, \alpha) < y + dy$  simultaneously

and so on.

We shall be concerned here not with the full scope of the probability distributions  $P$ ,  $Q$ , etc., but only with their first and second moments. We consider first the mean value of the random process  $c(t, \alpha)$ ,



$$m_c(t) = E[c(t, \alpha)] \\ = \int_{-\infty}^{\infty} x P_c(x; t) dx$$

where the operation  $E$ , taking the expected value, denotes an averaging over the ensemble index  $\alpha$ . A measure of the variation of  $c$  around its mean value is furnished by its variance:—

$$\sigma_c^2(t) = E[\{c(t, \alpha) - m_c(t)\}^2] \\ = \int_{-\infty}^{\infty} [x - m_c(t)]^2 P_c(x; t) dx$$

Primary information about the statistical relationship between values of  $c$  at different times is furnished by the auto-covariance function:—

$$\rho_c(\tau; t) = E[\{c(t, \alpha) - m_c(t)\} \\ \{c(t + \tau, \alpha) - m_c(t + \tau)\}] \\ = \int_{-\infty}^{\infty} \int_{-\infty}^{\infty} [x - m_c(t)] [y - m_c(t + \tau)] \\ Q_c(x, y; \tau; t) dx dy$$

It may be noted that:—

$$\rho_c(0; t) = \sigma_c^2(t)$$

In mixing studies one has to consider not one random process  $c(t, \alpha)$  in isolation, but rather two such processes  $c(t, \alpha)$ ,  $c^1(t, \alpha)$  jointly. The processes  $c$  and  $c^1$  are, in general, the concentration of some key component entering and leaving a mixing system. The joint statistics of  $c$  and  $c^1$  are defined by suitable generalizations of the distributions  $P_c, Q_c, \dots$ . Thus, one considers:—

$$P_{cc^1}(x; x^1; t) dx dx^1 = \text{the probability that } x < \\ c(t, \alpha) < x + dx \text{ and } x^1 < c^1(t, \alpha) < x^1 + dx^1 \\ \text{simultaneously}$$

etc. Primary information about the statistical relationship between values of  $c$  and  $c^1$  at different times is furnished by their cross-covariance function:—

$$\rho_{cc^1}(\tau; t) = E[\{c(t, \alpha) - m_c(t)\} \\ \{c^1(t + \tau, \alpha) - m_{c^1}(t + \tau)\}]$$

It will be important in what follows to single out from the general class of random processes those which are called stationary. The stationary

processes are those for which the probability distributions  $P, Q$ , etc. are independent of the origin of time, that is, those processes  $c$  for which:—

$$P_c(x; t) = P_c(x), \text{ and}$$

$$Q_c(x, y; \tau; t) = Q_c(x, y; \tau)$$

etc., independent of  $t$ . For a stationary process  $c$ , the mean and variance are constants:—

$$m_c(t) = m_c$$

$$\sigma_c^2(t) = \sigma_c^2$$

independent of  $t$ , and the auto-covariance function depends only on the lag  $\tau$ :—

$$\rho_c(\tau; t) = \rho_c(\tau)$$

independent of  $t$ .

If two random processes,  $c(t, \alpha)$  and  $c^1(t, \alpha)$  are separately stationary, then their separate probability distributions  $P_c, Q_c, \dots$  on the one hand, and  $P_{c^1}, Q_{c^1}, \dots$  on the other, are separately independent of  $t$ , with the consequences noted in the last paragraph. If, further, their joint probability distributions  $P_{cc^1}$ , etc. are independent of  $t$ , the two processes may be said to be jointly stationary. As a consequence of this, their cross-covariance function depends only on the lag  $\tau$ :—

$$\rho_{cc^1}(\tau; t) = \rho_{cc^1}(\tau)$$

independent of  $t$ .

In the body of this paper, the criterion of performance of a given mixing system will be taken to be the variance of a key concentration in the outlet stream. This criterion is adopted not because it is thought to be the most realistic, but because it seems to be the most accessible mathematically. Expressions will be derived in typical cases for the variance of the outlet stream concentration in terms of the covariance structure of the feed stream concentration. Section II will review the transient performance of cascades of continuous stirred mixers. Section III will discuss a typical problem with non-stationary feed stream concentration, and give the design relationships between the inlet and outlet concentration covariance functions. Section IV will discuss a similar problem with stationary feed stream concentration, and show

how the design relationships can be simplified by introducing the spectra of the inlet and outlet concentrations. Section V will consider a problem in discrete, rather than continuous time, which can be handled within the same statistical framework.

## II. CASCADES OF STIRRED MIXERS

Consider a cascade of continuous well-stirred tanks—the first feeding the second, the second feeding the third, and so on, all at the rate  $W \text{ ft}^3/\text{hr}$ . Let the volume of the  $n$ th tank be  $V_n \text{ ft}^3$ , and its nominal residence time therefore,

$$\theta_n = V_n/W \text{ hr.}$$

A straightforward material balance then shows that the concentration  $c_n(t)$  moles/ $\text{ft}^3$  of some material in (and leaving) the  $n$ th tank satisfies, as a function of time,  $t$ , hr, the differential equation:—

$$\frac{dc_n}{dt} = \frac{c_{n-1} - c_n}{\theta_n}; \quad n = 1, 2, \dots \quad (1)$$

In (1), the function  $c_0 = c_0(t)$  is the concentration of the material in question in the feed to the first tank.

We want from (1) information as to how variations in  $c_0(t)$  are propagated through the cascade to produce variations in  $c_n(t)$ . But this information should not include extraneous transients such as arise, for example, in start up. To achieve this, imagine the cascade to have been started up in the remote past, and solve the differential equations (1) under the initial conditions,

$$c_n(t) \text{ bounded as } t \rightarrow -\infty; \quad n = 1, 2, \dots \quad (2)$$

Under suitable regularity conditions on  $c_0(t)$  the mathematical system (1), (2) has the unique solution:—

$$c_n(t) = \int_0^t H_n(x) c_0(t-x) dx \quad (3)$$

where  $H_n(x)$  is the convolution of elementary exponentials (cf., e.g., [1])

$$H_n(x) = \frac{1}{\theta_1} e^{-x/\theta_1} * \frac{1}{\theta_2} e^{-x/\theta_2} * \dots * \frac{1}{\theta_n} e^{-x/\theta_n} \quad (4)$$

that is:—

$$H_1(x) = \frac{1}{\theta_1} e^{-x/\theta_1} \quad (5)$$

with

$$H_2(x) = H_1(x) * \frac{1}{\theta_2} e^{-x/\theta_2} \\ = \int_0^x H_1(x-u) \frac{1}{\theta_2} e^{-u/\theta_2} du$$

$$H_3(x) = H_2(x) * \frac{1}{\theta_3} e^{-x/\theta_3} \\ = \int_0^x H_2(x-u) \frac{1}{\theta_3} e^{-u/\theta_3} du$$

and so on. It might be pointed out that in the case of equal residence times in all stages:—

$$\theta_1 = \theta_2 = \dots = \theta_n = \theta$$

the kernel  $H_n(x)$  has the explicit form:—

$$H_n(x) = \frac{(x/\theta)^{n-1} e^{-x/\theta}}{(n-1)! \theta} \quad (6)$$

In Sections III and IV we shall treat the inlet and outlet concentrations as random processes in the sense of Section I. Accordingly we introduce their dependence on the ensemble index  $\alpha$  directly into (3) to give:—

$$c_n(t, \alpha) = \int_0^t H_n(x) c_0(t-x, \alpha) dx \quad (7)$$

This relation is of the general form studied extensively in certain control systems applications (cf., e.g., [2]), where the inlet concentration  $c_0$  is thought of as a generalized driving force:—

$$c_0(t, \alpha) = c(t, \alpha)$$

and the outlet concentration  $c_n$  as a generalized response,

$$c_n(t, \alpha) = c^1(t, \alpha)$$

For reasons of technical convenience, we write the connexion (7) in the form:—

$$c^1(t, \alpha) = \int_{-\infty}^{\infty} K(x) c(t-x, \alpha) dx \quad (8)$$

where:—

$$K(x) = \begin{cases} 0 & ; x < 0 \\ H_n(x) & ; x > 0 \end{cases} \quad (9)$$

In (9) the function  $H_n(x)$  is given in general by (4), with the important special cases (5), corresponding to only one mixing stage, and (6), corresponding to  $n$  identical stages.

The kernel  $K(x)$  in (8) may be characterized by its Fourier transform (cf., e.g., [3]) :—

$$L(\omega) = \int_{-\infty}^{\infty} K(x) e^{-i\omega x} dx \quad (10)$$

By (9),

$$L(\omega) = \int_0^{\infty} H_n(x) e^{-i\omega x} dx$$

with the particular forms (cf. [1]) :—

$$L(\omega) = \left\{ \begin{array}{l} \frac{1}{1+i\omega\theta_1} \cdot \frac{1}{1+i\omega\theta_2} \cdots \\ \frac{1}{1+i\omega\theta_n}, \text{ for the } H_n \text{ of (4)} \\ \frac{1}{1+i\omega\theta_1}, \text{ for the } H_n \text{ of (5)} \\ \frac{1}{(1+i\omega\theta)^n}, \text{ for the } H_n \text{ of (6)} \end{array} \right\} \quad (11)$$

The function  $L(\omega)$  is the transfer function of the system which transforms  $c$  into  $c^1$  (cf. [2]).

Section III will discuss the relation (8) for non-stationary inlet concentrations  $c$ , and Section IV, for stationary  $c$ .

### III. NON-STATIONARY INLET CONCENTRATIONS

We now consider the feed to a mixing system to have a key component with concentration  $c(t, x)$ , where the random process  $c(t, x)$  has mean  $m_c(t)$  and auto-covariance function  $\rho_c(\tau; t)$ , as defined in Section I. It may then be seen from (8) that the random process  $c^1(t, x)$  describing the outlet concentration of the key component has mean :—

$$m_c^1(t) = \int_{-\infty}^{\infty} K(x) m_c(t-x) dx \quad (12)$$

cross-covariance function with the inlet concentration :—

$$\rho_{cc^1}(\tau; t) = \int_{-\infty}^{\infty} K(x) \rho_c(\tau-x; t) dx \quad (13)$$

and auto-covariance function :—

$$\rho_c(\tau; t) = \int_{-\infty}^{\infty} K(x) \rho_{cc^1}(\tau+x; t-x) dx \quad (14)$$

To illustrate the use of these formulas we consider the feed stream to be made up in batches in such a way that the concentration  $c$  of the key component suffers a discrete change every  $h$  hr. Specifically, we imagine the batch concentrations to be drawn independently from a population with mean  $m_c$  and variance  $\sigma_c^2$ , both independent of  $t$ . If we synchronize the change-over times with the integral multiples of  $h$  on the  $t$ -scale, then the auto-covariance function of the feed stream concentration  $c$  is :—

$$\rho_c(\tau; t) = \begin{cases} \sigma_c^2 & ; \text{ if } t \text{ and } t+\tau \text{ lie between} \\ & \text{the same successive mul-} \\ & \text{tiples of } h \\ 0 & ; \text{ otherwise} \end{cases} \quad (15)$$

Finally we imagine the feed stream passed through a single stage of mixing with residence time  $\theta$  hr so that, from (9) and (5),

$$K(x) = \begin{cases} 0 & ; x < 0 \\ \frac{1}{\theta} e^{-x/\theta} & ; x > 0 \end{cases} \quad (16)$$

and ask how large we should take  $\theta$  to keep the variance of the outlet concentration  $c^1$  below an assigned level.

We note first that, since the integral of the kernel (16) is 1, the constant mean concentration  $m_c$  passes unchanged (as it ought) through the mixer; that is, by (12),  $m_{c^1} = m_c$ . Next, inserting (15) into (13) gives the cross-covariance function in the form :—

$$\rho_{cc^1}(\tau; t) = \sigma_c^2 f(\tau + \eta h) \quad (17)$$

where :—

$$f(u) = \begin{cases} 0 & ; u \leq 0 \\ 1 - e^{-u/\theta} & ; 0 \leq u \leq h \\ e^{(h-u)/\theta} - e^{-u/\theta} & ; h \leq u \end{cases}$$

In (17),  $\eta$  is the fractional part of  $t/h$ ; that is,

$$\eta = \frac{t}{h} - \left[ \frac{t}{h} \right] \quad (18)$$

where  $[z]$  is the largest integer not exceeding  $z$ . Substituting (17) into (14) gives the variance of the outlet concentration as:—

$$\begin{aligned} \sigma_{c^1}^2(t) &= \rho_{c^1}(0; t) \\ &= \sigma_c^2 \left( 1 - 2e^{-\eta h/\theta} + \left( 1 + \tanh \frac{h}{2\theta} \right) e^{-2\eta h/\theta} \right) \quad (19) \end{aligned}$$

In (19),  $\eta$  is given by (18) and varies between 0 and 1. The maximum value of (19) is assumed at the endpoints of the  $\eta$  interval, giving the (best) inequality:—

$$\sigma_{c^1}^2(t) \leq \sigma_c^2 \cdot \tanh \frac{h}{2\theta}, \text{ for all } t$$

Thus, to ensure that for all  $t$

$$\sigma_{c^1}(t) < \epsilon$$

for some assigned  $\epsilon$  between 0 and  $\sigma_c$ , choose  $\theta$  to make

$$\theta/h > \frac{1}{2 \operatorname{arctanh} \epsilon^2/\sigma_c^2}$$

Similar calculations can be made for cascades of mixers, but the complexity of the calculation mounts rapidly with the size of the cascade.

#### IV. STATIONARY INLET CONCENTRATIONS

If the random process  $c(t, x)$  describing a key concentration in the feed to a mixing system is stationary in the sense of Section I, then general considerations (cf. [2]) show that the corresponding outlet concentration  $c^1(t, x)$  given by (8) is also stationary, and that the inlet and outlet processes,  $c$  and  $c^1$ , are jointly stationary. One can of course see directly that the constant mean  $m_c$  of a stationary  $c$  passes unchanged (as it ought) through the mixing system; from (12),

$$m_{c^1} = m_c \int_{-\infty}^{\infty} K(x) dx = m_c$$

since, by (10) and (11),

$$\int_{-\infty}^{\infty} K(x) dx = L(0) = 1$$

Also, the general covariance relationships (13) and (14) show directly that the functions  $\rho_{cc^1}$  and  $\rho_{c^1}$  are independent of their second arguments if  $\rho_c$  is thus:—

$$\left. \begin{aligned} \rho_{cc^1}(\tau) &= \int_{-\infty}^{\infty} K(x) \rho_c(\tau - x) dx \\ \rho_{c^1}(\tau) &= \int_{-\infty}^{\infty} K(x) \rho_{cc^1}(\tau + x) dx \end{aligned} \right\} \quad (20)$$

The form of the equations (20) can be considerably simplified, and the tedious calculations in solving problems such as those in Section III in some measure avoided, by introducing Fourier transforms, when they exist, of the covariance functions  $\rho_c$

$$\left. \begin{aligned} S_c(\omega) &= \frac{1}{2\pi} \int_{-\infty}^{\infty} \rho_c(\tau) e^{i\omega\tau} d\tau \\ S_{c^1}(\omega) &= \frac{1}{2\pi} \int_{-\infty}^{\infty} \rho_{c^1}(\tau) e^{i\omega\tau} d\tau \\ S_{cc^1}(\omega) &= \frac{1}{2\pi} \int_{-\infty}^{\infty} \rho_{cc^1}(\tau) e^{i\omega\tau} d\tau \end{aligned} \right\} \quad (21)$$

The functions  $S_c$  and  $S_{c^1}$  are the power spectral densities of  $c$  and  $c^1$ , respectively; the function  $S_{cc^1}$  is the cross-power spectral density of  $c$  to  $c^1$ ; (cf. [2]). The transforms (21) can be inverted (cf. [3]) to express the covariances in terms of these spectral densities:—

$$\left. \begin{aligned} \rho_c(\tau) &= \int_{-\infty}^{\infty} S_c(\omega) e^{-i\omega\tau} d\omega \\ \rho_{c^1}(\tau) &= \int_{-\infty}^{\infty} S_{c^1}(\omega) e^{-i\omega\tau} d\omega \\ \rho_{cc^1}(\tau) &= \int_{-\infty}^{\infty} S_{cc^1}(\omega) e^{-i\omega\tau} d\omega \end{aligned} \right\} \quad (22)$$

The convolution form of the equations (20) permits writing them (cf. [3]) in terms of the spectra  $S$  as follows:—

$$\left. \begin{aligned} S_{cc^1}(\omega) &= \overline{L(\omega)} S_c(\omega) \\ S_{c^1}(\omega) &= L(\omega) S_{cc^1}(\omega) \end{aligned} \right\} \quad (23)$$

where  $L(\omega)$  is the transfer function defined in

(10). In (23) the bar denotes the operation of taking the complex conjugate value. From (23),

$$S_{c^1}(\omega) = |L(\omega)|^2 S_c(\omega)$$

and from (22):—

$$\rho_{c^1}(\tau) = \int_{-\infty}^{\infty} |L(\omega)|^2 S_c(\omega) e^{-i\omega\tau} d\omega$$

so that taking  $\tau = 0$  gives:—

$$\sigma_{c^1}^2 = \int_{-\infty}^{\infty} |L(\omega)|^2 S_c(\omega) d\omega \quad (24)$$

In (24),  $|L(\omega)|^2$  is the sum of the squares of the real and imaginary parts of  $L(\omega)$ , as will be illustrated in the sample problem to follow.

To illustrate the use of (24), we consider, as in the sample problem of section III, a feed stream in which the fluctuations in concentration  $c$  of a key component are to be smoothed out by passage through one mixing stage. If this mixer has residence time  $\theta$  hours, then the transfer function  $L(\omega)$  is given by (11) as:—

$$L(\omega) = \frac{1}{1 + i\omega\theta} \quad (25)$$

so that:—

$$|L(\omega)|^2 = \frac{1}{1 + \omega^2\theta^2} \quad (26)$$

The transfer function (25) corresponds to the kernel (16) in the sample problem of Section III. We take the inlet concentration  $c$  to have variance  $\sigma_c^2$  and characteristic time lag  $h$  hr for the decay of the dependence of neighbouring values of  $c$  on each other; specifically, we take

$$\rho_c(\tau) = \sigma_c^2 e^{-|\tau|/h} \quad (27)$$

where here  $|\tau|$  denotes merely the numerical value of the lag  $\tau$ . We ask how large we should take  $\theta$  to keep the variance of the outlet concentration  $c^1$  below an assigned level.

Substituting (27) into (21) gives the spectrum of the inlet concentration as:—

$$S_c(\omega) = \sigma_c^2 \cdot \frac{h}{\pi} \cdot \frac{1}{1 + \omega^2 h^2} \quad (28)$$

Substituting (26) and (28) into (24) gives the variance of the outlet concentration as:—

$$\sigma_{c^1}^2 = \frac{\sigma_c^2}{1 + \theta/h} \quad (29)$$

Thus, to ensure that  $\sigma_{c^1} < \epsilon$  for some assigned  $\epsilon$  between 0 and  $\sigma_c$ , choose  $\theta$  to make:—

$$\frac{\theta}{h} > \frac{\sigma_c^2}{\epsilon^2} - 1$$

Similar calculations can be made here for cascades of mixers without encountering the analytical complications of Section III. Suppose for example that in the foregoing problem the mixing system is taken to be two mixers in cascade, each of residence time  $\theta/2$  hr, so that the transfer function of the system is, by (11):—

$$L(\omega) = \frac{1}{(1 + i\omega\theta/2)^2} \quad (30)$$

rather than (25). Substituting (28) and (30) into (24) gives the variance of the outlet stream concentration as:—

$$\sigma_{c^1}^2 = \sigma_c^2 \frac{4 + \frac{\theta}{h}}{(2 + \frac{\theta}{h})^2}$$

which of course is always larger than the corresponding variance (29).

## V. A PROBLEM IN DISCRETE TIME

To exhibit the scope of the statistical methods described here, we conclude with an illustrative stage batch mixing problem. We imagine that batches of material, of uniform volume  $v$  ft<sup>3</sup> are prepared at times indexed by:—

$$n = \dots -2, -1, 0, 1, 2, \dots$$

and that the  $n$ th batch has the concentration  $c(n)$  moles/ft<sup>3</sup> in some critical component. As each batch is prepared it is fed into a blending tank containing  $V$  ft<sup>3</sup> of past material; the tank is thoroughly mixed, and then the same batch volume  $v$  is withdrawn. Let  $c^1(n)$  moles/ft<sup>3</sup> be the key concentration in the batch withdrawn just after the  $n$ th batch has been fed into the mixer and blended. A straightforward material balance then shows that  $c^1(n)$  satisfies the difference equation:—

$$c^1(n) - c^1(n-1) = v/V \{c(n) - c^1(n)\} \quad (31)$$

As in the cascade equations of Section II we want the solution of this difference equation which shows the dependence of  $c^1(n)$  on  $c(n)$  in a form uncontaminated by extraneous transients due to start up. This is achieved as before by imagining the mixing system to have been started in the remote past, and solving (31) under the initial condition:—

$$c^1(n) \text{ bounded as } n \rightarrow -\infty \quad (32)$$

Under suitable regularity conditions on  $c(n)$ , the mathematical system (31), (32) has the unique solution:—

$$c^1(n) = \sum_{i=0}^{\infty} H(i) c(n-i) \quad (33)$$

where

$$H(i) = \frac{(1+v/V)^{-i}}{(1+V/v)} \quad (34)$$

As in the continuous problems, the statistics arise in thinking of the concentrations as random processes:  $c(n, \alpha)$  for the inlet concentration, and  $c^1(n, \alpha)$  for the outlet concentration, where  $\alpha$  is the ensemble index which we may think of as ranging over duplicate physical systems operating under the same statistical conditions. We rewrite (33), (34) for the random processes  $c, c^1$ :—

$$c^1(n, \alpha) = \sum_{i=-\infty}^{\infty} K(i) c(n-i, \alpha) \quad (35)$$

with

$$K(i) = \begin{cases} 0 & ; i = -1, -2, -3, \dots \\ \frac{(1+v/V)^{-i}}{(1+V/v)} & ; i = 0, 1, 2, \dots \end{cases} \quad (36)$$

in analogy with (8) and (9). Further we define as in Section I the moments of these random processes:—

$$\left. \begin{aligned} m_c &= E[c(n, \alpha)] \\ m_{c^1} &= E[c^1(n, \alpha)] \\ \rho_c(v) &= E[\{c(n, \alpha) - m_c\} \{c(n+v, \alpha) - m_c\}]; \sigma_c^2 = \rho_c(0) \\ \rho_{c^1}(v) &= E[\{c^1(n, \alpha) - m_{c^1}\} \{c^1(n+v, \alpha) - m_{c^1}\}]; \sigma_{c^1}^2 = \rho_{c^1}(0) \\ \rho_{cc^1}(v) &= E[\{c(n, \alpha) - m_c\} \{c^1(n+v, \alpha) - m_{c^1}\}] \end{aligned} \right\} \quad (37)$$

all independent of the time index  $n$ . The operation  $E$  denotes, as before, an averaging over the ensemble index  $\alpha$ . (These definitions are made only for what corresponds to the stationary case of Section I).

Applying (37) to (35) shows first that:—

$$m_{c^1} = m_c$$

as it ought, since by (36):—

$$\sum_{i=-\infty}^{\infty} K(i) = 1$$

and second that:—

$$\left. \begin{aligned} \rho_{cc^1}(v) &= \sum_{i=-\infty}^{\infty} K(i) \rho_c(v-i) \\ \rho_{c^1}(v) &= \sum_{i=-\infty}^{\infty} K(i) \rho_{cc^1}(v+i) \end{aligned} \right\} \quad (38)$$

in analogy with (20). Combining the two equations (38) gives:—

$$\rho_{c^1}(v) = \sum_{i=-\infty}^{\infty} \sum_{j=-\infty}^{\infty} K(i) K(j) \rho_c(v+i-j)$$

which, on taking  $v=0$ , gives for the variance of the outlet concentration  $c^1$ :—

$$\sigma_{c^1}^2 = \sum_{i=-\infty}^{\infty} \sum_{j=-\infty}^{\infty} K(i) K(j) \rho_c(i-j) \quad (39)$$

We can, by analogy with Section IV, introduce forms of the spectral densities  $S$  appropriate to the discrete time processes  $c(n, \alpha)$ ,  $c^1(n, \alpha)$ . These are defined to be the Fourier sums, when they exist:—

$$\left\{ \begin{aligned} S_c(\lambda) &= \frac{1}{2\pi} \sum_{v=-\infty}^{\infty} \rho_c(v) e^{i\lambda v} \\ S_{c^1}(\lambda) &= \frac{1}{2\pi} \sum_{v=-\infty}^{\infty} \rho_{c^1}(v) e^{i\lambda v} \\ S_{cc^1}(\lambda) &= \frac{1}{2\pi} \sum_{v=-\infty}^{\infty} \rho_{cc^1}(v) e^{i\lambda v} \end{aligned} \right.$$



corresponding to (21), with the inverses :—

$$\begin{cases} \rho_c(v) = \int_{-\pi}^{\pi} S_c(\lambda) e^{-i\lambda v} d\lambda \\ \rho_{c^*}(v) = \int_{-\pi}^{\pi} S_{c^*}(\lambda) e^{-i\lambda v} d\lambda \\ \rho_{cc^*}(v) = \int_{-\pi}^{\pi} S_{cc^*}(\lambda) e^{-i\lambda v} d\lambda \end{cases}$$

corresponding to (22). If we introduce further a discrete time analogue to the system transfer function (10) :—

$$L(\lambda) = \sum_{j=-\infty}^{\infty} K(j) e^{-i\lambda j}$$

then equations (38) give :—

$$\begin{cases} S_{c^*}(\lambda) = \overline{L(\lambda)} S_c(\lambda) \\ S_{c^*}(\lambda) = L(\lambda) S_{c^*}(\lambda) \end{cases}$$

corresponding to (23), and equation (39) gives :—

$$\sigma_{c^*}^2 = \int_{-\pi}^{\pi} |L(\lambda)|^2 S_c(\lambda) d\lambda$$

corresponding to (24). We shall not, however, use this formulation in the example which follows.

To illustrate the application of (39), we consider the simple case where the key concentrations  $c(n, \alpha)$  in the feeds are independent from batch to batch, that is, where :—

$$\rho_c(v) = \begin{cases} \sigma_c^2 & ; v = 0 \\ 0 & ; v \neq 0 \end{cases}$$

Equations (39) and (36) then give :—

$$\sigma_{c^*}^2 = \frac{\sigma_c^2}{1 + 2V/v}$$

Thus, to ensure that  $\sigma_{c^*} < \epsilon$  for some assigned  $\epsilon$  between 0 and  $\sigma_c$ , choose  $V$  to make :—

$$\frac{V}{v} > \frac{1}{2} \left( \frac{\sigma_c^2}{\epsilon^2} - 1 \right)$$

*Acknowledgement*—The author is indebted to R. DeBAUN and J. HOROWITZ of the American Cyanamid Company for many stimulating and helpful discussions on these problems.

## REFERENCES

- [1] CHURCHILL R. V. *Modern Operational Mathematics in Engineering* Chap. II. McGraw-Hill, New York 1944.
- [2] LANING J. H., JR. and BATTIN R. H. *Random Processes in Automatic Control* Chap. V. McGraw-Hill, New York 1956.
- [3] WIENER N. *The Fourier Integral and Certain of its Applications*. Cambridge University Press 1933.
- [4] DANCKWERTS P. V. and SELLERS E. S. *Industr. Chem.* 1951 p. 305.
- [5] DANCKWERTS P. V. *Chem. Engng. Sci.* 1953 2 1.

## Ternary vapour-liquid equilibria in the system: benzene-*cyclohexane*-methyl *isobutyl* ketone

P. DAKSHINAMURTY, G. JAYARAMA RAO, M. V. R. ACHARYA and C. VENKATA RAO

Department of Chemical Technology, Andhra University, Waltair.

(Received 21 September 1957)

**Abstract**—Isobaric vapour-liquid equilibrium data of the ternary system benzene-*cyclohexane*-methyl *isobutyl* ketone were determined at 760 mm Hg total pressure using a modified Colburn still. The activity coefficient data for all the experimental points were correlated satisfactorily by Wohl's three suffix Margules ternary equations with a ternary constant. It was concluded that methyl *isobutyl* ketone might be used as an entrainer in the separation of benzene-*cyclohexane* mixtures into pure components. No ternary azeotrope was observed.

**Résumé**—Les données d'équilibre des isobares vapeur-liquide du système ternaire benzène-*cyclohexane*-méthyl *isobutyl* cétone ont été déterminées à une pression totale de 760 mm Hg en utilisant l'appareil de Colburn modifié. Les coefficients d'activité pour tous les points expérimentaux ont été reliés de façon satisfaisante par les équations 3 aires de MARGULES à 3 indices de WOHL, avec une constante ternaire. L'auteur conclut que la méthyl *isobutyl* cétone peut être utilisée comme entraîneur dans la séparation des mélanges benzène-*cyclohexane* en leurs composants purs. Il n'a pas observé d'azéotrope ternaire.

**Zusammenfassung**—Die Werte für das isobare Dampf-Flüssigkeits-Gleichgewicht des ternären Systems Benzol-Cyclohexan-Methylisobutylketon wurden bei 760 Torr Gesamtdruck in einer abgeänderten Colburn-Apparatur bestimmt. Die Werte des Aktivitätskoeffizienten für alle Messpunkte wurden befriedigend korreliert durch ternäre Margulesgleichungen vom Drei-Suffix-Typ nach WOHL mit einer ternären Konstanten. Es wurde geschlossen, dass Methylisobutylketon als Schleppmittel zur Zerlegung von Benzol-Cyclohexan-Mischungen in die reinen Komponenten geeignet ist. Kein ternäres Azeotrop wurde beobachtet.

In the purification of benzene from small amounts of higher non-aromatic hydrocarbons a lower non-aromatic hydrocarbon such as *cyclohexane*, which forms an azeotrope with benzene is added and this azeotropic mixture is removed as an overhead product, while the higher boiling impurities are left as residue. The hydrocarbon products obtained at the top of the column can then be fractionated into pure components adopting azeotropic or extractive distillation techniques, using a polar solvent such as alcohol or ketone.

Design of the plant for separation of this type requires prior knowledge of vapour-liquid equilibria of the mixtures encountered. This investigation was undertaken with a view to studying the separation of benzene-*cyclohexane* mixtures into pure components using methyl

*isobutyl* ketone as a solvent. As the vapour-liquid equilibria of all the constituent binaries benzene-*cyclohexane* [1], benzene-methyl *isobutyl* ketone [2], and *cyclohexane*-methyl *isobutyl* ketone [2] are available in the literature, the ternary vapour-liquid equilibrium data of the system benzene-*cyclohexane*-methyl *isobutyl* ketone were obtained at 760 mm total pressure.

### Materials used

**Benzene:** Baker analysed reagent grade benzene was fractionated in a glass column and the fraction distilling over at 80-10°C was collected and used.

**Cyclohexane:** *Cyclohexane* supplied by Light & Co. was subjected fractional distillation and the fraction distilling over at 80-6°C was collected and used.

Table 1. Physical properties

Chemical	Density at 30°		Refractive index at 30°C		Boiling point at 760 mm	
	Lit.	Obs.	Lit.	Obs.	Lit.	Obs.
Benzene	0.86828 [8]	0.86749	1.49486 [8]	1.4950	80.103 [8]	80.1
Cyclohexane	0.76928 [8]	0.76910	1.42090 [8]	1.4210	80.738 [8]	80.6
Methyl isobutyl ketone	0.79100 [21]	0.78986	1.39190 [21]	1.3912	115.900 [21]	116.0

Methyl isobutyl ketone: Laboratory reagent B.D.H. grade methyl isobutyl ketone was fractionated and the fraction distilling over at 115.9° was collected and used.

The physical properties of the chemicals used in this investigation are compared with the literature values and are given in Table 1.

#### ANALYTICAL METHODS USED

Both refractive index and specific gravity were used to fix the composition of a ternary mixture. In brief the method consists of mixing known quantities of the three components in which the mole ratio of two components was held constant and determining the two physical properties. A large scale plot, 50 × 50 cm, of the physical property *vs.* the composition of the component, whose mole number is at variance with the mole ratio of the other two components as parameter, resulting in a family of curves, was prepared.

The physical properties were next smoothed at even values of the composition and cross-plotted on a 50 cm side isosceles triangle; this chart was used to analyse the unknown ternary mixtures. To test the validity of this analytical method several known mixtures were analysed and the results showed an average deviation of 1 per cent. The refractive indices were determined at  $30 \pm 0.1^\circ\text{C}$  for sodium light using Abbe's precision refractometer, capable of reading to 0.0005. Water was circulated through the prism jackets maintained at 30°C by Fisher's Unitized constant temperature bath.

The equilibrium still used and the technique of its operation adopted are the same as reported previously [3]. The vapour liquid equilibrium

data and the values of experimental and calculated activity coefficients are given in Table 2. The smoothed analytical data are shown in Fig. 1.

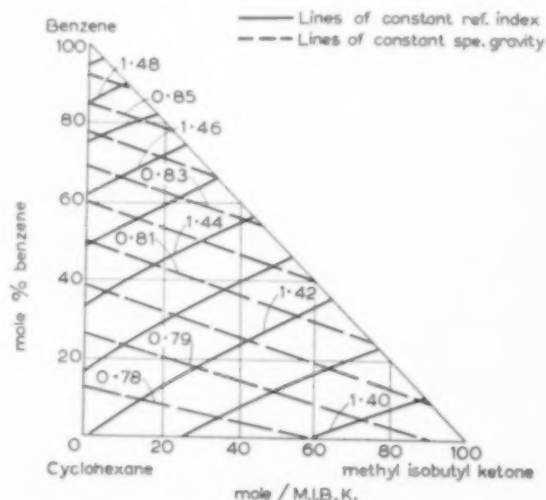


Fig. 1. Smoothed data of refractive index and specific gravity *v.* composition at 30°C in the system benzene-cyclohexane-methyl isobutyl ketone.

#### CALCULATION OF ACTIVITY COEFFICIENTS

Vapour liquid equilibrium data may be critically evaluated readily and extended by the use of activity coefficients. When the vapour phase is considered ideal the activity coefficient of a component in a mixture of *n* components is given by

$$\gamma_i = \frac{P_i x_i}{\pi y_i}$$

For cases when the deviations of the gas phase could not be ignored, BENEDICT *et al.* [4] expressed the activity coefficient as:—

Table 2. Vapour-liquid equilibria in the system benzene-cyclohexane-methyl isobutyl ketone at 760 mm Hg. total pressure

S. No.	Temp. (°C)	$x_1$	$x_2$	$y_1$	$y_2$	$\gamma_1$ Obs.	$\gamma_1$ Calc.	$\gamma_2$ Obs.	$\gamma_2$ Calc.	$\gamma_3$ Obs.	$\gamma_3$ Calc.
1	95.2	42.00	1.50	67.25	4.25	1.041	1.067	1.908	1.796	0.9515	0.9840
2	94.9	38.75	1.75	62.00	5.50	1.025	1.028	2.127	1.809	1.0210	0.9970
3	95.1	37.25	1.50	61.00	6.50	1.066	1.003	2.190	1.779	1.0070	0.9972
4	96.0	34.50	3.25	56.50	9.00	1.019	1.007	1.851	1.698	1.0200	0.9954
5	91.3	45.75	4.25	67.75	9.25	1.055	1.003	1.539	1.782	1.0130	0.9993
6	90.3	44.25	6.00	64.75	12.75	1.065	1.042	1.632	1.717	1.0250	0.9982
7	88.8	41.25	12.50	54.75	25.25	1.028	1.014	1.632	1.717	1.0250	1.0020
8	87.2	38.50	17.00	49.50	33.25	1.045	1.026	1.627	1.557	0.9491	1.0020
9	86.5	36.00	21.50	43.25	40.25	0.9979	1.039	1.585	1.502	0.9729	1.0210
10	88.5	26.25	39.25	31.25	35.50	1.040	1.087	1.269	1.284	1.0310	1.0830
11	83.8	24.25	43.75	29.00	59.00	1.072	1.101	1.234	1.238	1.0350	1.1370
12	84.6	20.50	44.75	24.75	61.75	1.058	1.131	1.235	1.245	1.0410	1.1200
13	85.5	19.25	40.75	24.75	57.75	1.089	1.103	1.226	1.278	1.0510	1.0740
14	86.4	18.00	37.75	24.00	57.75	1.109	1.129	1.302	1.316	1.0130	1.0500
15	90.0	16.25	29.75	22.75	54.00	1.054	1.139	1.406	1.001	0.9647	1.0080
16	100.0	10.25	9.25	19.75	32.25	1.095	1.072	2.103	1.475	0.9620	0.9900
17	93.2	31.00	7.00	38.50	20.50	1.068	1.028	2.077	1.671	1.0030	0.9915
18	90.0	46.50	5.00	65.50	13.50	1.061	1.005	2.022	1.762	0.9979	0.9992
19	88.8	52.50	5.50	68.50	13.50	1.021	1.015	1.957	1.752	0.9790	1.0030
20	87.6	57.50	5.75	74.75	10.50	1.037	0.996	1.490	1.740	0.9497	1.0030
21	86.6	62.75	3.75	77.25	7.50	1.053	1.001	1.692	1.782	0.9888	1.0080
22	86.0	66.00	3.75	80.50	7.75	1.029	0.996	1.780	1.799	0.9917	1.0080
23	85.5	56.00	9.75	71.00	10.50	1.084	1.134	1.321	1.652	1.1360	1.0280
24	84.9	42.25	23.00	50.00	36.25	1.031	1.021	1.405	1.452	1.0510	1.0510
25	91.2	17.25	25.00	25.25	49.25	1.065	1.119	1.478	1.436	0.9574	0.9938
26	90.4	4.50	37.50	6.00	67.50	0.991	1.252	1.378	1.345	1.0000	1.0100
27	86.4	7.75	49.06	10.50	71.75	1.167	1.227	1.247	1.246	1.0280	1.0516
28	86.5	3.25	53.25	5.00	76.25	1.277	1.275	1.216	1.229	1.0800	1.0960
29	81.8	1.00	88.50	1.25	92.50	1.185	1.353	1.009	1.018	1.7550	1.8770
30	81.8	4.50	80.50	7.00	85.50	1.474	1.298	1.028	1.039	1.4270	1.6270
31	81.4	13.00	71.75	15.50	76.75	1.144	1.081	1.050	1.059	1.6180	1.4460
32	80.8	23.00	61.75	27.00	66.25	1.147	1.147	1.070	1.145	1.3480	1.4860
33	80.2	31.25	64.00	34.00	61.25	1.075	1.096	1.151	1.174	1.1580	1.4350
34	80.0	38.75	49.00	41.00	54.00	1.060	1.075	1.125	1.126	1.2510	1.4170
35	81.3	34.50	46.25	38.25	54.25	1.064	1.070	1.151	1.277	1.1800	1.2540
36	81.0	42.75	40.75	45.25	45.75	1.036	1.045	1.185	1.220	1.1940	1.2800
37	80.5	43.75	39.75	50.25	43.00	1.089	1.076	1.154	1.282	1.2630	1.1950
38	80.1	32.75	5.25	93.25	6.00	1.000	1.000	1.163	1.411	1.1740	1.0560
39	81.2	88.00	5.00	91.25	7.50	0.993	0.990	1.345	1.481	0.9262	1.0510
40	80.4	83.25	10.00	85.50	11.75	1.013	1.001	1.183	1.137	1.2590	1.0960
41	80.8	71.25	16.25	73.00	23.00	1.001	0.990	1.415	1.408	0.9723	1.1260
42	80.4	65.00	24.50	67.25	29.00	1.022	1.007	1.194	1.313	1.1050	1.1700
43	81.2	61.50	22.50	63.75	31.25	1.003	1.001	1.389	1.375	1.0670	1.1460
44	79.4	52.5	40.50	53.00	43.50	1.056	1.046	1.116	1.81	1.4080	1.4060
45	79.2	47.00	45.00	49.25	49.25	1.079	1.061	1.099	1.149	1.4180	1.4510
46	79.3	48.50	42.00	50.00	46.00	1.057	1.064	1.141	1.172	1.4220	1.4050
47	79.4	48.25	42.75	50.00	47.25	1.060	1.051	1.173	1.166	1.3410	1.4090
48	81.0	87.50	27.00	58.75	35.75	0.986	1.008	1.308	1.327	1.0760	1.1900

$$\gamma_i = z_i \frac{P_i x_i}{\pi y_i}$$

where

$$z_i = \exp_{10} \left[ \frac{(P_i - \pi)(V_i - \beta_i)}{2.303 RT} \right]$$

The terms  $P_i$ ,  $V_i$ ,  $\beta_i$  are all functions of temperature and values of these were found at various temperatures between 80 and 116°C. Consequently

it was possible to express  $Z$  directly in terms of temperature. The second virial coefficient  $\beta$  was calculated using the equation given by WOHL [5]:

$$\beta = \frac{RT_c}{P_c} \left( 0.197 - 0.012 T_r - \frac{0.4}{T_r} - \frac{0.146}{T_r^{3/2}} \right)$$

The critical constants for benzene and cyclohexane are obtained from PERRY [6] and those of methyl isobutyl ketone are calculated by the

method given by HOUGEN, WATSON and RAGATZ [7]. The vapour pressure data of the three components benzene, cyclohexane, and methyl isobutyl ketone are taken from the existing literature. For each component  $\log P \cdot 1000/T$  was plotted and a mean straight line was drawn for each case; these lines are represented by the following equations,

$$\text{Benzene [8]} \log P = 7.65501 - \frac{1685.7266}{(t + 273)}$$

$$\text{Cyclohexane [9]} \log P = 6.84498 - \frac{1203.526}{(t + 222.863)}$$

Methyl isobutyl ketone

$$[10] \log P = 7.9592 - \frac{1975.0}{t + 273}$$

#### CORRELATION AND DISCUSSION OF THE DATA

Among the various equations [11, to 15] developed for correlating ternary vapour liquid equilibrium data those of WOHL [12] are comprehensive and find wide application. The applicability of the ternary WOHL [12], LI and COULL [15] or WHITE [11] equations is restricted by the condition:—

$$A_{32}/A_{23} = (A_{31}/A_{13})(A_{12}/A_{21})$$

which is not satisfied in the present case. Hence an attempt was made to correlate the data, with WOHL's [12] three suffix Margules equations, which utilize six binary constants and one ternary constant.

The end values of the system benzene-cyclohexane were obtained by correlating the data of RICHARDS and HARGREAVES [1] with WOHL's two suffix equations; the other two have been reported earlier [2] and are given below:—

$$\begin{array}{ll} A_{12} = 0.158 & A_{21} = 0.158 \\ A_{23} = 0.10 & A_{32} = 0.41 \\ A_{13} = 0 & A_{31} = 0 \end{array}$$

As a first approximation  $C$  was assumed to be zero and the activity coefficients were calculated; good agreement was not obtained between the calculated and experimental values. In order to obtain a more satisfactory fit of the data, about 13 values of  $C$  were computed from experimental

ternary measurements using appropriate equations and compositions as suggested by WOHL [12]; they were averaged to give a value of  $-0.26$ .

By inserting these seven constants into the three suffix Margules equations of WOHL [12] the following equations are obtained:—

$$\log \gamma_1 = 0.158 x_2^2 + x_2(-0.25 x_3 + 0.62 x_3^2) + 0.26 x_2 x_3 (1 - 2 x_1)$$

$$\log \gamma_2 = x_3^2(0.1 + 0.62 x_2) + x_1(0.158 + 0.568 x_3) + 0.26 x_1 x_3 (1 - 2 x_2)$$

$$\log \gamma_3 x_1^2(0.41 - 0.62 x_3) + x_1 x_2(0.252 - 0.62 x_3) + 0.26 x_1 x_2 (1 - 2 x_3)$$

In Table 2 the experimental and calculated activity coefficient data for each experimental run are compared; satisfactory agreement was obtained in most cases. The average error between calculated and experimental activity coefficients in  $\gamma_1$ ,  $\gamma_2$  and  $\gamma_3$  are respectively 2.4 per cent, 4 per cent and 4.5 per cent and these errors are within reasonable limits of experimental accuracy. Hence the three suffix Margules equations represent the data fairly well with the ternary constant  $C = -0.026$ .

No ternary azeotrope was observed in the present system.

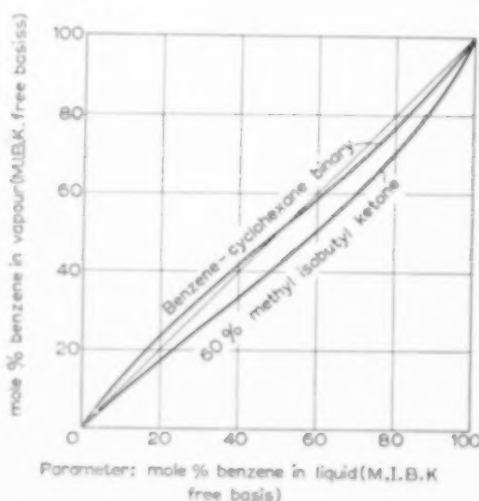


FIG. 2. Mole % benzene in liquid (methyl isobutyl ketone free basis). The effect of methyl isobutyl ketone on benzene-cyclohexane vapour-liquid equilibria.



The experimental ternary vapour-liquid equilibrium data were smoothed and plotted on a solvent free basis, that is, on a basis free from methyl isobutyl ketone. Fig. 2 shows that the benzene-cyclohexane azeotrope was completely eliminated when the solvent concentration was about 60 per cent. Thus the solvent depresses the relative volatility of benzene and increases that of cyclohexane, thus causing a separation to take place. However further increase of the solvent concentration did not increase the relative volatility of the binary mixture to any considerable extent.

### CONCLUSIONS

Ternary vapour-liquid equilibrium data of the system benzene-cyclohexane-methyl isobutyl ketone were determined at 760 mm Hg. total pressure using a modified Colburn still. The activity coefficient data of all the experimental runs were correlated satisfactorily by Wohl's three suffix Margules equations employing six binary constants and one ternary constant. It was found that there is a ternary effect and prediction of ternary data from binaries alone would lead to error.

Although ternary data can be predicted from

constituent binaries as an approximation, for the reliable establishment of vapour-liquid equilibrium relationships at least a few ternary measurements are necessary to account for the ternary effects, as observed by earlier workers [2, 16, to 20]. No ternary azeotrope was observed. Methyl isobutyl ketone might be used as an entrainer in the separation of benzene-cyclohexane mixtures into pure components by extractive distillation.

### NOTATION

- $A_1, A_2, A_3$ , etc. = the end values of the activity coefficient curves  
 $C$  = ternary constant  
 $\beta$  = virial coefficient of component  $i$   
 $\pi$  = total pressure of the system  
 $P_i$  = vapour pressure of pure components at the temperature of the system  
 $E$  = gas constant  
 $T$  = absolute temperature  
 $\gamma$  = activity coefficient of component  $i$  of the system  
 $x$  = mole fraction of component in liquid  
 $y$  = mole fraction of component in vapour  
 $v$  = molal volume of liquid  
 $z$  = factor introduced to account for vapour phase deviations  
 Subscripts, 1, 2, 3,  $i, j$  refer to the components.

### REFERENCES

- [1] RICHARDS A. R. and HARGREAVES E. *Industr. Engng. Chem. (Industr.)* 1944 **36** 805.
- [2] DAKSHINAMURTY P., JAYARAMA RAO G., ACHARYA, M. V. R. and VENKATA RAO C. *J. Sci. Industr. Res.*, 1957 **16B** No. 8 340.
- [3] DAKSHINAMURTY P. and VENKATA RAO C. *J. Sci. Res.* 1956 **15B** No. 3 118.
- [4] BENEDICT M., JOHNSON C. A., SOLMON E. E. and RUBIN L. C. S. *Trans. Amer. Inst. Chem. Engrs. Industr.* 1945 **41** 371.
- [5] WOHL K. Z. *Phys. Chem.* 1929 **2B** 77.
- [6] PERRY T. H. *Chemical Engineers Handbook*. McGraw-Hill, New York 1950.
- [7] HOGGEN O. A., WATSON K. M. and RAGATZ R. A. *Chemical Process Principles*, Part I. John Wiley & Sons, New York, 1955.
- [8] TIMMERMAN J., *Physical Constants of Pure Organic Compounds*. Elsevier, New York 1950.
- [9] JORDON T. E. *Vapour Pressures of Pure Organic Solvents*. Interscience Inc., New York 1954.
- [10] KARR A. E., SCHEIBEL E. G., BOWES W. M. and OTHMER D. F., *Industr. Engng. Chem. (Industr.)* 1951 **43** 961.
- [11] WHITE R. R. *Trans. Amer. Inst. Chem. Engrs.* 1945 **41** 539.
- [12] WOHL K. *Trans. Amer. Inst. Chem. Engrs.* 1946 **42** 215.
- [13] REDLICH O. and KISTER A. T. *Industr. Engng. Chem. (Industr.)* 1948 **40** 345.
- [14] EDWARDS B. S., HASHMALL F., GILMONT R. and OTHMER D. F. *Industr. Engng. Chem. (Industr.)* 1954 **46** 194.
- [15] LI Y. and COULL T. J. *Inst. Pet.* 1948 **34** 692.
- [16] ACHARYA M. V. R., D.Sc. Thesis, Andhra University 1954.
- [17] KURMANADHA RAO K. V., D.Sc. Thesis, Andhra University 1956.
- [18] KRISHNAMURTY V. V. G., D.Sc. Thesis, Andhra University 1955.
- [19] MERTES T. S. and COLBURN A. P. *Industr. Engng. Chem.* 1947 **39** 787.
- [20] THORNTON J. D. and GARNER F. A. J. *Appl. Chem.* 1951 Supplement No 1 61.
- [21] WEISBERGER A., PROSKANES E. D., REDDICK T. A. and TOOPS E. E. *Organic Solvents*. Interscience Inc., New York 1955.

## A note on mean residence-times in steady flows of arbitrary complexity

D. B. SPALDING

Imperial College of Science and Technology, London

(Received 24 January 1958)

**Abstract**—The mean residence-time of a tracer injected into a steady incompressible flow of arbitrary complexity is shown to be equal to the vessel volume enclosed between inlet and outlet planes divided by the volumetric flow rate, provided that the tracer is prevented from diffusing upstream of the injection plane. Velocities and effective diffusion coefficients may vary with position, but not with concentration or time.

If the tracer is not prevented from diffusing upstream of the injector plane, the mean residence-time exceeds the above by an amount equal to the effective longitudinal diffusion coefficient in the inlet pipe, divided by the square of the velocity in that pipe.

**Résumé**—L'auteur montre que le temps de contact moyen d'un traceur introduit dans un fluide incompressible de complexité arbitraire, lors de l'écoulement permanent, est égal au rapport du volume du récipient compris entre les plans d'entrée et de sortie et de la vitesse d'écoulement volumique, à condition d'empêcher la diffusion en amont du plan d'injection. Les vitesses et coefficients effectifs de diffusion peuvent varier avec la position, mais ne varient pas en fonction de la concentration ou du temps.

Si le traceur diffuse en amont du plan d'injection, la durée de contact est supérieure à celle décrite précédemment d'une quantité égale au coefficient effectif de diffusion longitudinale dans la tubulure d'entrée divisé par la carré de la vitesse dans ce tube.

**Zusammenfassung**—Die mittlere Verweilzeit eines Indikators, der in eine stationäre, inkompressible Strömung beliebiger Anordnung injiziert wird, ist, wie gezeigt wird, gleich dem Behältervolumen zwischen Eintritts- und Austrittsebene geteilt durch den Volumenstrom, vorausgesetzt, dass der Indikator nicht von der Injektionsebene stromaufwärts diffundiert. Geschwindigkeiten und effektive Diffusionskoeffizienten können von Ort zu Ort, nicht aber mit der Konzentration oder der Zeit variieren.

Wenn der Indikator von der Injektionsstelle stromaufwärts diffundieren kann, wird die mittlere Verweilzeit grösser als die oben angegebene, und zwar um einen Betrag gleich dem effektiven Längsdiffusionskoeffizienten im Eintrittsrohr, geteilt durch das Quadrat der Geschwindigkeit in diesem Rohr.

### 1. PURPOSE OF NOTE

If a pulse of tracer material is injected uniformly across the inlet duct to a vessel of volume  $V$ , through which incompressible fluid flows steadily, and the concentration of tracer is measured vs. time at the outlet section, a simple formula [1] for the mean residence-time  $\theta_m$  (time from instant of injection to instant of appearance at exit of an element of tracer, averaged over all tracer elements) is

$$\theta_m = V/v \quad (1)$$

where  $v$  is the volumetric rate of fluid flow.

This note examines the conditions under which this formula is valid. It will be shown that it holds if the tracer material is prevented from diffusing upstream at the injector plane, provided that the effective diffusion coefficients and velocities are independent of concentration, even for flows of arbitrary complexity. If upstream diffusion at the injector plane can occur,

the formula underestimates the mean residence-time.

## 2. STATEMENT OF PROBLEM FOR INJECTOR PLANE IMPERMEABLE TO TRACER

Consider first the vessel shown in Fig. 1. At time  $\theta = 0$  a small tracer quantity  $S$  is suddenly injected uniformly into the fluid crossing the inlet plane 1. A "sieve" prevents the tracer from diffusing upstream. An analysis device measures the concentration of tracer  $c_2$  at the outlet plane 2. The volume of vessel and duct between the two planes is  $V$ . The flow velocities can be regarded as uniform across each of the planes 1 and 2.

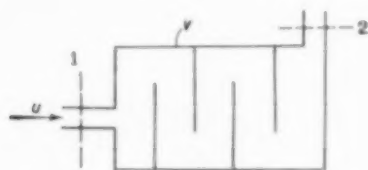


FIG. 1. The flow system considered.

The analysis device gives a result such as is illustrated in Fig. 2. We have to find the value

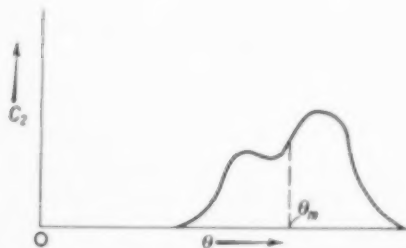


FIG. 2. Typical concentration time diagram at outlet.

of the mean residence-time which, in accordance with the above definition, is given by

$$\theta_m = \frac{\int_0^{\infty} c_2 \theta d\theta}{\int_0^{\infty} c_2 d\theta} \quad (2)$$

## 3. ANALYSIS

### Equation of conservation

It will be supposed that the tracer travels by convection and diffusion. Then its concentration  $c$  at any point obeys the equation

$$\partial c / \partial \theta = \nabla (D \nabla c) - \nabla (\mathbf{q} c) \quad (3)$$

where  $\mathbf{q}$  is the local velocity vector, and  $D$  is the local effective (laminar and turbulent) diffusivity. Both  $\mathbf{q}$  and  $D$  vary with position, but not with concentration or time.

### Theorem 1

Integrating the equation from  $\theta = 0$  to  $\theta = \infty$ , (3) becomes

$$c_{\infty} - c_0 = \nabla (D \nabla \int_0^{\infty} c d\theta) - \nabla (\mathbf{q} \int_0^{\infty} c d\theta) \quad (4)$$

Now at all points,  $c_{\infty} = 0$ ; for at long enough times no tracer material remains. Also, for points downstream of the injector plane,  $c_0 = 0$ ; for the tracer takes a finite time to reach such points in finite concentrations. The L.H.S. of (4) is therefore zero.

For convenience, put

$$I \equiv \int_0^{\infty} c d\theta \quad (5)$$

Then (4) becomes

$$\nabla (D \nabla I) - \nabla (\mathbf{q} I) = 0 \quad (6)$$

This will be recognised as the steady-state diffusion equation in the absence of sources. Without formal analysis (which could of course be given), it is easy to see that, since gradients of  $c$ , and therefore of  $I$ , are zero at the vessel walls, the only possible solution is

$$\begin{aligned} I &= \text{const. everywhere} \\ &= I \text{ for inlet stream} \\ &= S/v \end{aligned} \quad (7)$$

Equation (7) represents the first theorem, which is obvious enough. It means among other things that, if a steady stream (train of equal pulses) of tracer is injected, the concentration is uniform throughout the vessel.

**Theorem 2**

To approach  $\theta_m$ , we first multiply equation (3) by  $\theta$ , and then integrate from  $\theta = 0$  to  $\theta = \infty$ , obtaining

$$\int_{\theta=0}^{\theta=\infty} \theta dc = \nabla \int_0^{\infty} c \theta d\theta - \nabla (q \int_0^{\infty} c \theta d\theta) \quad (8)$$

The L.H.S. may be written as

$$\int_{\theta=0}^{\theta=\infty} \theta dc = [\theta c]_0^{\infty} - \int_0^{\infty} c d\theta = 0 - I, \quad (9)$$

N.B. (In order that the symbols within the square bracket shall represent zero at the upper limit,  $c$  must fall off more rapidly than  $1/\theta$ . It always does so; for otherwise  $I$  would not be finite).

Putting, for convenience,

$$J \equiv \int_0^{\infty} c \theta d\theta, \quad (10)$$

equation (8) now becomes

$$\nabla (D \nabla J) - \nabla (q J) + I = 0 \quad (11)$$

Equation (11) will be recognised as the steady-state diffusion equation with a distributed source term  $I$ , which Theorem 1 has shown to have constant magnitude. The solution to the equation can again immediately be written down without formal analysis (which of course could again easily be given). Thinking of  $J$  as representing enthalpy and  $I$  as a heat source, and noting that wall gradients of  $c$ , and so of  $J$ , are zero, it is evident that the problem is akin to that of fluid flow through a heater. Since the total "heat input rate" is  $IV$ , it is clear that the difference between  $J$  at outlet and  $J$  at inlet is given by

$$v(J_2 - J_1) = IV \quad (12)$$

Now  $J_1$ , if we take for clarity a plane just upstream of 1, is evidently zero. Therefore

$$vJ_2 = IV \quad (13)$$

Reverting to the earlier notation, this can be written as

$$v \int_0^{\infty} c_2 \theta d\theta = V \int_0^{\infty} c_2 d\theta \quad (14)$$

Introducing  $\theta_m$  from (2), we have therefore proved that

$$\theta_m = V/v \quad (15)$$

which is our "simple formula" (1).

This is Theorem 2. A somewhat different proof has previously been given by DANCKWERTS [1]. It will be noted that the theorem holds irrespective of the flow pattern in the vessel. There may even be regions of recirculation in the vessel where the streamlines are closed. Changes in flow pattern will introduce changes in the shape of the curve of Fig. 2, but we have not had to make any assumption about this shape, being concerned only with the position of the centroid of the area beneath it.

#### 4. THE CASE OF A PERMEABLE INLET PLANE

We now carry out the corresponding analysis for the case in which the "sieve" is absent from the inlet duct, so that tracer material is free to diffuse upstream.

$$\text{Distribution of } \int_0^{\infty} c d\theta$$

No change in the analysis is needed in the derivation of Theorem 1 for the region downstream of plane 1. There  $I = S/v$  still holds. We now have to consider the distribution of  $I$  in the inlet duct.

Let the area of the duct be  $A_1$ , so that the flow velocity is  $v/A_1$ . Let the diffusion coefficient in the duct have the uniform value  $D_1$ . Then equation (6) for this region runs

$$D_1 \frac{d^2 I}{dx^2} - \frac{v}{A_1} \frac{dI}{dx} = 0 \quad (16)$$

where  $x$  = distance along the inlet duct in the stream direction.

The solution of this equation, with the boundary conditions  $I = S/v$  at  $x = x_1$  (inlet plane), and  $I = 0$  at  $x = -\infty$  (far upstream), is

$$x_1 < x: I = (S/v) \exp[v(x - x_1)/D_1 A_1] \quad (17)$$

This means that  $I$  falls off exponentially in an upstream direction.

### Determination of $\theta_m$ : Theorem 3

The previous analyses leading to (11) is still valid; the solution for  $J_2$  will be seen to differ however. For ease of physical understanding, we will continue to regard  $I$  as a heat input term; no rigour is lost thereby.

The total "heat input rate" now contains two terms, one for the vessel as before, namely  $SV/v$ , and another for the inlet duct. The latter must be written as  $\int_{-\infty}^{x_1} I A_1 dx$ . Introducing equation (17), valid in this region, we have:

$$\int_{-\infty}^{x_1} I A_1 dx = (S A_1 / v) \int_{-\infty}^{x_1} \exp [v(x - x_1) / D_1 A_1] dx \\ = S D_1 A_1^2 / v^2 \quad (18)$$

The solution of (11) is therefore

$$v J_2 = SV/v + S D_1 A_1^2 / v^2 \quad (19)$$

Introducing the original notation as before, a new expression for the mean residence-time is obtained, namely

$$\theta_m = \frac{V}{v} + \frac{D_1 A_1^2}{v^2} \quad (20)$$

This is Theorem 3. The second term may be interpreted as a correction to the "simple formula," necessary because some of the tracer material lengthens its residence-time by diffusing upstream before being swept downstream. Alternatively  $D_1 A_1^2 / v$  could be treated as a correction which must be added to the vessel volume  $V$  to account for the permeability of the inlet plane.

### 5. DISCUSSION

The result contained in equation (20) may be regarded as a generalisation to flows of arbitrary complexity of a result reported recently by LEVENSPIEL and SMITH [2], for the case of constant-area flow with a uniform diffusion coefficient.

However, the suggestion of these authors that, in complex flows, an average value of diffusion coefficient should be used in the residence-time correction, appears to be ill-founded: it is the diffusion coefficient in the inlet pipe which matters. This will often be much smaller than the average.

It also appears that the time-correction increases as the square of the intake area. This means that the effect of an impermeable injector plane can always be obtained by reducing the cross-section of the inlet duct in proportion to the other dimensions of the vessel. In many practical cases therefore the correction will be entirely negligible.

### 6. REFERENCES

- [1] DANCEWERTS P. V. *Chem. Engng. Sci.* 1957 **2** 1.
- [2] LEVENSPIEL O. and SMITH W. K. *Chem. Engng. Sci.* 1957 **6** 227.

## Local residence-times in continuous-flow systems

P. V. DANCKWERTS

Imperial College of Science and Technology, London.

(Received 24 January 1958)

**Summary**—If a tracer is injected at the inlet of a continuous-flow system in the form of a step or pulse signal, the course of the subsequent change in concentration at a point within the system, can be used to determine quantitatively the average "age" as an indication of the degree of stagnation of the material at this point.

**Résumé**—L'injection d'un traceur, à l'alimentation d'un système en écoulement continu, sous la forme d'un signal discontinu ou d'un signal d'impulsion permet de déterminer quantitativement la vitesse de remplacement ou le degré de stagnation de la matière, en un point du système, par suite des fluctuations de concentration en ce point.

**Zusammenfassung**—Wenn ein Indikator stossweise in den Eintritt eines kontinuierlichen Strömungssystems injiziert wird, kann man den Verlauf der nachfolgenden Konzentrationsänderung an einem Punkt innerhalb des Systems zur quantitativen Bestimmung der Verdrängungsgeschwindigkeit oder der Aufenthaltsdauer des Stoffes in diesem Punkt verwenden.

ELSEWHERE in this issue (p. 74), SPALDING shows that if a pulse consisting of a quantity of tracer is injected at the inlet of a steady-state flow system at  $t = 0$ , then the quantity

$$\int_0^{\infty} c \cdot dt$$

(where  $c$  is the local concentration of tracer at time  $t$  after injection) will have the same value at every point in the system. This suggests a method of determining the rate of replacement or degree of stagnation of the material in different parts of the system.

SPALDING's proposition is discussed further in the Appendix, where it is shown that the distribution of "ages" of the material in a volume-element around the point at which  $c$  is measured can be deduced from the variation of  $c$  with  $t$ . (The "age" of a particle of material is the time elapsed since it entered the system). The fraction of the material having ages between  $t$ ,  $(t + dt)$  is  $(vc/Q) \cdot dt$ , where  $v$  is the rate of flow of material through the system, and  $Q$  the quantity of tracer injected.

It follows that the average age,  $\bar{\theta}$ , of the

material at the point of measurement could be determined by evaluating graphically the integral

$$\bar{\theta} = \frac{v}{Q} \int_0^{\infty} ct \cdot dt.$$

In practice this may be hard to evaluate because of uncertainties about the tail of the curve. For many purposes the median age,  $\tau$ , will be just as useful as an index of the local rate of replacement. Half the material at the point has an age greater than  $\tau$ ; hence

$$\int_0^{\tau} c \cdot dt = \frac{1}{2} \frac{Q}{v}$$

The value of  $\tau$  is easily found by plotting  $c$  against  $t$  until the area under the curve is equal to  $Q/2v$ .

The same information can be obtained by raising the concentration of tracer in the inlet stream at  $t = 0$  from zero to a steady value  $C$ . The value of  $c/C$  at the point of measurement at time  $t$  is then equal to the fraction of the material having an age less than  $t$ , and the median age is equal to the value of  $t$  at which  $c/C$  reaches  $\frac{1}{2}$ .



These techniques offer a quantitative method of investigating rates of replacement of material in various parts of a continuous-flow plant (or of air in a room or water in a pond). For instance, a contour map of median ages throughout the plant might be made, and would show up clearly dead spots and by-passing effects. In general one would expect the median or average ages near the inlet to approach zero, and their values near the outlet to approach those for the material in the whole stream leaving the system. However, in stagnant pockets the age of the material might be considerably greater than that of the leaving stream, and channelling or by-passing effects would be shown up as regions where the age was relatively low.

## APPENDIX

A quantity  $Q$  of tracer is injected into the inflowing

stream. If  $Q$  is finite, the injection cannot be truly instantaneous; it will be assumed that it occurs at a constant rate over a short time-interval  $\delta t$ . Let the distribution function for the ages ( $\theta$ ) of the particles of material in the volume element, which contains a quantity  $\delta m$  of material be  $f(\theta)$ . At any time  $t$  after injection the age of the tracer will be between  $t$ ,  $(t + \delta t)$ , and hence the fraction of the material in the volume-element having the same age as the tracer is  $f(t) \cdot \delta t$ . Since a quantity  $v \cdot \delta t$  entered the system with the pulse of tracer, and therefore has the same age, the ratio of tracer to other material entering during the pulse was  $Q/v \cdot \delta t$ . Provided therefore that tracer and other material migrate together, the quantity of tracer in the specified volume-element at time  $t$  is

$$\frac{Q}{v \cdot \delta t} f(t) \cdot \delta t \cdot \delta m = \frac{Q f(t)}{v} \cdot \delta m$$

and hence the ratio  $c$ , of tracer to the whole of the other material in the volume element is given by

$$c = Q \cdot f(t)/v.$$

## Shorter Communications

### Lateral diffusion with liquid flow through a packed bed of ion-exchange particles

(Received 6 March 1958)

#### INTRODUCTION

SOME difficulties encountered with the introduction and the distribution of feed streams into a packed bed of ion-exchange resin particles led us to a method for measuring apparent radial diffusivities in fixed beds at low *Re*-numbers. In this method a constant downward flow of a solution containing ions *A* through a cylindrical fixed bed of known height is maintained. Another solution, with the same concentration of *A* but containing an additional amount of ions *B*, is fed through a narrow capillary placed in the axis of the bed and a few centimeters below the top. The average liquid velocity in the injection tube is made equal to the superficial velocity of the main stream. After a sufficiently long time of operation under constant conditions the ion composition in the resin particles is in equilibrium with the liquid composition; the distribution of the latter is determined by the spreading of the injected liquid by axial convective and radial diffusional transport, and under equilibrium conditions it would be the same as for a bed of inert particles with the same geometric structure. If now the flow experiment is discontinued and the resin bed is washed with water, the total amount of *B*-ions on the ion-exchange particles can be determined by elution with a concentrated solution containing e.g. *A*-ions and by subsequent titration. This total amount is a measure of the spreading of the injected liquid and therefore of the apparent radial diffusivity.

The measurements reported here were performed with a narrow size fraction of nearly spherical Dowex 50 × 8 cation-exchange particles with an average diameter  $d_p = 0.75$  mm. The main flow consisted of a dilute solution of NaCl in water (concentration  $c_0$ ); the injected flow contained the same amount of NaCl plus a relatively high excess concentration,  $\Delta c$ , of HCl. The resin was originally charged with Na<sup>+</sup>. As a consequence of the high total concentration near the injection point the resin particles would tend to shrink somewhat; on the other hand the displacement of Na<sup>+</sup> by H<sup>+</sup> causes the particles to swell. The above conditions were chosen in order to secure a small net swelling effect of the particles so that no local high porosities and channelling was to be expected.

The relationship between the total amount of H<sup>+</sup>-ions in the resin phase and the radial diffusivity  $D_r$  will be given in the next section.

#### THEORY

Under the steady state conditions described above, the excess,  $\Delta c$ , in H<sup>+</sup>-ion concentration in the liquid as a function of the axial distance from the injection point,

$z$ , and of the radial distance from the axis,  $r$ , is approximately given by

$$\Delta c = \frac{\Delta c_i A_i \bar{v}}{4 \pi D_r z} \exp\left(-\frac{r^2 \bar{v}}{4 D_r z}\right) \quad (1)$$

In the derivation of this equation it has been assumed that axial transport by diffusion is negligible and that the radial diffusion takes place from an infinitely thin line source into a radially infinite medium. In an actual experiment the injected stream has a finite cross-sectional area,  $A_i$ , so that in the very neighbourhood of the injection point equation (1) would not be valid. Further, the bed is radially confined, i.e. cylindrical with a radius  $R_p$ . However, if the region containing the bulk of the diffusing material is large with respect to the dimension of the injection tube but small with respect to the bed diameter, equation (1) is a very good approximation of the actual concentration distribution. Since this applies to the experiments to be described, equation (1) will be used as a basis for further calculation. Finally, equation (1) is valid only for the case where the approach velocities of the injected liquid and of the main stream are equal ( $= v_0$ ); also this condition was obeyed in the experiments.

In the present case of the exchange of univalent ions with a monofunctional resin the equilibrium relationship between the ion compositions in the liquid and in the resin can be expressed as

$$\frac{x(1-y)}{y(1-x)} = K, \quad (2)$$

where  $x$  and  $y$  are the relative concentrations or fractions of the displacing ions in the liquid and resin phase respectively (see e.g. [1]).

With

$$x = \frac{\Delta c}{\Delta c + c_0},$$

and equation (2) we may write for  $y$ :

$$y = \frac{\Delta c}{\Delta c + Kc_0}. \quad (3)$$

The total amount of H<sup>+</sup>-ions present in the resin phase in the length interval  $0 < z < L$  is given by

$$m_H = q \int_0^L dz \int_0^\infty y 2\pi r dr, \quad (4)$$

where  $q$  is the capacity of the ion-exchanger per unit volume of bed.

After substitution of equations (1) and (3) into (4) the latter can be integrated to give

$$m_H = \frac{q \Delta c_i A_i L}{2K_0} \left( 1 + \lambda \ln \left( 1 + \frac{1}{\lambda} \right) - \frac{1}{\lambda} \ln (1 + \lambda) \right), \quad (5)$$

with

$$\lambda = \frac{4 \pi K c_0 D_r L}{\Delta c_i A_i \bar{v}}, \quad (6)$$

When  $\lambda$  changes from 0 to  $\infty$ , the expression between brackets in equation (5) varies from 0 to 2. If the conditions of the experiment ( $c_0$ ,  $\Delta c_i$ ,  $A_i$ ,  $L$  and  $\bar{v}$ ) and the properties of the system ( $q$  and  $K$ ) are known, equations (5) and (6) can be used for the calculation of  $D_r$  from the experimentally determined value of  $m_H$ .

Apart from the experimental requirements connected with the validity of equation (1), the method postulates that the spreading of the injected excess concentration can be described by means of a constant radial diffusion coefficient.

#### RESULTS

The values of the various quantities for these experiments were

$A_i = 3.36 \times 10^{-6} \text{ m}^2$  (inner diameter of injection tube = 2.07 mm),

$c_0 = 0.010 \text{ kg-equiv. Na}^+\text{-ions/m}^3$  (except for run no. 10 where  $c_0 = 0.10$ ),

$\Delta c_i = 1.0 \text{ kg-equiv. H}^+\text{-ions/m}^3$ ,

$K = 1.7$  (determined separately, see also [2]),

$q = 2.1 \text{ kg-equiv./m}^3$  (also determined separately),

$\epsilon = 0.40$  ( $= v_0/\bar{v}$ ).

The other experimental conditions (the tube diameter  $2 R_t$ ,  $L$  and  $v_0$ ) are given in Table 1, together with the

$m_H$ -values found and the values of  $\lambda$  and  $\bar{v}/D_r$  calculated from the data by means of equations (5) and (6). The values of  $D_r$  obtained vary between 0.4 and  $3.3 \times 10^{-7} \text{ m}^2/\text{sec}$ , i.e. a few orders of magnitude greater than the coefficients of molecular diffusion of electrolytes in water. Since radial diffusion in packed beds is frequently expressed in terms of the dimensionless group  $\bar{v} d_p/D_r$  (a Péclet number), the value of this number is indicated in Table 1 together with  $Re_p$ , the Reynolds number based on the particle diameter and the superficial flow velocity.

It is seen from Table 1 that the values of  $\bar{v} d_p/D_r$  are fairly constant and that no significant dependence on Reynolds number exists. Runs no. 3, 8, 10 and 11, with nearly equal values of  $v_0$ , give practically equal results for  $\bar{v} d_p/D_r$ , although 3 and 8 differ in tube diameter, 8 and 10 in the value of  $c_0$  and 8 and 11 in the length  $L$ . This indicates that very probably the spreading of the excess concentration may be treated as a diffusional process with constant diffusivity and it justifies the application of equation (1) to these experiments. The latter can also be checked by more detailed calculations.

A comparison of these results with other work is of interest. BERNARD and WILHELM [3] measured lateral diffusivities in packed beds in the region  $5 < Re_p < 2,000$ . The value of  $\bar{v} d_p/D_r$  proved to be of the order of 10, but variations were observed between 5 and 20. Later on, LATINEN [4, 5] continued this work; his experiments showed that  $\bar{v} d_p/D_r$  had a constant value of about 11 for  $Re_p > 200$ , but that at lower  $Re$ -numbers this value increased. The latter results have been represented in Fig. 1. LATINEN's explanation for this effect, i.e. that as the flow becomes more laminar, the injected liquid is less thoroughly mixed between the particles and becomes more striated with a preference to its original lateral position, is entirely plausible; this was also borne out by visual observation with a model. It is, therefore, surprising that the average value of  $\bar{v} d_p/D_r$ , of about 26,

Table 1

No.	Temp. (°C)	$2 R_t$ ( $10^{-3} \text{ m}$ )	$L$ (m)	$v_0$ ( $10^{-3} \frac{\text{m}}{\text{sec}}$ )	$m_H$ ( $10^{-6} \text{ kg-equiv.}$ )	$\lambda$ —	$\bar{v}/D_r$ ( $10^4 \text{ m}^{-1}$ )	$\bar{v} d_p/D_r$ —	$v_0 d_p/v$ —
1	17	37.5	0.229	1.40	34.8	0.48	3.0	23	1.05
2	19	37.5	0.229	1.99	33.0	0.44	3.3	25	1.46
3	17	37.5	0.231	2.99	33.0	0.43	3.4	26	2.08
4	14	62.2	0.210	0.62	28.3	0.39	3.4	26	0.40
5	16	62.2	0.211	0.82	28.9	0.40	3.35	25	0.55
6	16	62.2	0.210	1.06	25.7	0.32	4.1	31	0.72
7	15	62.2	0.209	1.83	26.2	0.34	3.9	29	1.21
8	14	62.2	0.209	3.07	29.2	0.42	3.2	24	1.96
9	14	62.2	0.210	4.47	28.2	0.38	3.5	26	2.86
10	17	62.2	0.210	3.07	6.35	3.70	3.6	27	2.13
11	17	62.2	0.317	3.07	51.8	0.37	3.5	26	2.13

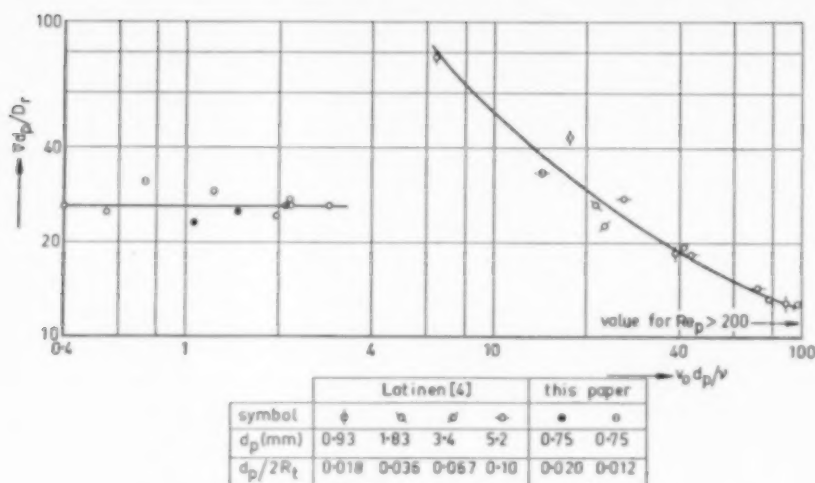


FIG. 1. Measured radial diffusivities compared with LATINEN's results.

obtained with the present experiments in a range of still smaller  $Re$ -numbers, is much smaller than would be expected on the basis of Latinen's results and considerations. Since, however, we cannot find any reason for which the method used here and its results would be entirely wrong, we think that a further investigation along these lines would be interesting.

M. E. HARTMAN

Laboratorium voor Fysische Technologie C. J. H. WEVERS

Technische Hogeschool, Delft, Netherlands H. KRAMERS

## NOTATION

$A_i$  = cross-sectional area of injection tube ( $m^2$ )  
 $c_0$  = concentration of  $Na^+$ -ions in main and injected stream (kg-equiv./ $m^3$ )  
 $\Delta c$  = excess concentration of  $H^+$ -ions in the liquid (kg-equiv./ $m^3$ )

 $d_p$  = average particle diameter (m) $D_r$  = apparent lateral (or radial) diffusivity ( $m^2/sec$ ) $K$  = equilibrium constant, equation (2) $L$  = height of the packed bed, measured from injection point (m) $m_H$  = total amount of  $H^+$ -ions bound by the resin (kg-equiv.) $q$  = capacity of the ion-exchanger (kg-equiv./ $m^3$  of fixed bed) $r$  = radial distance from the axis (m) $\bar{v}$  = average liquid velocity in the bed (m/sec) $v_0$  = liquid velocity based on the empty cross-section (m/sec) $x$  = relative concentration of  $H^+$ -ions in the liquid (—) $y$  = relative concentration of  $H^+$ -ions in the resin (—) $z$  = distance downstream from the injection point (m) $\epsilon$  = porosity of the bed (—) $Re_p = v_0 d_p / \nu$  (—)

## REFERENCES

- [1] KUNIN R. and MYERS R. J. *Ion-exchange resins*, John Wiley New York 1952.
- [2] WEVERS C. J. H. *Research on ion exchangers by means of the percolation technique* Doctor's thesis, Delft 1957 (In Dutch).
- [3] BERNARD R. A. and WILHELM R. H. *Chem. Engng. Progr.* 1950 **46** 233.
- [4] LATINEN G. A., *Mechanisms of fluid-phase Mixing in Fixed and Fluidized Beds of Uniformly Sized Spherical Particles*, Ph.D. dissertation, Princeton Univ. 1951.
- [5] WILHELM R. H. *Chem. Engng. Progr.* 1953 **49** 150.

## Book Reviews

J. ZERNIKE : *Chemical Phase Theory*. Klumer's Pub. Co. Ltd., Netherlands 1957, 666 diagrams, 493 pp.

This book gives a very thorough account of the subject which in English is usually referred to as "The phase rule", that is to say it deals with the phase relations in systems containing one or more components. Up till very recently the most comprehensive treatment of the subject available was probably the series of volumes edited by H. W. B. ROOZENOOM, published in German; however, beginning as it did in 1901, the data given in this work are far from up to date. ZERNIKE's book contains an account of the subject in some 493 pages which, according to the author, covers literature references up to 1954, and refers to no less than about 680 actual systems in illustration of the theory. The subject matter is treated as follows: derivation of the phase rule 18 pp.; one-component systems 17 pp.; binary systems 213 pp.; ternary systems 139 pp.; more complex systems 39 pp.; metastable systems 26 pp.; and answers to problems 20 pp.

The data to which reference is made above serve as illustrations to the general theoretical discussion of the subject: it would appear that the theoretical development and discussion is treated throughout in a scientifically satisfactory manner. On the other hand the English style is not above criticism and makes the reading of the book at times somewhat difficult.

As examples of awkward turns of phrase two sentences from p. 11 may be quoted: "through the membrane . . . the carbon dioxide diffuses in this form that two ions of  $\text{HCO}_3$  go from right to left, and . . ." "Here we have a very pronounced example that . . . the vapour pressure . . . is . . .".

The reviewer also has a minor quarrel with the author over the use of certain words: for instance (p. 120) "monotonous curve" should surely be "monotonic curve"; (p. 63) "have a common tangent with the liquidus in the extreme" is surely apt to be misread, as the author is referring to an extreme value; nor does he really like the word "multijugary" (multi-component?). The author introduces "singularly" for "one-component", and "chaoticus" for "gas-phase boundary curve"; these may be useful innovations, although "chaoticus" has got to compete with "vaporus" introduced by other authors.

One of the most interesting chapters is the one on metastable states, a somewhat unusual aspect of the subject. This deals for instance at considerable length with the sulphur system; it also discusses a number of other less important systems with metastable phases, including what the author calls pseudo-mixed crystals, but which are normally described as cases of adsorption on the solid phase.

As pointed out by the author, the text book by RICCI *The Phase Rule and Heterogeneous Equilibrium* appeared whilst ZERNIKE's work was still in manuscript. The two books undoubtedly cover much the same field, but in such an all-embracing subject as phase theory there is certainly room for two text books in the English language.

To sum up ZERNIKE's book constitutes a comprehensive and sound scientific survey of the phase theory, very fully illustrated with examples from actual systems. Some criticism can be levelled against the book on the grounds of style, and it may be hoped that this will be improved in a future edition.

R. F. STRICKLAND-CONSTABLE

## SELECTION OF CURRENT SOVIET PAPERS OF INTEREST TO CHEMICAL ENGINEERS

- S. N. GANZ : General principles of absorption processes in high-speed rotary absorbers. *Zh. prikl. Khim.* 1957 **30** 1604.
- I. V. LYUBIMOV and N. I. SMIRNOV : Dynamic activity of absorbents. *Zh. prikl. Khim.* 1957 **30** 1691.
- V. V. KAPAROV and YU. I. DITNERSKI : Equation for the calculation of limiting velocities of flow in packed columns. *Zh. prikl. Khim.* 1957 **30** 1698.
- V. I. ATROSHCHENKO and N. A. GAVRYA : Influence of inert gases on the synthesis of ammonia. *Zh. prikl. Khim.* 1957 **30** 1741.
- I. P. MUKHILENOV : Dynamics of a layer of liquid in a gas. *Zh. prikl. Khim.* 1957 **30** 1750.
- V. B. FALKOVSKI, YU. I. MELNIKOV and A. V. VETROVA : Dynamics of chemisorption in bubbling columns. *Zh. prikl. Khim.* 1957 **30** 1756.
- R. S. FRAIMAN : On kinetics of the process of rectification. *Zh. prikl. Khim.* 1947 **30** 1763.
- V. B. KOGAN : On the theory of extractive rectification. *Zh. prikl. Khim.* 1957 **30** 1863.
- I. P. MUKHILENOV : Investigation of layers of moving foam in sieve-type equipment. *Zh. prikl. Khim.* 1958 **31** 45.
- I. G. PLIT : On the theory of absorption complicated by simultaneous chemical reaction in the liquid phase. *Zh. prikl. Khim.* 1958 **31** 54.
- S. N. GANZ : Absorption of nitrogen oxides by solid sorbents. *Zh. prikl. Khim.* 1958 **31** 66.
- N. D. GORCHAKOV and I. I. POGODIN : Desorption of solvents from activated carbon with inert gases. *Zh. prikl. Khim.* 1958 **31** 60.
- A. G. AMELIN : Simplification in the method of purification of gas in manufacture of sulphuric acid by the contact process. *Khim. Prom.* 1957 463.
- V. G. FASTOVSKI and YU. V. PETROVSKI : Rectification process for the production of pure crypton. *Khim. Prom.* 1957 476.
- I. G. ROMANKOV, A. S. NOZDRAVSKI, A. I. SILMAN, N. B. RASHKOVSKAYA and Z. A. BEREZOVSKAYA : Separation of finely dispersed suspensions of poor filtering properties using centrifuges of the mounted basket type. *Khim. Prom.* 1957 480.
- YA. M. VARSHAVSKI and S. E. VEISBERG : Thermodynamic and kinetic peculiarities of reactions of the isotopic form of hydrogen. *Uspekhi Khim.* 1957 **26** 1434.
- A. P. KARNAUKHOV and A. B. KISELEV : Contribution to the theory of corpuscular structure of adsorbents. Capillary condensation in the space between regularly packed spheres. *Zh. fiz. Khim.* 1957 **31** 2635.
- I. R. KRISHEVSKI, N. E. KHAZANOVA and L. R. LINSHITS : Liquid-vapour equilibria in the system benzene-methanol at high pressures. *Zh. fiz. Khim.* 1957 **31** 2711.



# Selection of Current Soviet Papers of Interest to Chemical Engineers

- M. V. TOVIN and E. V. SAVINOVA : Kinetics of non-steady state processes at the gas-liquid interface II. Effect of adsorption layers on the rate of non-steady evaporation of water. *Zh. fiz. Khim.* 1957 **31** 2717.
- A. M. EUSGEV : On the theory of liquids. *Zh. fiz. Khim.* 1957 **31** 2414.
- L. P. FILPOV : The use of the similarity principle in characterising the properties of liquids IV. Viscosity. *Zh. fiz. Khim.* 1957 **31** 2435.
- M. V. TOVIN and E. V. SAVINOVA : The non-steady state kinetics of processes at gas-liquid interface I. Kinetics of evaporation of water in the non-steady state. *Zh. fiz. Khim.* 1957 **31** 2145.
- F. P. DOUZHENKO : A test of the Panchenkov equation. (Temperature dependence of the viscosity coefficient for binary liquid mixtures.) *Zh. fiz. Khim.* 1957 **31** 2517.
- N. A. FUKS : On the theory of evaporation of small drops. *Zh. tekhn. Fiz.* 1958 **28** 159.
- A. A. KULYEV and P. N. NASLEDOV : On diffusion of mercury into selenium. *Zh. tekhn. Fiz.* 1958 **22** 259.
- M. G. MANOV : On the mean rate of steam flow and steam expenditure in nozzles of high vacuum pumps. *Zh. tekhn. Fiz.* 1958 **22** 316.
- L. N. GRIGORIEV and A. G. USMANOV : Heat transfer to boiling binary mixtures. *Zh. tekhn. Fiz.* 1958 **28** 325.

## SOME CURRENT PAPERS IN OTHER JOURNALS

### CHEMICAL ENGINEERING PROGRESS Vol. 54, No. 6, June 1958

	PAGE
K. D. TIMMERHAUS, D. H. WEITZEL and T. M. FLYNN : Low temperature distillation of hydrogen isotopes ..	35
G. W. SWIFT, J. A. CHRISTY, A. A. HECKES and F. KURATA : Determining viscosities of liquefied gaseous hydrocarbons at low temperatures and high pressure .. .. .	47
R. V. L. HALL : Copper alloys for corrosion resistance .. .. .	51
T. T. MILLER : Projecting the profitability of new products .. .. .	56
J. HAPPEL and C. J. MARSEL : High-energy hydrocarbon fuels .. .. .	60
E. L. NEU, H. T. KOBATA and P. W. LEPPLE : Precoat scale-up from laboratory-size filter test leaf .. .. .	65
E. J. HENLEY, N. F. BARR, S. THOMSON and E. R. JOHNSON : Scale-up of radiation effects .. .. .	69
H. J. FLETCHER, D. E. HOOK, WILLIAM POULOS and W. R. COLLINGS : Interconnected pilot plant - laboratory system .. .. .	73

### CHEMICAL ENGINEERING PROGRESS Vol. 54, No. 7, July 1958

Plant operators report on Safety in Air and Ammonia Plants - I .. .. .	35
W. G. STRUNK : Preparation and properties of unsymmetrical dimethylhydrazine .. .. .	45
D. F. OTTHER : Acetic acid recovery methods .. .. .	48
JAMES F. ZIEVERS : Automation of filtration equipment .. .. .	53
E. J. CROSBY and W. R. MARSHALL, JR. : Effects of drying conditions on the properties of spray-dried particles ..	56
RALPH LANDAU : Chemical engineering in West Germany .. .. .	64

## ANNOUNCEMENT OF MEETING

### JAHRESTREFFEN 1958 DER VERFAHRENS-INGENIEURE

in Berlin vom 6 bis 8 Oktober

#### Vorläufiges Programm

Eröffnung und Begrüssung durch Prof. Dr. K. RIESS, Leverkusen  
Geleitworte des Bundesministers für Atomkernenergie u. Wasserwirtschaft, Prof. Dr.-Ing. S. BALKE, Bad Godesberg

#### PLENARVORTRÄGE

- Prof. Dr. K. Specht, Köln  
Der Einfluss der technischen Entwicklung auf die Struktur der Gesellschaft
- Prof. D.-Ing. H. Piloty, München  
Grundprinzipien der elektronischen Rechenautomaten

#### FACHVORTRÄGE

- Dr. G. Grass, Duisburg  
Über den Einfluss von Störungen der Strömung auf den Wärmeübergang an Wasser
- Dipl.-Ing. R. Ernst, Aachen  
Mechanismus der Wärmeübertragung in Fließbetten
- Prof. E. F. Boon, Delft  
Versuche an Dichtungen für rotierende Wellen
- Privatdozent Dr. H. Jung, Stuttgart  
Neuere Auffassungen über die Probleme der Festigkeit bei Hochdruck-Apparaten
- Prof. Dr. H. Kölbel und Dipl.-Ing. J. Schulze, Berlin  
Methoden und Daten zur Ermittlung des Anlagekapitalbedarfs bei der Projektierung verfahrenstechnischer Anlagen
- Dr.-Ing. R. Söhngen, Leverkusen  
Rationalisierung verfahrenstechnischer Anlagen durch Verwendung von Normeinheiten (Lagerbehälter, Pumpen, Rührwerke, Filterpressen, Destillierkolonnen, Messgeräte, Wärmeaustauscher)
- Dr.-Ing. W. Leidenfrost, Aachen  
Wärmeforschung in USA (Erfahrungen aus einem 20 monatigen Studienaufenthalt)
- Dr. G. Weiss, Butzbach  
Dekontaminierung von radioaktivem Abwasser
- Obering. E. Borgwardt, Berlin  
Filterung von radioaktiv verseuchter Luft
- Dr. H. Götte, Frankfurt-Griesheim  
Anwendung von radioaktiven Stoffen in der Verfahrenstechnik
- Prof. Dr. H. E. Rose, London  
Betrachtungen zur Korngrößen-Analyse
- Privatdozent Dr. W. Siemes, Berlin  
Förderung von körnigem Gut in geneigten Fließbetten
- Prof. Dr. P. Grassmann, Zürich  
Wärme- und Stoffaustausch zwischen zwei fluiden Phasen
- Prof. Dr. W. Niebergall, Berlin  
Anlagen zur Druckdestillation von Ammoniakwasser

Am 8. Oktober finden Besichtigungen von Industriebetrieben Berlins statt. Nähere Auskünfte über die Tagung erteilt die Geschäftsstelle der VDI-Fachgruppe Verfahrenstechnik, Frankfurt/Main, Rheingau Allee 25.

## CHEMICAL ENGINEERING SCIENCE

### PAPERS TO BE PUBLISHED IN FUTURE ISSUES

- M. RAJA RAO and C. VENKATA RAO : Flooding rates in packed liquid extraction towers
- R. A. SEHR : The thermal conductivity of catalyst particles
- F. J. ZUIDERWEG and A. HARMANS : The influence of surface phenomena on the performance of distillation columns
- A. S. SAID : The non-homogenous chromatographic column
- F. H. GARNER and R. B. KEY : Mass-transfer from single solid spheres - I. Transfer at low Reynolds numbers
- R. B. KEY and F. H. GARNER : Mass-transfer from single solid spheres - II. Transfer in free convection
- G. H. P. BRAS : The graphical determination of changes in the gas phase due to simultaneous heat and mass transfer
- J. J. CARBERRY : Some remarks on chemical equilibrium and kinetics in the nitrogen oxides-water system
- T. MIZUSHINA, N. HASHIMOTO and N. NAKAJIMA : Design of cooler condensers for gas-vapour mixtures
- J. BUITEN : The final stage in the removal of the lighter component of a binary mixture by batch rectification
- I. SORGATO : Some properties of the activity coefficient
- P. BORTOLINI : Kinetics of water-gas conversion reaction
- G. BOYE-CHRISTENSEN and S. G. TERJESEN : The action of surface active agents on mass transfer in liquid-liquid extraction
- T. MIZUSHINA, J. OISHI and N. HASHIMOTO : Method of calculation for the absorption accompanied with heat liberation
- A. ACRIVOS : On the rate of mass transfer from a gas to a moving liquid film
- R. ARIS and N. R. AMUNDSON : Statistical analysis of a reactor. Linear theory
- C. J. HOOGENDOORN : Gas/liquid flow in horizontal pipes

---

### EDITORIAL ANNOUNCEMENT

In the interests of keeping readers currently informed on the significant papers being published in the U.S.S.R. of interest to chemical engineers, arrangements have been made for a competent editor with a good knowledge of Russian to scan the Soviet literature and list the authors and titles of articles which might be of advantage to our readers. Translations or photostats of the article can be supplied on request by the Pergamon Institute (a non-profit making foundation) at a nominal charge. All orders for translations of Russian articles listed should be addressed to the Administrative Secretary of the Pergamon Institute at either 4 Fitzroy Square, London, W.1., or 122 East 55th Street, New York 22, which ever is more convenient.

## ERRATA

K. KLAMER and D. W. VAN KREVELEN. Studies on ion-exchange – I. General introduction *Chem. Engng. Sci.* 1958 7 197

p. 198, 1st column, 11th line from bottom : phenolsulphonic

p. 200, 1st column, 6th line from bottom : Fig. 3(b)

p. 202, equation (8) should read :

$$q_{\text{Na}^+} = f(c_{\text{Na}^+}, c_{\text{H}^+})$$

p. 202, equation (11) should read :

$$\left(\frac{\delta x}{\delta t}\right)_x = \frac{av}{a\gamma + Sf'_a(x)}$$

p. 203, 2nd column, 6th line from bottom : *for* to be replaced by *through*

p. 202, 1st column, 5th line from top :  $q_{\text{Na}^+}$

K. KLAMER, J. C. H. LINSSSEN and D. W. VAN KREVELEN. Studies on ion-exchange – II. Determination of ion-exchange equilibria. *Chem. Engng. Sci.* 1958 7 204

p. 205, 4th line from top : *schr verschiedene Natur* to be replaced by *Polyfunktionalität*

p. 206, 2nd column, 13th line from top :

$$(f_a(x_1^-) - f_c^-(x_2^-)), \text{ because } f_c^-(x_2^-)$$

to be replaced by :

$$(f_a(x_1^-) - f_c^+(x_2^-)), \text{ because } f_c^+(x_2^-)$$

p. 207, equation 9 should read :

$$x^2 = \frac{K}{c_{\text{H}^+} + K} \frac{c_{\text{H}^+}}{c}$$

p. 213, under Notation : the dimensions of  $c$  are :  $(ML^{-3})$

VOL  
9  
1958/